Experiment Station to Observe The Solar Charge Station Behaviour For a Year Period

By

Farah TATAR

A Dissertation Submitted to the Graduate School in Partial Fulfillment of the Requirements for the Degree of

MASTER OF SCIENCE

Department: Energy Engineering
Major: Energy Engineering
(Energy and Power Systems)

Izmir Institute of Technology
Izmir, Turkey

September, 2003

We approve the thesis of **Farah TATAR**

Date of Signature

-- 11.09.2003

Prof. Dr.-Ing. Gürbüz ATAGÜNDÜZ
Supervisor
Energy Engineering (Energy and Power Systems)

-- 11.09.2003

Assoc. Prof. Dr. Mehmet GÜNEŞ
Co-Supervisor
Department of Physics

-- 11.09.2003

Prof. Dr. Ali GÜNGÖR
Department of Mechanical Engineering

-- 11.09.2003

Prof. Dr. Necdet ÖZBALTA
Department of Mechanical Engineering

-- 11.09.2003

Assoc. Prof. Dr. Barış ÖZERDEM
Department of Mechanical Engineering

-- 11.09.2003

Prof. Dr.-Ing. Gürbüz ATAGÜNDÜZ
Head of Interdisciplinary
Energy Engineering (Energy and Power Systems)

ACKNOWLEDGEMENT

I am deeply indebted to my advisor, Prof. Dr.-Ing. Gürbüz Atagündüz, for his constant support. He carefully guided me throughout the pursuit of my Masters Degree at Izmir Institute of Technology. His ideas and suggestions have been invaluable to this thesis.

I would also like to thank my co-advisors Assoc. Prof. Dr. Mehmet Güneş and Asst. Prof. Dr. Salih Dinleyici and the members of my committee Prof. Dr. Ali Güngör and Prof. Dr. Necdet Özbalta from Ege University and Assoc. Prof. Dr. Barış Özerdem, who attend my defense. Their advice and patience is appreciated.

I am grateful to my Institute, İzmir Institute of Technology for supporting financial assistantship throughout my Master of Science education

I would like to thank Prof. Dr. Gazanfer Harzadın from Tartes for his invaluable advice on the construction and production of Omega Type Solar Charge Station and for his help about the experiment station equipment. A special thanks also goes to the Department of Construction Works, who mounted the photovoltaic station to the Classrooms Building rooftop and did the necessary connections and wiring.

I would also like to acknowledge Scientific Research Projects Commission of Izmir Institute of Technology, who supported my project. This study would not be ended without their help and support.

I am indebted to the preceding graduate students from The Department of Energy Engineering before me: Aylin Çantay, Fatih Bacaksız and Pınar İlker Alkan.

I would also like to thank drivers of Iztech for their tireless efforts when I need transportation.

Lastly, I would like to thank my family and my friends for their support. They were always there when needed.

ABSTRACT

The main purpose of this project is to set-up an experiment station, which will investigate the behavior of a portable "Solar Charge Station" that charges electric or hybrid vehicles, which work at the city centers.

The solar charge station is constructed on Classrooms Building in Engineering Faculty of Izmir Institute of Technology. Sixteen monocrystalline silicon photovoltaic modules having the dimensions of $1.293m \times 0.329m \times 0.034m$ and 55W power rating are used as the photovoltaic generator of the solar charge station. Modules are mounted as if they create an "*Omega Shape*" which gives its name to the station (*Omega Type Solar Charge Station*). Vertical and tilted reflectors are used to enhance the electricity generation. Generated electricity is used to charge a lead acid battery, which is protected by five solar charge regulators in order to prevent discharging and overcharging. 50 W halogen lamps working with direct current are chosen as the loads. The system is analyzed both theoretically and experimentally. Theoretical results have shown that Omega Type Solar Charge Station generates more or less steady electricity, approximately 240 MJ through a year period. The reflectors operate better in winter than in summer, theoretically. According to the stations shape, it uses less space on rooftops. Experiments have shown that efficiency of the charge station during summer is considerably high. The efficiencies calculated by using direct solar radiation on inclined surface is 31.65315%, for the experiment on 21.08.2003, 27.90379% for the experiment carried out without reflectors on 11.09.2003 and 35.70939% for the experiment carried out with optimum inclination angles for September, on 12.09.2003. Omega shape of the station and the reflectors increase the efficiency more or less 3% in summer and 16% in winter, theoretically. The usage of reflectors, also, reduces total cost of the station if the energy gain is considered.

ÖZ

Projenin ana amacı, elektrikle şehir merkezlerinde çalışan otomobil ve otobüslerin akülerini, güneş enerjisi ile şarj edebilecek bir portatif "Güneş Şarj İstasyonu"nu yıl boyunca inceleyecek deney istasyonunun kurulmasıdır.

Güneş Şarj İstasyonu, İzmir Yüksek Teknoloji Enstitüsü, Mühendislik Fakültesi Derslikler Binası'nın çatısına kurulmuştur. Güneş Şarj istasyonunun fotovoltaik jeneratörü, on altı tane $1.293m \times 0.329m \times 0.034m$ boyutlarında 55 W güce sahip mono-kristal silisyum fotovoltaik modülden oluşmaktadır. Modüller, istasyona adını veren (*Omega Tipi Güneş Şarj İstasyonu*) "Omega Şekli"ni oluşturacak şekilde dizilmiştir. Dikey ve eğik reflektörler, elektrik üretimini arttırmak için kullanılmıştır. Üretilen elektrik, beş adet şarj regülatörü tarafından aşırı dolma ve boşalmaya karşı korunan bir kurşun-asit aküyü şarj etmek için kullanılmıştır. Yük olarak, doğru akım ile çalışan 50 W' lık halojen lambalar seçilmiştir. Sistem hem teorik hem de deneysel olarak incelenmiştir. Teorik sonuçlar göstermiştir ki, Omega Tipi Güneş Şarj İstasyonu yıl boyunca sabite yakın elektrik üretir (yıl boyunca 240 MJ). Teorik olarak reflektörler kışın, yaza göre daha verimli çalışırlar. İstasyonun şekli, çatılarda daha az yer kaplamasına sebep olur. Deneyler göstermiştir ki, istasyonun günlük verimi, yaz döneminde oldukça yüksektir. 21.08.2003 günü, eğik düzleme gelen direkt güneş radyasyonu kullanılarak %31.65315, 11.09.2003 günü yapılan reflektörsüz deneyde %27.90379 ve Eylül ayı için optimum modül eğimleri ile yapılan deneyde %35.70939 olarak hesaplanmıştır. Omega şekli ve reflektörler sayesinde, teorik olarak, yazın yaklaşık %3 ve kışın %16 verim artışı hesaplanmıştır. Reflektör kullanımı, ayrıca, kazanılan ek enerji düşünüldüğünde maliyetin daha az olmasını sağlamıştır.

TABLE OF CONTENTS

LIST OF FIGURES

LIST OF TABLES

NOMENCLATURE

A: Area, m^2

A_{sh}: Shaded area, m^2

A_{she}: Effective shaded area, m^2

a_m: absorbance of the photovoltaic module

E: Equation of time

GU: length of the shadow on horizontal surface, m

GU_β: length of the shadow on inclined surface, m

H: Height, m

h: Altitude angle, °

I_o^*: Solar constant, W/m^2

I_{on}^*: Extraterrestrial radiation, W/m^2

$I_{o\beta}^*$: Instantaneous extraterrestrial solar radiation on inclined surface, W/m^2

I_{oz}^*: Instantaneous extraterrestrial solar radiation on horizontal surface, W/m^2

$I_{oh\beta}$: Hourly extraterrestrial solar radiation on inclined surface, J/m^2

I_{ohz}: Hourly extraterrestrial solar radiation on horizontal surface, J/m^2

$I_{on\beta}$: Daily extraterrestrial solar radiation on inclined surface, J/m^2

$I_{on\beta}$: Daily extraterrestrial solar radiation on horizontal surface, J/m^2

$I_{cı}^*$: Clear sky, direct radiation, W/m^2

$I_{cı\beta}^*$: Clear sky direct radiation on an inclined surface, W/m^2

I_{cu}^*: Clear sky direct radiation on a horizontal surface, W/m^2

I_{cd}^*: Clear sky diffuse radiation, W/m^2

$I_{cd\beta}^*$: Clear sky diffuse radiation on an inclined surface, W/m^2

I_{cdz}^*: Clear sky diffuse radiation on a horizontal surface, W/m^2

$I_{ct\beta}^*$: Clear sky total radiation on a horizontal surface, W/m^2

I_{ctz}^*: Clear sky total radiation on a horizontal surface, W/m^2

$I_{oR}^{*'}$: Instantaneous reflected solar energy per unit time and area, W/m^2

$Q_{oR}^{*'}$: Instantaneous total reflected solar energy, W

Q_{ohR}' : Hourly total reflected solar energy, J

Q_{oht} : Hourly total energy falling and reflected, J

I: Ampere, A

L: Length, m

n : Number of day, n

r_R: Reflectance of the photovoltaic module

W: Width, m

U: Voltage, V

t: Time, s

Greek Letters

θ: Angle of incidence, °

θ': Angle of incidence of reflected beam, °

δ: Declination, °

ϕ: Latitude, °

β: Slope, °

γ: Surface azimuth angle,°

γ_s: Solar azimuth angle, °

γ_s': Solar azimuth angle of the reflected beam, °

ω: Hour angle, °

ω_s: Sunset and sunrise hour angle for horizontal surface

θ_z: Zenith angle, °

τ_1: Atmospheric transmittance for direct radiation

Superscripts

$'$: Reflected

*: Per unit time

Subscripts

$_e$: Effective

$_h$: Hourly

$_m$: Module

$_r$: Reflector

$_{sh}$: Shaded

$_t$: Total

$_\beta$: Tilted

Chapter 1

INTRODUCTION

The World Bank estimates that the world population will be about 8.5 billion by the year 2025. It is evident that with increasing number of people the energy demand will increase rapidly which enhances the air pollution and the green house effect [1]. Additionally, China, which has a rapid population increase (China has its 5th census on 1 November 2000 and it is 1.295.330.000), becomes industrialized and it is obvious that its energy demand will be supported by the coal reserves, which has not been used yet. This will also increase the pollution, the greenhouse effect and the smog. The only way is to quit the usage of fossil fuels and turn our face to clean, sustainable and renewable energy.

Since the onset of the industrial revolution in the mid 19th century, some 290 Gt Carbon have been oxidized from fossil fuels and released to the atmosphere. The known fossil fuel resource base represents a further carbon volume of some 5000 Gt Carbon indicating that there are good reserves of coal, gas and oil (as well as uranium), although there is still some uncertainty. The technical potential of renewable energy sources is far higher though it currently meets only around 20% of the global energy demand, mainly as traditional biomass and hydropower. Modern renewable energy systems have the technical potential to provide all global energy services in sustainable ways and with low or virtually zero greenhouse gas emissions [2].

Transportation has an important role on the explained gas emissions. Nearly 30% of the CO_2 emissions are because of the transportation. Electro or hybrid vehicles also named as zero or low emission vehicles can be a solution to the problem. Research and development studies carried out all over the world for the improvement of the vehicles that do not use fossil fuels [1].

If the electricity demand of the hybrid or electric vehicles is met by the utility grid power that use fossil fuels, the main idea of decreasing emissions is not satisfied. The aim is to charge the batteries of the electric vehicle by means of a clean energy resource, photovoltaic modules. Thus, clean energy will always be used in the energy chain.

"*Omega Type Solar Charge Station*" is designed to charge the batteries of an electric or hybrid vehicle. The owner of the idea, Atagündüz [1,3], created it on the bases of a previous study for the fields of heliostats of solar thermal power plant in the Ege University and the theoretical design of the station was made during a study in Germany.

The originality of the station comes from the orientation of the 16 photovoltaic modules that are used. The modules are mounted as if they formed an omega shape and created a fixed mirror area, which also acts as if it were a Sun-tracking array.

As it is important to increase the efficiency, and as it is well known that a solar-tracking system has a higher efficiency but a higher cost, than a stationary system acting as a tracking system with low cost will be more efficient.

The current high cost of the photovoltaic modules make it interesting to enhance the energy collection of the devices by using several methods. In Omega Type Solar Charge Station booster reflectors are used to increase the energy collection by the array. Widespread applications of the photovoltaic systems are restricted due to their relatively high capital cost and low efficiency. The cost of a plane reflector is less than 5% of the cost of the PV system, while it can theoretically provide more than 15% yearly enhancement in solar energy collection, therefore reflectors are very promising as an ideal method of improving the efficiency of the arrays [4].

It is known that solar energy is diffuse and discontinues, it is available during the day but not at night. With the design of the Omega Type Solar Charge Station, this disordered behavior of the solar energy is minimized and more or less a stable energy is obtained. One of the major problems of solar energy, less energy in winter, can be solved with the reflectors. Monthly enhancement factor in the photovoltaic modules output energy reaches its maximum value in the winter season; while it reaches its minimum value in the summer season, so a linear electricity generation due to the reflectors through the whole year occurs.

The circular shape of omega gives another advantage to the station, which is area it needs for the mounting of the construction. As it is a rule of the nature, circular shape has a less area requirement. The station is mounted on the "Classroom's Building" rooftop in Faculty of Engineering in Iztech Campus, Urla-Izmir.

In this thesis, both the theoretical and experimental analysis of the "Omega Type Solar Charge Station" will be proposed. The first chapter is a brief introduction to the study. Following chapter, Chapter 2, is "Literature Survey" that is carried out from the selection of the thesis to the end. After the literature survey, a brief explanation of the theory of solar radiation and photovoltaic systems are given in Chapter 3. Pursuing chapter gives the calculation methods used in this study, which is Chapter 4. The extraterrestrial and terrestrial solar radiation calculations in Chapter 4, theoretical section, are done with the existing methods in the literature that are given in Chapter 3. Chapter 5 is the experimental section of the study including experimental set-up and experimental procedure Sections. Comprehensive knowledge about the orientation of the photovoltaic modules, the dimensions and the orientation of the reflectors, the measurement devices that are used in the experiments and the procedure followed can be found in Chapter 5. The results and their interpretations are given in Chapter 6. It includes the theoretical analysis of the omega type solar charge station and also some other possible orientations of the photovoltaic modules, the effects of reflectors, single module efficiencies and the whole array efficiency. A brief summary and the conclusions of the study are given in Chapter 7.

Chapter 2

LITERATURE SURVEY

In the discussions of the Grand Design for the 21st century's civilization life, great attention is focused on the *3E-Trilemma*. That is, for the activation of economic development (*E: Economy*), we do need an increase of the energy expense (*E: Energy*). However, it induces environmental problems (*E: Environment*) by more emissions of pollutant gases. On the contrary, if the political option chooses the suppression of pollutant gas emission, it inactivates the economical development. This is 3E-Trilemma [5].

Figure 2.1 shows an illustration of the cyclic correlation of the Economy, Energy and Environment. Here, importance is placed on the change in the circuit from the infrastructure of fossil fuel energy supply to that of renewable energy development and supply.

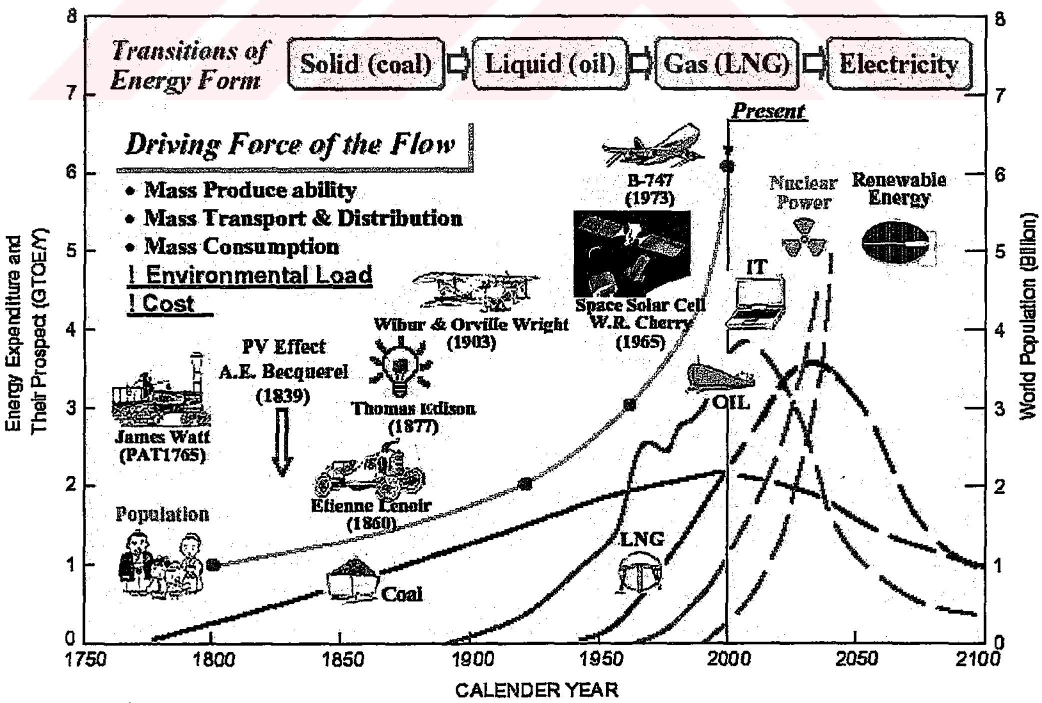

Figure 2.1 Change in the civilization life with energy resource [5].

World energy demands are assumed to double within the next 20 years [6]. Figure 2.2 is the transitions of world population and total energy demands.

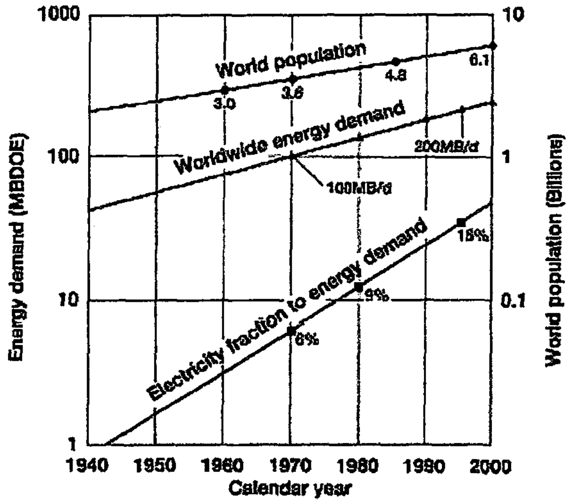

Figure 2.2 Transitions of world population, total energy demands. Percentages are the ratios of electricity to the total energy [5].

Table 2.1 shows the electricity generation sources and their percentages for the year 2000 and Table 2.2 shows the pollutant emission factors for electricity generation for different energy sources in the world.

Table 2.1 Net electricity generation from various fuels, in 2000 [7].

Fuel	**Kilowatt-hours (Millions)**	**Percentage of total electricity generation**
Non-renewable and hydro	3,799,944	97.79
Renewable:		
Biomass	39,498	1.04
Waste combustion	24,590	0.56
Geothermal	14,197	0.37
Wind	4,953	0.13
Solar	844	0.02.
Total renewable	84,082	2.31

Table 2.2 Pollutant emission factors for electricity generation (g/kWh) [5].

Energy source	CO_2	NO_2	SO_x
Coal	322.8	1.8	3.400
Oil	258.5	0.88	1.700
Natural gas	178.0	0.9	0.001
Nuclear	7.8	0.003	0.030
Photovoltaic	5.3	0.007	0.020
Biomass	0.0	0.6	0.140
Geothermal	51.5	TR	TR
Wind	6.7	TR	TR
Solar thermal	3.3	TR	TR
Hydropower	5.9	TR	TR

TR=trace.

It is obvious that with increasing population, the world's energy and electricity demand is increasing as shown in Figure 2.2. Since the electricity is being generated from non-renewable sources, Table 2.1, the pollutant emissions especially CO_2 will increase rapidly as given in Table 2.2.

Fossil fuels are being depleted at a faster rate than ever before. Global warming and its climatic change are becoming serious concern for governments worldwide. There is, thus, an urgent need for much more efficient and environmentally friendly energy resources to be exploited worldwide [6].

30% of the CO_2 emissions found in the atmosphere are caused by the transportation, which is due to the internal combustion engine vehicles. Introducing electric or hybrid cars (zero or low emission vehicles) can be a solution to this huge environmental problem [1,3]. But if the batteries of the electric cars are charged with conventionally generated electricity, the idea of reducing pollutant emissions will not be satisfied.

Under these conditions, there is growing interest for renewable and environment-friendly energy sources such as solar energy, on which some kind of sustainable growth may be based. Solar energy is indeed a renewable source of energy, the use of which avoids most of the negative externalities due to the use of fossil fuels.

The production of electrical power from solar energy may practically be implemented through two main technologies (Meyers, 1983), which are [8]:

- Solar-thermodynamic power plants, in which solar heat is concentrated through suitable mirror systems, to feed a conventional power plant; and
- Solar photovoltaic systems, in which energy is produced as a direct result of the conversion of the energy of the solar ray using the so-called "P*hotovoltaic Effect*". The photovoltaic effect is the basic physical process through which a photovoltaic device converts sunlight into electricity. In 1839, nineteen-year-old Edmund Becquerel, a French experimental physicist, discovered the photovoltaic effect while experimenting with an electrolytic cell made up of two metal electrodes. Becquerel found that certain materials would produce small amounts of electric current when exposed to light (discussed with more details in Section 3.2.1.1).

On the other hand, Turkey is an energy importing country with more than half of the energy requirements being supplied by imports, and air pollution is becoming a great environmental concern in the country. In this regard, renewable energy resources appear to be one of the most efficient and effective solutions for sustainable energy development and environmental pollution prevention in Turkey [9]. That's why we have to give our efforts to the R & D studies about renewable energy sources, especially solar energy and photovoltaics.

Solar PV technology provides a technologically feasible solution to societies current health and environmental dilemmas posed by the reliance on fossil fuel based power generation. Solar energy is already economically viable in many applications, and will continue to expand as production continues to increase in scale. PV energy production represents an environmentally beneficial and sustainable method of maintaining an energy intensive standard of living, which will enable development without compromising those who will live in the future to do the same [10]. Although photovoltaics are a savior for an environmental point of view, it is not well developed for an economical point of view and another "E", Efficiency of the photovoltaics becomes important.

Many working in the field of photovoltaics believe that 'first generation' silicon wafer-based solar cells sooner or later will be replaced by a 'second generation' of lower cost thin-film technology, probably also involving a different semiconductor. Historically, CdS, a-Si, CuInSe2, CdTe and, more recently, thin-film Si has been regarded as key thin-film candidates. Since any mature solar cell technology is likely to evolve to the stage where costs are dominated by those of the constituent materials, be it silicon wafers or glass sheet, it is argued that photovoltaics will evolve, in its most mature form, to a 'third generation' of high-efficiency thin-film technology. By high efficiency, what is meant is energy conversion values double or triple the 15–20% range presently targeted. Tandem cells provide the best-known example of such high-efficiency approaches, where merely adding more cells of different band gap to a stack can increase efficiency. However, a range of other better-integrated approaches is possible that offer similar efficiency to an infinite stack of such tandem cells. When photons of sunlight strike a PV cell, only the photons with a certain level of energy are able to free electrons from their atomic bonds to produce an electric current. This level of energy, known as the band-gap energy, is defined as the amount of energy required to dislodge an electron from its covalent bond and allow it to become part of an electrical circuit. The energy that photons possess is called the "photon energy." This energy must be at least as high as the band-gap energy for a photon to free an electron. However, photons with energy higher than the band-gap energy will expend the extra energy as heat when freeing the electrons. So, it's important for a PV cell to be "tuned" (through slight modifications to the semiconductor's molecular structure) to maximize the photon energy. After all, one key to obtaining an efficient PV cell is to convert as much sunlight into electricity as possible [11].

Photovoltaics are optimized and rated with respect to standard test conditions (STC), i.e. for an irradiation of 1000 W/m^2, a module temperature of 25°C and the standard spectrum AM 1.5. However these conditions do not correspond to real operating conditions of photovoltaics: in Freiburg, Germany, 50% of the total irradiation is in the interval below 600 W/m^2, but in Sudan, Africa, this amounts to 20% only. Module temperature varies between -20°C and 80°C, light incidence angles between 0° and 90°. As a consequence, the performance of PV modules under real conditions can be up to 30% (on a monthly scale) lower than at STC, depending on the weather and module/cell design [12].

A cost effective method to increase photovoltaic efficiency is using "*Booster Reflectors*" that reflects the solar radiation to the modules [13]. The use of inexpensive plane reflectors to enhance the solar energy collection of photovoltaics can provide acceptable efficiencies at higher operating temperatures [14]. Several types of reflectors can be used to increase sophistication, cost and enhancement coefficients. With reflectors, the increase in energy gain can range from 20 to 250%, depending on the type of equipment and season [15]. Figure 2.3 shows some types of reflector-photovoltaic systems.

The studies carried out by G. E. Ahmad and H. M. S. Hussein, for a complete year of experiments under different climatic conditions are shown in Figure 2.4 and Figure 2.5 [16]. Figure 2.4 shows the variation in the average daily output energy and efficiency of photovoltaic modules with and without reflector. The figure indicates that the reflector provides a large enhancement in the average daily output energy and efficiency of the photovoltaic module, especially in the winter season as shown in Figure 2.5. It shows that the monthly enhancement factor in the photovoltaic module output energy reaches its maximum value in the winter season, while it reaches its minimum value in the summer season. These results confirm the theoretical results previously published by the authors [14].

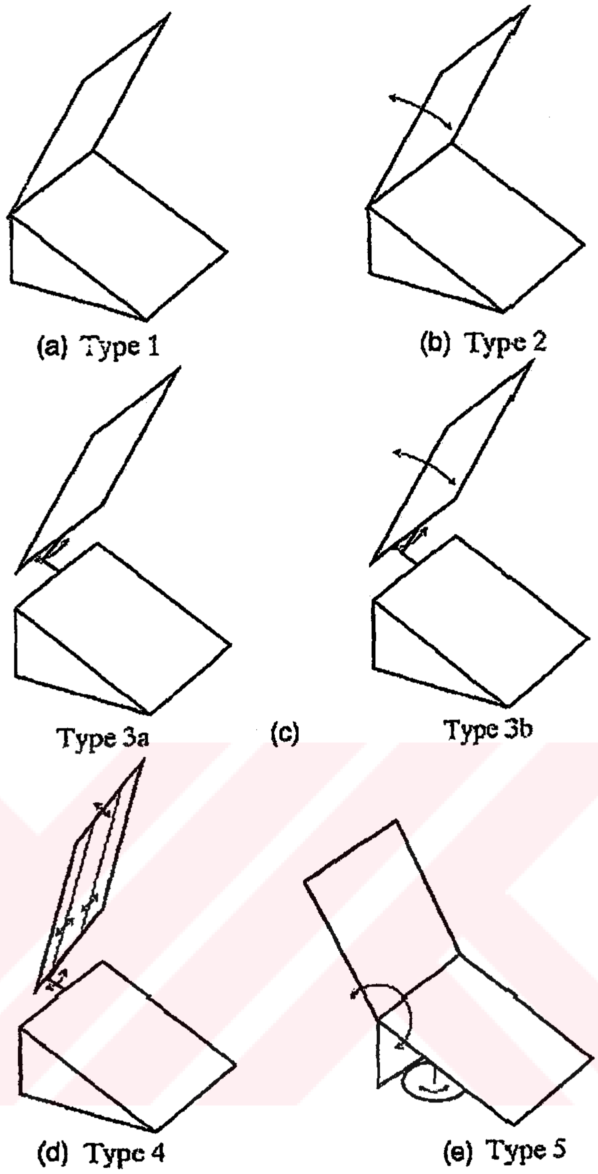

Figure 2.3 Schematic representation of the different types of photovoltaic panels using reflection of sunbeams: (a) reflector with a fixed position; (b) reflector with changing inclination; (c) reflector that follows changes of the azimuth angle (type 3a) and the same with changing inclination as well (type 3b); (d) reflector with flaps for changing its width; (e) Sun-tracking collector/photovoltaic panel with fixed reflector [15].

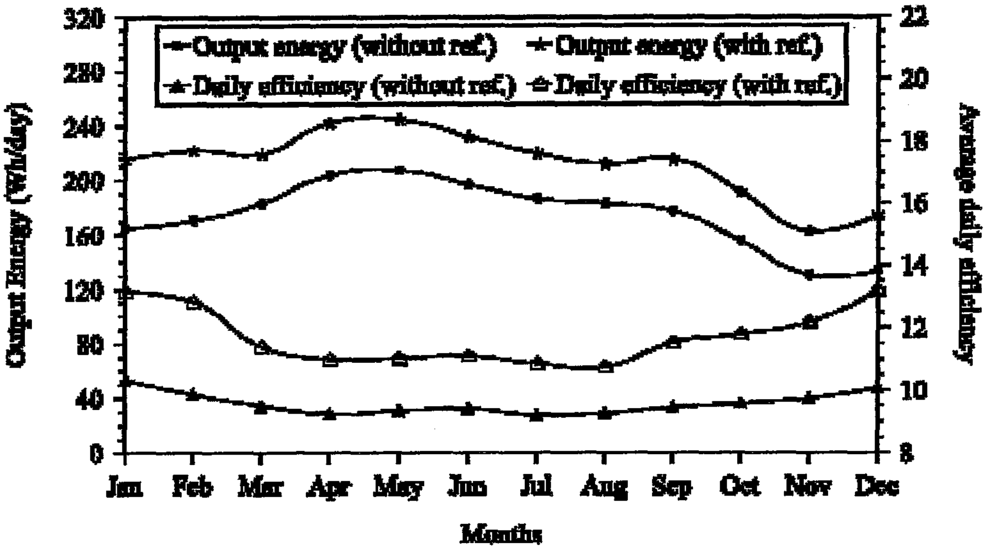

Figure 2.4 Variation of the average daily output energy and efficiency of two photovoltaic modules with and without reflectors [16].

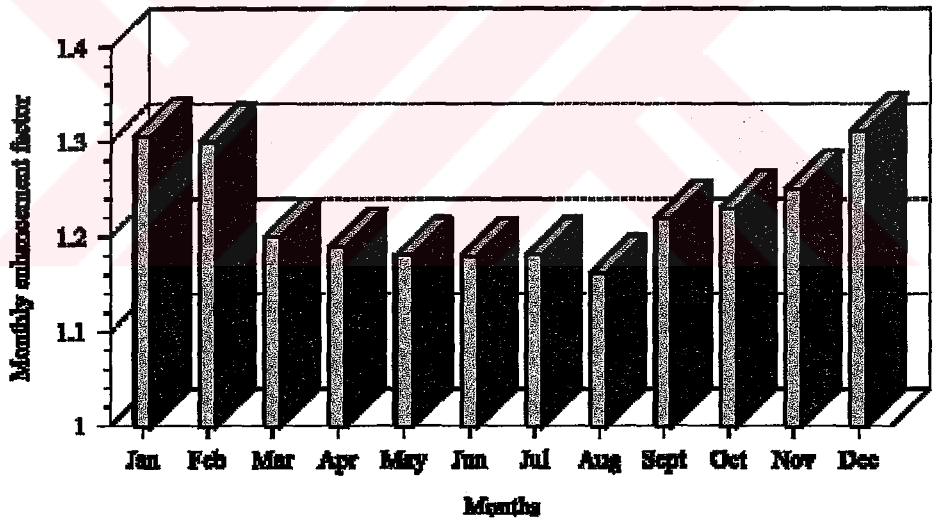

Figure 2.5 Variation of the monthly enhancement factor in the performance of the photovoltaic module augmented by a plane reflector through a complete year [16].

If economy viability is achieved, a large-scale deployment of photovoltaics could be triggered. The evidence indicates that the photovoltaic industry may be on the verge of rapid expansion as economies of scale improve production economies, government programs encourage deployment and more large-scale applications of the photovoltaic technology become viable [17].

Chapter 3

THEORY

The Sun is the provider of the energy needed to sustain life in our solar system. It is important to know its nature to understand the energy it radiates into space. The first part of Chapter 3, Section 3.1, is a brief introduction to Solar Radiation including The Sun, solar constant, solar spectrum and the position of the Sun in the sky.

The second part, Section 3.2 of Chapter 3 includes Photovoltaic Systems, its components and applications. The last part of the chapter, Section 3.3, contains some knowledge about Electro Cars, which is one of the application areas of photovoltaics.

3.1 Solar Radiation

3.1.1 The Sun

The Sun has been worshipped as a life-giver to our planet since ancient times. The industrial ages gave us the understanding of sunlight as an energy source. This discovery has never been more important than now as we realize that the exploitation of fossil energy sources may be affecting the planet's ambient.

The energy supply from the Sun is truly enormous: on average, the Earth's surface receives about 1.2×10^{17} W of solar power. This means that in less than one hour enough energy is supplied to the Earth to satisfy the entire energy demand of the human population over the whole year. Indeed, it is the energy of sunlight assimilated by biological organisms over millions of years that has made possible the industrial growth as we know it today. Most of the other renewable means of power generation also depend on the Sun as the primary source: hydroelectric, wind and wave power all have the same origin [18].

The Sun is a continuous fusion reactor and several thermonuclear fusion reactions have been suggested to supply the energy radiated by the Sun. The one considered the most important is a process in which hydrogen combines to form helium, Equation (3.1)and (3.2) [19].

$$4H^1 \rightarrow 2He^4 + 2e^+ + 2v \tag{3.1}$$

or

$$2p \rightarrow 2n + 2e^+ + 2v \tag{3.2}$$

This reaction is highly exothermic and a huge energy, for each He nucleus 25.5 eV or 1.5×10^8 kcal/gram, occurs. Researches have shown that Hydrogen amount present in the Sun is enough for nearly 10^{11} years [20].

In this reaction, mass is converted to energy according to Einstein's famous formula, $E = mc^2$. As a result of it, the surface of the Sun is maintained at a temperature of approximately 5800 K and at a density 100 times greater than water. This energy is radiated from the Sun uniformly in all directions, in close agreement with Planck's blackbody radiation formula [21].

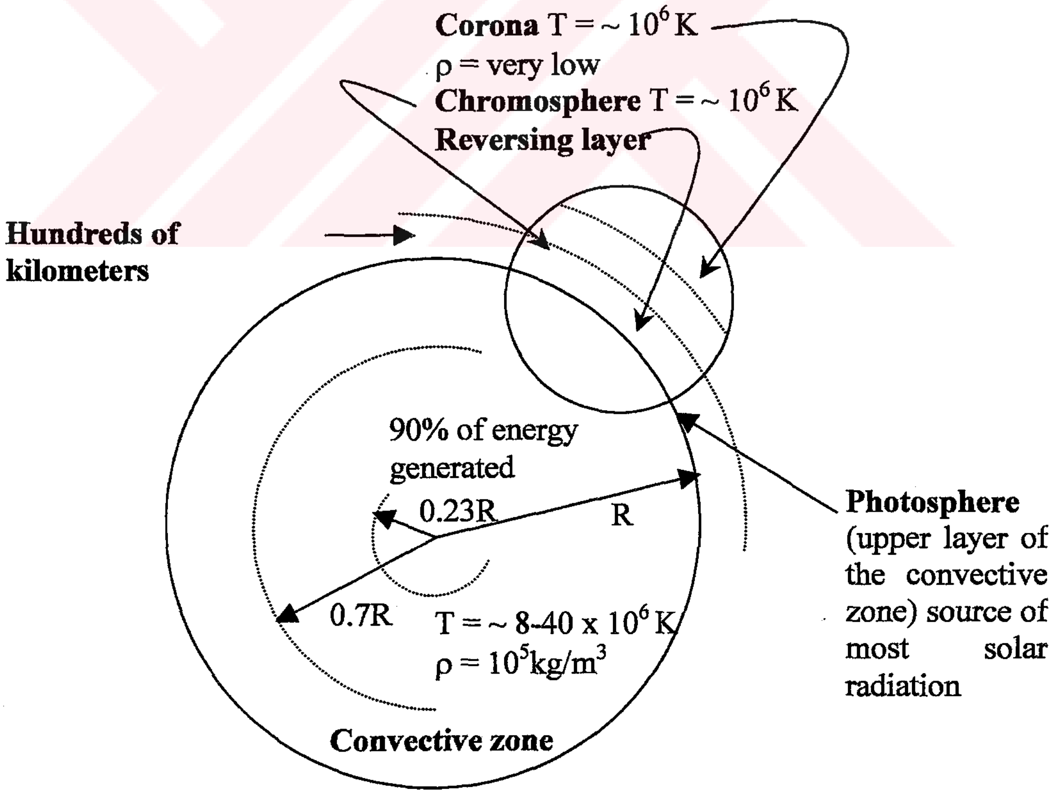

Figure 3.1 The structure of the Sun [19].

A schematic structure of the Sun is shown in Figure 3.1. It is estimated that 90% of the energy generated in the region of 0 to 0.23R (where R is the radius of the Sun), which contains 40% of the mass of the Sun.

At a distance 0.7R from the center, the temperature has dropped about 130,000 K and the density has dropped to 70 kg/m3; here convection process begin to become important, and the zone from 0.7 to 1.0R is known as the convective zone. Within this zone the temperature drops to about 5000 K and the density to about 10-5kg/m3 [19].

3.1.2 Energy From The Sun

3.1.2.1 Solar Constant

By the time the solar radiation from the Sun has travelled 93 million miles to the Earth, the total extraterrestrial energy density (radiation outside the atmosphere of the Earth) decreases to 1367 W/m^2 and is often referred as the **solar constant** [18, 19, 20, 21].

Figure 2.2 shows the geometry of the Sun-Earth relations. The eccentricity of the Earth's orbit is such that the distance between the Sun and the Earth varies by 1.7%.

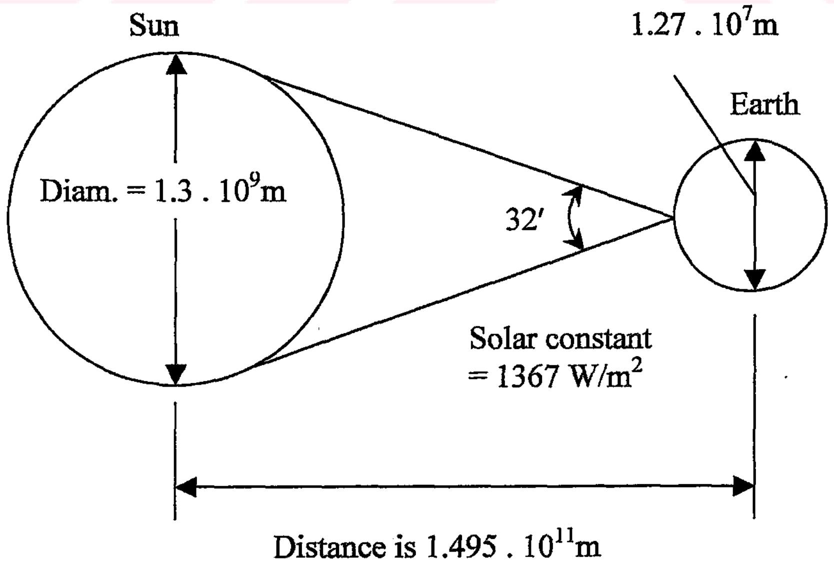

Figure 3.2 Sun-Earth relationships [19].

At a distance of one astronomical unit, 1.495×10^{11} m, the mean Sun-Earth distance, the Sun subtends an angle of 32′. The radiation emitted by the Sun and its spatial relationship to the Earth result in a nearly fixed intensity of solar radiation outside of the Earth's atmosphere. It is the energy of the Sun, per unit time received on a unit area of surface perpendicular to the direction of the propagation of the radiation, at mean Sun distance, outside of the atmosphere, which is explained above as the **solar constant,** I_0^*, [19].

3.1.2.2 Extraterrestrial Solar Radiation and The Solar Spectrum

The energy from the thermonuclear fusion reactions in the sun is radiated away from the Sun uniformly in all directions, in close agreement with Planck's blackbody radiation formula

$$w_\lambda = \frac{2\pi hc^2\lambda^{-5}}{e^{\frac{hc}{\lambda kT}}-1} \quad \text{(W/m}^2\text{/unit wavelength in meters)} \tag{3.3}$$

where $h = 6.63\times10^{-34}$ watt sec^2 (Planck's Constant),

$k = 1.38\times10^{-23}$ Joule/K (Boltzmann's constant)

λ = Wavelength in meters and c = speed of light (m/s).

Part of the energy from the fusion process heats the chromosphere, the outer layer of the Sun that is much cooler than the interior of the Sun, and the radiation from the chromosphere becomes the solar radiation incident on Earth. The solar radiation is not much different from the radiation of any object that is heated to about 5800 K except that the 'surface' of the Sun is heated by the fusion process. The radiation spans a large range of wavelengths from 200 nm to more that 50000 nm with the peak around 500 nm (Figure 3.3). Approximately 47% of the incident extraterrestrial solar radiation is in the visible wavelengths from 380 nm to 780 nm. The infrared portion of the spectrum with wavelengths greater than 780 nm account for another 46% of the incident energy and the ultraviolet portion of the spectrum is with wavelengths below 380 nm accounts for 7% of the extraterrestrial solar radiation [21].

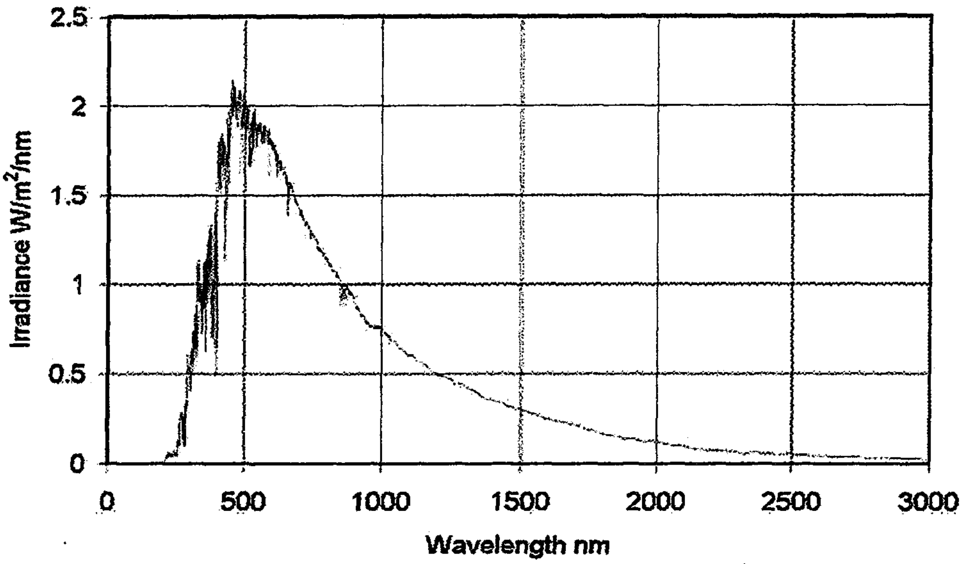

Figure 3.3 Extraterrestrial solar spectrum [21].

The solar constant, I_0^*, value (1367 W/m^2) varies by ±3% as the Earth orbits the Sun. The Earth's closest approach to the Sun occurs around January 4th and it is farthest from the Sun around July 5th. The extraterrestrial radiation is [19]

$$I_{on}^* = I_o^*(1 + 0.033 \cdot \cos\frac{360 \cdot n}{365}) \text{ (W/m}^2\text{)} \tag{3.4}$$

where n is the day of the year. For example, January 15 is year day 15 and February 15 is year day 46. There are 365 or 366 days in a year depending if the year is a leap year [20]. The variation of extraterrestrial solar radiation with time of year (n) is shown in

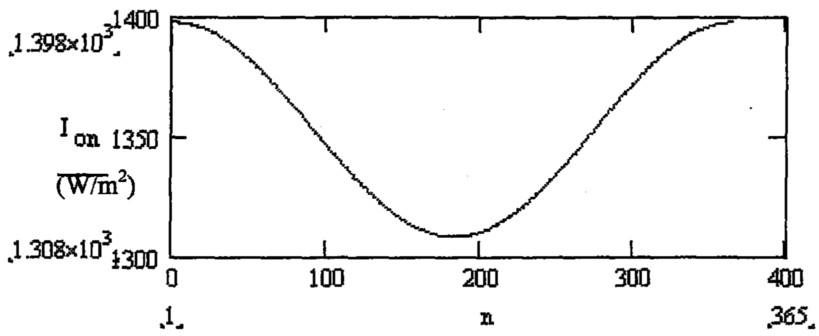

Figure 3.4 Variation of extraterrestrial solar radiation with time of year [22].

3.1.3 Definitions

In order to understand the basics of the solar radiation, effect of atmosphere and the components of the solar radiation and some useful equations, it is important to know some definitions, which are given below [19].

Air mass (AM) is a concept that characterizes the effect of a clear atmosphere on sunlight, equal to the relative length of the direct beam path through the atmosphere. On a clear summer day at sea level, the radiation from the Sun at zenith corresponds to air mass 1; at other times, the air mass is approximately equal to $1/\cos\theta_z$, where θ_Z is the zenith angle [18].

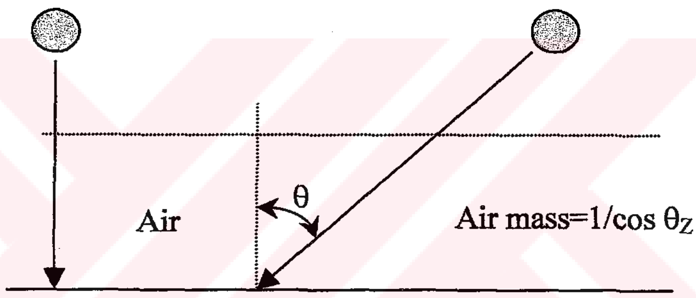

Figure 3.5 Representation of Air mass, schematically.

Near noon on a day without clouds, about 25% of the solar radiation is scattered and absorbed as it passes through the atmosphere. Therefore about 1000 W/m^2 of the incident solar radiation reaches the Earth's surface without being significantly scattered. This radiation, coming from the direction of the Sun, is called **direct radiation (or beam radiation)** [19].

Some of the scattered sunlight is scattered back into space and some of it also reaches the surface of the Earth. The scattered radiation reaching the Earth's surface is called **diffuse radiation.** Some radiation is also scattered off the Earth's surface and then re-scattered by the atmosphere to the observer. This is also part of the diffuse radiation the observer sees. This amount can be significant in areas in which the ground is covered with snow [19].

The **total solar radiation** on a horizontal surface is called **global radiation** and it is the total of incident diffuse radiation and the direct normal irradiance projected onto the horizontal surface. If the surface under study is tilted with respect to the horizontal, the total irradiance is the incident diffuse radiation plus the direct normal irradiance projected onto the tilted surface plus ground reflected radiation that is incident on the tilted surface [19].

Irradiance or Solar Flux, W/m^2, is the rate at which radiant energy is incident on a surface, per unit area of surface. The symbol I is used for solar irradiance, with appropriate subscripts for direct, diffuse and global radiation [19].

Irradiation or Radiant Exposure, J/m^2, is the incident energy per unit area on a surface, found by integration of irradiance over a specified time, usually an hour or a day. **Insolation** is a term applying specifically to solar energy irradiation.

Solar time is the time used in all of the Sun-Angle relationships such as Equations (3.9), (3.10) or (3.11); because the Sun moves along the ecliptic rather than along the equator and the distance between the Earth and the Sun is not constant, the apparent motion of the Sun contains an irregular component and the apparent solar time does not coincide with the time measured by conventional clocks. It is necessary to convert standard time to solar time by applying two corrections. First, there is constant correction for the difference in longitude between the observer's meridian (longitude) and the meridian on which the local standard time is based (two hours forward from Greenwich, 30° East Meridian for Turkey). The Sun takes 4 minutes to transverse 1° of longitude. The second correction is from the equation of time, which takes into account the perturbations in the Earth's rate of rotation that affect the time the Sun crosses the observer's meridian. The difference in minutes between solar time and standard time is

$$\text{Solar time} - \text{standard time} = 4\,(L_{st} - L_{loc}) + E \qquad (3.5)$$

Where L_{st} is the standard meridian for the local time zone. L_{loc} is the longitude of the location we are dealing. The equation of time E (in minutes) is determined from the Equation (3.6)[19].

$$E = 229.2(0.000075 + 0.001868\cos B - 0.032077\sin B - 0.014615\cos 2B - 0.04089\sin 2B) \tag{3.6}$$

where

$$B = (n-1)\frac{360}{365} \tag{3.7}$$

and n = day of the year, thus $1 \le n \le 365$.

3.1.4 Direction of Beam Radiation; The Angle of Incidence

The geometric relationships between a plane of any particular orientation relative to the Earth at any time (whether the plane is fixed or moving relative to the Earth) and the incoming beam solar radiation, the **angle of incidence**, that is, the position of the Sun relative to that plane, can be described in terms of several angles [Benford and Bock (1939)]. The angles are as follows [1]:

θ **Angle of incidence**, it is the angle between the sunbeam and the normal vector of the inclined surface.

δ **Declination**, it is the angular height of the Sun at solar noon with respect to the plane of the Equator, north positive and it takes values $-23{,}45° < \delta < +23{,}45°$.

According to the Figure 3.6, it can be seen that the declination angle is the angle between Sun, Earth and the equatorial plane. It is given by (Cooper, 1969) [19]:

$$\delta = 23.45\sin\left(360\frac{284+n}{365}\right) \tag{3.8}$$

n, which is the day of the year, can be obtained from Table 3.1.

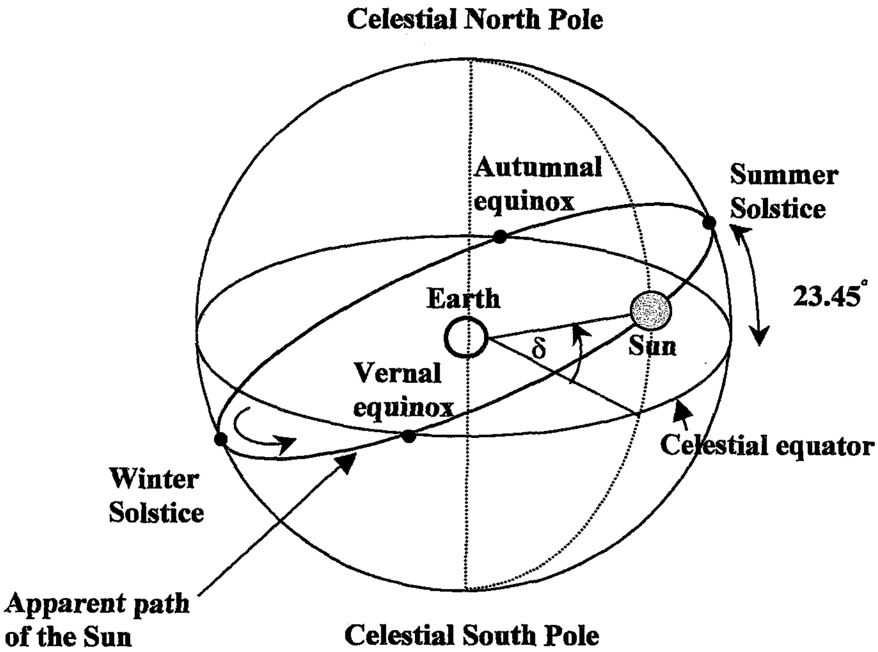

Figure 3.6 Celestial sphere with the apparent yearly motion.

Table 3.1 Recommended Average Days for Months [19].

		For the Average day of the Month	
Month	***n* for *i*th Day of Month**	**Date**	***n*, Day of Year**
January	i	17	17
February	31 + i	16	47
March	59 + i	16	75
April	90 + i	15	105
May	120 + i	15	135
June	151 + i	11	162
July	181 + i	17	198
August	212 + i	16	228
September	243 + i	15	258
October	273 + i	15	288
November	304 + i	14	318
December	334 + i	10	344

ϕ **Latitude,** it is angular location north or south of the Equator, north positive.

β **Slope,** it is the angle between the inclined surface and the horizontal plane.

γ **Surface azimuth angle,** it is the angle in the horizontal plane between the projection of the surface normal vector of the inclined surface and the south indicating line according to a reference point.

ω **Hour angle,** it is the angular displacement of the Sun east or west of the local meridian due to rotation of the Earth on its axis at 15° per hour. It takes morning negative and afternoon positive values. At the solar noon it is zero, ω=0.

Additional angles are defined that describe the position of the Sun in the sky:

θ_z **Zenith angle,** the angle between the vertical and the line to the Sun, i.e., the angle of incidence of beam radiation on a horizontal surface.

h **Solar altitude angle,** the angle between the horizontal and the line to the Sun, i.e., the compliment of the zenith angle.

γ_s **Solar azimuth angle,** the angular displacement from south of the projection of beam radiation on the horizontal plane, shown in Figure 3.9.

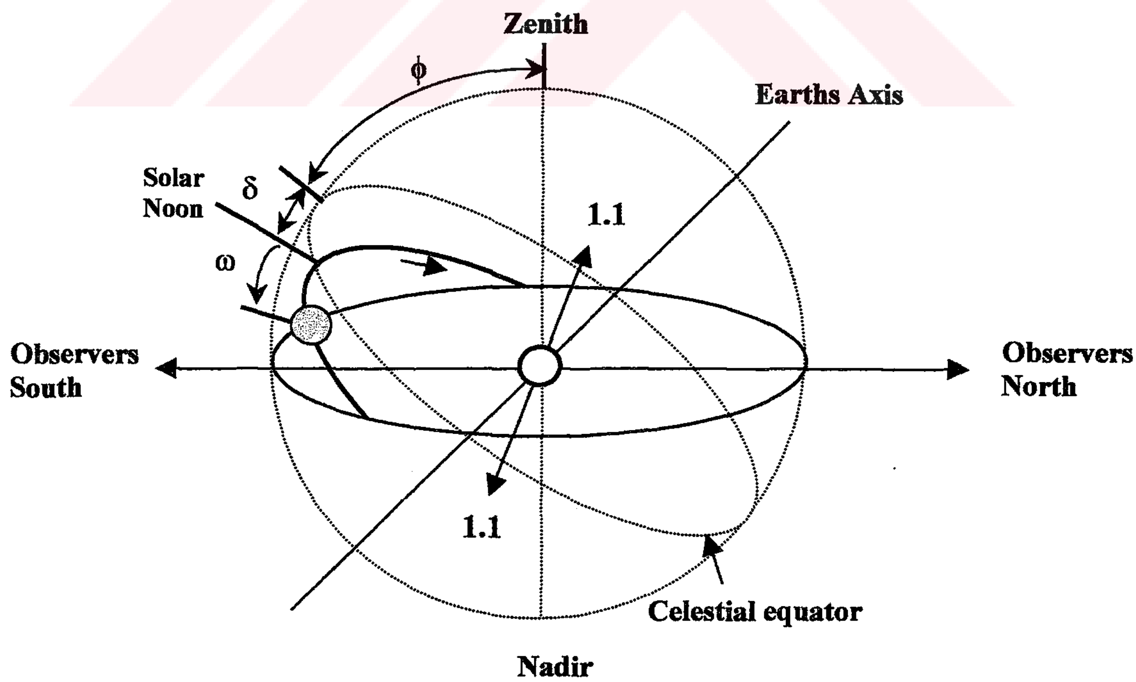

Figure 3.7 The local zenith - nadir coordinate system showing the apparent daily motion of the Sun.

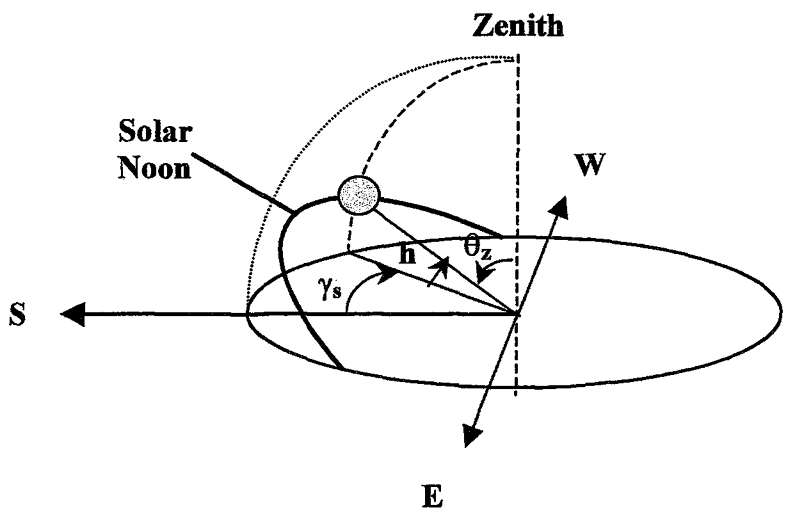

Figure 3.8 Definition of the azimuth, solar elevation and the zenith angle.

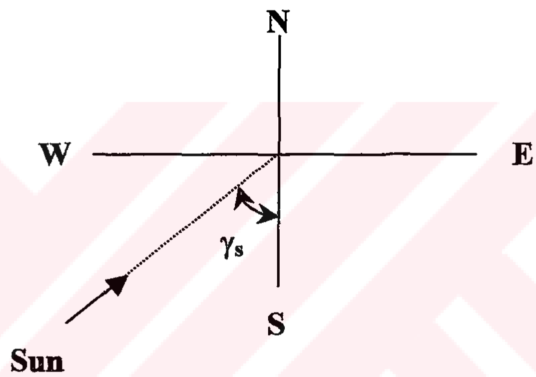

Figure 3.9 Solar azimuth angle.

As it is said before, angle of incidence, θ, is described with the relations between angles explained above [19,20]

$$\cos\theta = \sin\delta\sin\phi\sin\beta - \sin\delta\cos\phi\sin\beta\cos\gamma + \cos\delta\cos\phi\cos\beta\cos\omega \\ + \cos\delta\sin\beta\sin\gamma\sin\omega \qquad (3.9)$$

and

$$\cos\theta = \cos\theta_z\cos\beta + \sin\theta_z\sin\beta\cos(\gamma_s - \gamma) \qquad (3.10)$$

The cosine of solar azimuth angle is [19,20]

$$\cos\gamma_s = \frac{-\cos\phi\sin\delta + \sin\phi\cos\delta\cos\omega}{\sin\theta_z} \tag{3.11}$$

There are several commonly occurring cases for which Equation (3.9) is simplified. For fixed surfaces sloped toward the south or north that is with a surface azimuth angle γ of 0° or 180°, which is a very common situation, the last term drops out [19,20]

$$\cos\theta = \sin\delta\sin\phi\sin\beta - \sin\delta\cos\phi\sin\beta\cos\gamma + \cos\delta\cos\phi\cos\beta\cos\omega \tag{3.12}$$

For vertical surfaces, $\beta = 90°$ and the equation becomes [19, 20]

$$\cos\theta = -\sin\delta\cos\phi\sin\beta\cos\gamma + \cos\delta\cos\phi\cos\beta\cos\omega + \cos\delta\sin\beta\sin\gamma\sin\omega \tag{3.13}$$

For horizontal surfaces, the angle of incidence is the zenith angle of the Sun, θ_z. Its value must be between 0°and 90° when the Sun is above the horizon. For this situation, $\beta = 0°$ and Equation (3.9) for sunset and sunrise becomes [20]

$$\cos\theta_z = \sin\phi\sin\delta + \cos\phi\cos\delta\cos\omega \tag{3.14}$$

In Equation (3.14), hour angle ω can be taken as ω_s to show that it is for sunset and sunrise. For sunrise its value is negative (-) and for sunset it is positive (+).

From Equation (3.14) ω_s is calculated to be [20]

$$\omega_s = \arccos(-\tan\phi\tan\delta) \tag{3.15}$$

To calculate the sunrise and sunset hour angles on an inclined surface, we know that at sunrise and sunset $\theta = 90°$ and Equation (3.9) becomes [20]

$$0 = A - B + C\cos\omega + D\cos\omega + E\sin\omega \tag{3.16}$$

where

$$A = \sin\delta\sin\phi\cos\beta$$
$$B = \sin\delta\cos\phi\sin\beta\cos\gamma$$
$$C = \cos\delta\cos\phi\cos\beta$$
$$D = \cos\delta\sin\phi\sin\beta\cos\gamma$$
$$E = \cos\delta\sin\beta\sin\gamma$$

For an inclined surface the hour angle is ω_β and sunrise and sunset hour angles are respectively $\omega_{\beta,r}$ and $\omega_{\beta,s}$. By using the necessary trigonometric relationships ω_β from Equation (3.16) is [20]

$$\omega_\beta = \arccos\left(\frac{-N \mp \sqrt{N^2 - 4MP}}{2M}\right) \tag{3.17}$$

Here,

A-B = K; C+D = L; $L^2 + E^2 = M$; 2KL = N; $K^2 - E^2 = P$

Equation (3.17) has 2 roots, which are [20]

$$\omega_{\beta,1} = \arccos\left(\frac{-N - \sqrt{N^2 - 4MP}}{2M}\right) \tag{3.18}$$

$$\omega_{\beta,2} = \arccos\left(\frac{-N + \sqrt{N^2 - 4MP}}{2M}\right) \tag{3.19}$$

The values obtained from Equations (3.18) and (3.19) are compared with the $-\omega_s$ and $+\omega_s$ values calculated from the Equation (3.16)to determine $\omega_{\beta,r}$ and $\omega_{\beta,s}$.

Figure 3.10 is the schematic representation of the explained hour angles.

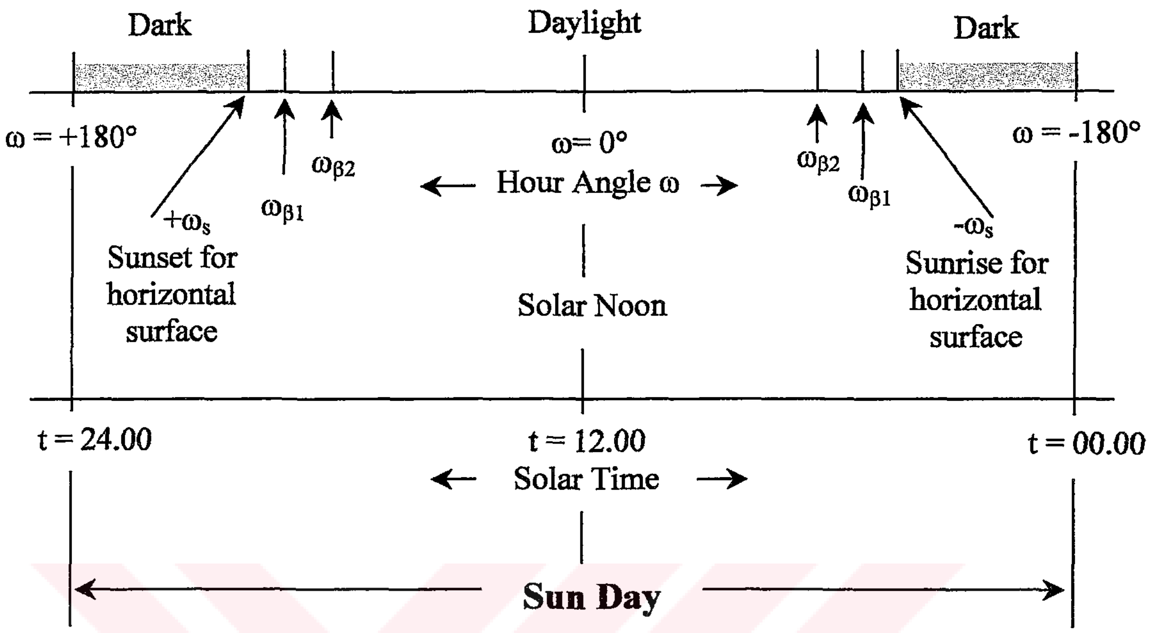

Figure 3.10 Sunrise and sunset hour angles for horizontal and inclined surfaces.

Surface azimuth angle of the inclined surface, γ, is important to determine the values of $\omega_{\beta,r}$ and $\omega_{\beta,s}$ [20].

1. Region, for $\gamma = 0°$:

The roots of Equation (3.17) are equal and

$$\omega_{\beta 1} = \omega_{\beta 2} = \arccos(\frac{-N}{2M}) \tag{3.20}$$

For sunrise and sunset

$$\omega_{\beta,r} = \text{Max}\,(-\omega_{\beta}, -\omega_s) \tag{3.21}$$

$$\omega_{\beta,s} = \text{Min}\,(\omega_{\beta}, \omega_s) \tag{3.22}$$

2. Region, for - 180° < γ < 0°:

At first the sunrise and sunset hour angles for the inclined surface, $\omega_{\beta 1}$ and $\omega_{\beta 2}$, must be compared with each other and after with $-\omega_s$ and $+\omega_s$.

For sunrise and sunset

$$\omega_{\beta, r} = \text{Max}\,(\,-\text{Max}\,(\omega_{\beta 1}, \omega_{\beta 2}), -\omega_s) \tag{3.23}$$

$$\omega_{\beta, s} = \text{Min}\,(\,\text{Min}\,(\omega_{\beta 1}, \omega_{\beta 2}), \omega_s) \tag{3.24}$$

3. Region, for 0° < γ < +180°:

The procedure looks like the one in the 2. Region

For sunrise and sunset

$$\omega_{\beta, r} = \text{Max}\,(\,-\text{Min}\,(\omega_{\beta 1}, \omega_{\beta 2}), -\omega_s) \tag{3.25}$$

$$\omega_{\beta, s} = \text{Min}\,(\,\text{Max}\,(\omega_{\beta 1}, \omega_{\beta 2}), \omega_s) \tag{3.26}$$

4. Region, for γ = ± 180°

Like 1. Region, sunrise and sunset hour angles are symmetrical and equal.

$\omega_{\beta 1} = \omega_{\beta 2}$

For sunrise and sunset

$$\omega_{\beta, r} = \text{Max}\,(-\omega_\beta, -\omega_s) \tag{3.27}$$

$$\omega_{\beta, s} = \text{Min}\,(\omega_\beta, \omega_s) \tag{3.28}$$

3.1.5 Extraterrestrial Solar Radiation on Inclined Surfaces

Instantaneous, hourly and daily extraterrestrial solar radiations on inclined surface are going to be calculated respectively. Instantaneous, hourly and daily extraterrestrial solar radiations on horizontal surface are going to be calculated for the special situation of $\beta = 0°$.

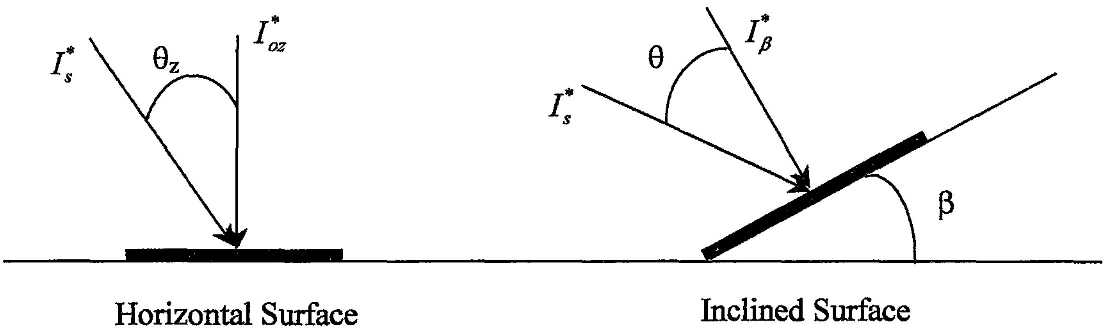

Figure 3.11 Extraterrestrial solar radiation calculations for horizontal and inclined surfaces.

As can be seen from the Figure 3.11, ***instantaneous extraterrestrial solar radiation*** on an inclined surface with an inclination angle β is [19, 20]

$$I_{o\beta}^* = I_s^* \cos\theta \qquad (3.29)$$

and for a horizontal surface is

$$I_{oz}^* = I_s^* \cos\theta_z \qquad (3.30)$$

I_s^* is the extraterrestrial solar radiation on the surface, for unit time and unit area (W/m^2) and it is taken as I_{on}^*, which can be calculated with the help of Equation (3.4).

Hourly extraterrestrial solar radiation on an inclined surface with an inclination angle β is [19, 20]

$$\int_{t_1}^{t_2} I_\beta^* dt = I_{oh\beta} \qquad (3.31)$$

Hourly extraterrestrial solar radiation on a horizontal surface is [19, 20]

$$\int_{t_1}^{t_2} I_z^* dt = I_{ohz} \qquad (3.32)$$

Here,

$$t = \frac{24 \cdot 3600}{2\pi}\omega + 12 \cdot 3600 \ \text{[s]}$$

$$dt = \frac{24 \cdot 3600}{2\pi} d\omega$$

For t_2 - t_1 = 1 hour and ω_2 - ω_1 = 15 using Equations (3.29) and (3.31) for inclined surface and Equations (3.30) and (3.32) for horizontal surface we obtain respectively [19, 20]

$$\int_{t_1}^{t_2} I_{on}^* \cos\theta dt = I_{oh\beta} = \frac{24 \cdot 3600}{2\pi} \int_{\omega_1}^{\omega_2} I_{on}^* \cos\theta d\omega \tag{3.33}$$

$$\int_{t_1}^{t_2} I_{on}^* \cos\theta_z dt = I_{ohz} = \frac{24 \cdot 3600}{2\pi} \int_{\omega_1}^{\omega_2} I_{on}^* \cos\theta_z d\omega \tag{3.34}$$

If $\cos\theta$ and $\cos\theta_z$ are put into their places in the Equations (3.33) and (3.34) the equations mostly used to determine hourly extraterrestrial solar radiation values for inclined and horizontal surfaces are obtained by taking the necessary integrals [19, 20].

$$\begin{aligned} I_{oh\beta} = {} & \frac{24 \cdot 3600}{2\pi} \cdot I_o^*(1 + 0.033 \cdot \cos\frac{360n}{365}) \cdot [\sin\delta \sin\phi \cos\beta \\ & \frac{2\pi}{360}(\omega_2 - \omega_1) - \sin\delta \cos\phi \sin\beta \cos\gamma \frac{2\pi}{360}(\omega_2 - \omega_1) \\ & + \cos\delta \cos\phi \cos\beta(\sin\omega_2 - \sin\omega_1) + \cos\delta \sin\phi \sin\beta \\ & \cos\gamma(\sin\omega_2 - \sin\omega_1) - \cos\delta \sin\beta \sin\gamma(\cos\omega_2 - \cos\omega_1)](J/m^2) \end{aligned} \tag{3.35}$$

$$\begin{aligned} I_{ohz} = {} & \frac{24 \cdot 3600}{2\pi} \cdot I_o^*(1 + 0.033 \cdot \cos\frac{360n}{365}) \cdot [\sin\delta \sin\phi \cos\phi \\ & \frac{2\pi}{360}(\omega_2 - \omega_1) + \cos\delta \cos\phi(\sin\omega_2 - \sin\omega_1)](J/m^2) \end{aligned} \tag{3.36}$$

If ***daily extraterrestrial solar radiation*** for inclined and horizontal surfaces is needed, the same procedure holds but instead of ω_1 and ω_2, sunrise and sunset hour angles $\omega_{\beta,r}$, $\omega_{\beta,s}$ (for inclined surfaces) and hour angle ω_s (for horizontal surfaces) are used [19, 20].

$$
\begin{aligned}
I_{on\beta} = & \frac{24 \cdot 3600}{2\pi} \cdot I_o^*(1+0.033 \cdot \cos\frac{360n}{365}) \cdot [\sin\delta \sin\phi \cos\beta \\
& \frac{2\pi}{360}(\omega_{\beta,s} - \omega_{\beta,r}) - \sin\delta \cos\phi \sin\beta \cos\gamma \frac{2\pi}{360}(\omega_{\beta,s} - \omega_{\beta,r}) \\
& + \cos\delta \cos\phi \cos\beta(\sin\omega_{\beta,s} - \sin\omega_{\beta,r}) + \cos\delta \sin\phi \sin\beta \\
& \cos\gamma(\sin\omega_{\beta,s} - \sin\omega_{\beta,r}) - \cos\delta \sin\beta \sin\gamma(\cos\omega_{\beta,s} - \cos\omega_{\beta,r})](J/m^2)
\end{aligned}
\tag{3.37}
$$

$$
\begin{aligned}
I_{onz} = & \frac{24 \cdot 3600}{2\pi} \cdot I_o^*(1+0.033 \cdot \cos\frac{360n}{365}) \cdot [\sin\delta \sin\phi \cos\phi \\
& \frac{2\pi}{360}(\omega_{\beta,s} - \omega_{\beta,r}) + \cos\delta \cos\phi(\sin\omega_{\beta,s} - \sin\omega_{\beta,r})](J/m^2)
\end{aligned}
\tag{3.38}
$$

3.1.5.1 Ratio of Direct Radiation on Tilted Surface to that on Horizontal Surface

For purposes of solar process design and performance calculations, it is often necessary to calculate the hourly radiation on a tilted surface of a collector from measurements or estimates of solar radiation on a horizontal surface. The most commonly available data are total radiation for hours or days on the horizontal surface, whereas the need is for direct and diffuse radiation on the plane of the collector.

The geometric factor R_b, the ratio of direct radiation on the tilted surface to that on a horizontal surface at any time, can be calculated exactly by appropriate use of Equation (3.9). Figure 3.11 indicates the angle of incidence of direct radiation on the horizontal and tilted surfaces. The ratio $\frac{I_{o\beta}^*}{I_{oz}^*}$ is given by [19, 20]

$$R_b = \frac{I_{o\beta}^*}{I_{oz}^*} = \frac{I_s^* \cos\theta}{I_s^* \cos\theta_z} = \frac{\cos\theta}{\cos\theta_z} \tag{3.39}$$

Solar process performance calculations are very often done on an hourly basis. Hottel and Woertz (1942) calculated R_b values for the most common cases. They also showed a graphical method and this graphical method has been revised by Whiller (1975) [19].

3.1.6 Effect of Atmosphere on Solar Radiation

In extraterrestrial solar radiation calculations, we assume that atmosphere on Earth does not effect the radiation but this is not a realistic approach. Calculating the amount of the energy, which reaches the Earth, is not an easy procedure. The amount is related to the atmospheric conditions that have a statistical character. The energy balance of the Earth is given in Figure 3.12.

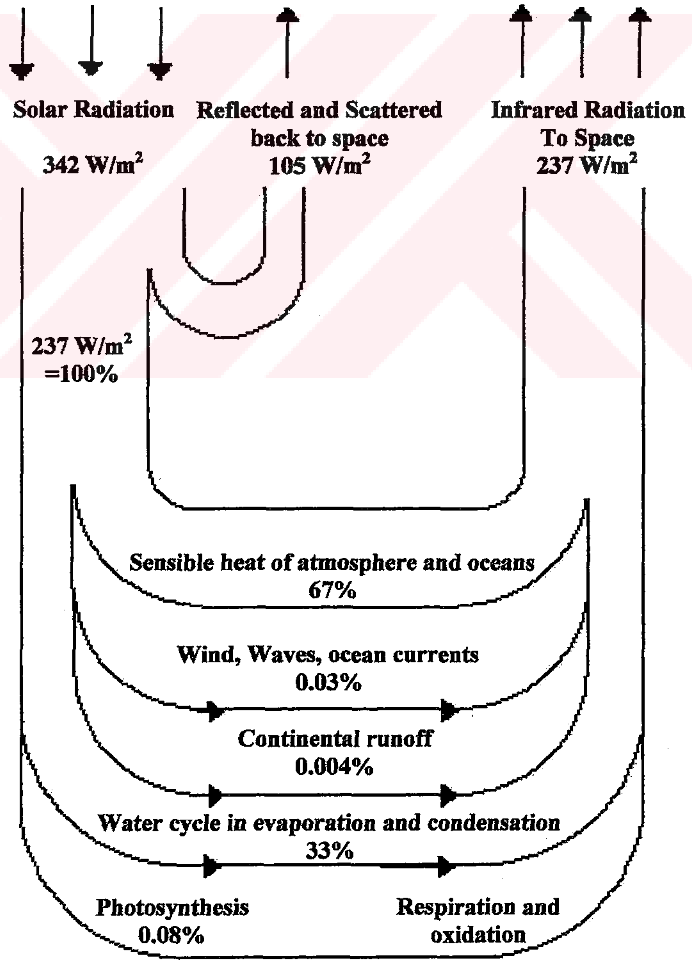

Figure 3.12 Energy balance of the Earth. The average incident solar radiation is equal to a quarter of the solar constant [18].

The effects of the atmosphere in scattering and absorbing radiation are variable with time as atmospheric conditions and air mass change. It is useful to define a standard "clear" sky and calculate the hourly and daily radiation, which would be received on an inclined and a horizontal surface under these standard conditions [19].

Hottel (1976) has presented a method for estimating the direct radiation transmitted through clear atmospheres which takes into account zenith angle and altitude for a standard atmosphere and for four climate types. The atmospheric transmittance for direct radiation, τ_1, is given in the form [20].

$$\tau_1 = a_0 + a_1 \exp\left(\frac{-k}{\cos\theta_z}\right) \tag{3.40}$$

The constants a_0, a_1 and k for the standard atmosphere with 23 km visibility are found from a_0^*, a_1^* and k^* that are given for altitudes less than 2.5 km by [20]

$$a_0^* = 0.4237 - 0.00821(6 - A)^2 \tag{3.41}$$

$$a_1^* = 0.5055 - 0.00595(6.5 - A)^2 \tag{3.42}$$

$$k^* = 0.2711 + 0.01858(2.5 - A)^2 \tag{3.43}$$

In these equations A is the altitude for the observer in kilometers. Correction factors are applied to a_0^*, a_1^* and k^* to allow for changes in climate types. The correction factors [20]

$$r_0 = a_0 / a_0^* \qquad r_1 = a_1 / a_1^* \qquad r_k = k / k^* \tag{3.44}$$

are given in Table 3.2. Thus the transmittance of the atmosphere for direct radiation can be determined for any zenith angle and any altitude up to 2.5 km. The clear sky direct radiation for an altitude A is then [20]

$$I_{c\tau}^* = I_{on}^* \cdot \tau_\tau \tag{3.45}$$

Table 3.2 Correction Factors for Climate Types [19, 20].

Climate Type	r_0	r_1	r_k
Tropical	0.95	0.98	1.02
Midlatitude Summer	0.97	0.99	1.02
Subarctic Summer	0.99	0.99	1.01
Midlatitude Winter	1.03	1.01	1.00

In Equation (3.45) I^*_{on} is found from Equation (3.4). For a clear sky and at any altitude A, direct radiation on an inclined surface becomes [20]

$$I^*_{cl\beta} = I^*_{on} \cdot \tau_l \cdot \cos\theta \tag{3.46}$$

For the same conditions direct radiation on a horizontal surface is [20]

$$I^*_{cl} = I^*_{on} \cdot \tau_l \cdot \cos\theta_z \tag{3.47}$$

It is also possible to estimate the diffuse radiation for clear sky and for an altitude A. according to Liu and Jordan for a clear sky, the correlation between the direct radiation transmittance, τ_l, and the diffuse radiation transmittance, τ_d, is [20]

$$\tau_d = 0.2710 - 0.2939 \cdot \tau_l \tag{3.48}$$

Using Equation (3.48) we obtain the necessary equation to calculate the diffuse radiation on an inclined surface for clear sky [20]

$$I^*_{cd\beta} = I^*_{on} \cdot \tau_d \cdot \cos\theta \tag{3.49}$$

and on a horizontal surface for clear sky [20]

$$I_{cdz}^{*} = I_{on}^{*} \cdot \tau_d \cdot \cos\theta_z \tag{3.50}$$

Thus the total solar radiation for an inclined surface from the Equations (3.46) and (3.49) is [20]

$$I_{ct\beta}^{*} = I_{ci\beta}^{*} + I_{cd\beta}^{*} \tag{3.51}$$

The total solar radiation on a horizontal surface from the Equations (3.47) and (3.50) is [20]

$$I_{ctz}^{*} = I_{cu}^{*} + I_{cdz}^{*} \tag{3.52}$$

3.1.6.1 Direct an Diffuse Components of Hourly Radiation

Data measured by pyranometers give instantaneous total solar radiation values. In photovoltaic applications this total solar radiation data is used to estimate the direct that is also called beam radiation and the diffuse radiation. The direct component of the total solar radiation is used to generate electricity by the photovoltaic device. There are some useful correlations that are used to estimate the direct solar radiation data from the measured total radiation data.

$$\frac{I_{dhz}}{I_{thz}} = 1.00 - 0.1 \times \left(\frac{I_{thz}}{I_{ctz}}\right) \tag{3.53}$$

Equation (3.53) holds for $0 \le \frac{I_{thz}}{I_{ctz}} < 0.48$.

$$\frac{I_{dhz}}{I_{thz}} = 1.11 + 0.039 \times \left(\frac{I_{thz}}{I_{ctz}}\right) - 0.789 \times \left(\frac{I_{thz}}{I_{ctz}}\right) \tag{3.54}$$

Equation (3.54) holds for $0.48 \le \frac{I_{thz}}{I_{ctz}} < 1.11$.

$$\frac{I_{dhz}}{I_{thz}} = 0.2 \tag{3.55}$$

Equation (3.55) holds for $\frac{I_{thz}}{I_{ctz}} \geq 1.11$.

Direct solar radiation is now calculated by using Equations (3.53), (3.54), (3.55) as

$$I_{ihz} = I_{thz} + I_{dhz} \tag{3.56}$$

where I_{ihz} stands for hourly direct solar radiation on horizontal surfaces.

3.2 Photovoltaic Systems

PV systems constitute an environmentally friendly alternative way for energy production using the energy from the Sun. They operate quietly without emissions, can be installed quickly, and are modular, which has the advantage that more units can be added if the load increases. Their long lifetimes and little maintenance requirements make them an ideal solution for remote applications when used as autonomous (stand alone) systems. This is currently the most common use of PV systems. More recently, PV systems are being used to supplement the conventional power generation in industrialized countries. Their advantage is that they can be located close to the sites where the electricity is to be consumed. Being located near the end-user, they can reduce transmission and distribution costs and, under some circumstances, can provide with peak load high quality power and increase reliability of electrical services delivered [18, 19].

In general a PV system includes a PV generator, an auxiliary generator which can be a diesel or petroleum generator set to provide back-up when there is not enough sun, an accumulator (usually a lead-acid battery) to store the energy, and a load which can work with direct current (DC) (for example, lighting, telecommunication equipment) and/or alternative current (AC) (most appliances in the conventional market). The system also usually includes some form of a power conditioning - power electronic equipment that provides an interface between the components giving protection and control [21]. Except for the PV generator, all components belong to what we might call conventional technology.

In this section, the PV system components, basic PV system configurations, and common PV applications will be mentioned briefly.

3.2.1 Photovoltaic System Components

Photovoltaic systems that produce electricity are made up of interconnected components that individually serve a specific function. Modularity has become one of the major advantages of solar electrical systems. As our needs grow, individual components can be replaced or added to provide increased capacity. The basic components of a photovoltaic system are

- Photovoltaic Generator
- Inverter
- Batteries
- Loads
- Wiring

Each component of a system is explained briefly.

3.2.1.1 Photovoltaic Generator

3.2.1.1.1 Photovoltaic Cell

Photovoltaic: adj. providing a source of electric current under the influence of light or similar radiation.

With such a broad definition, a large range of physical effects qualifies for description as photovoltaic. Bequerel is usually credited as being the first to demonstrate the photovoltaic effect in 1839 by illuminating Pt electrodes coated with AgCl or AgBr inserted into acidic solution, as in Figure 3.13 [23].

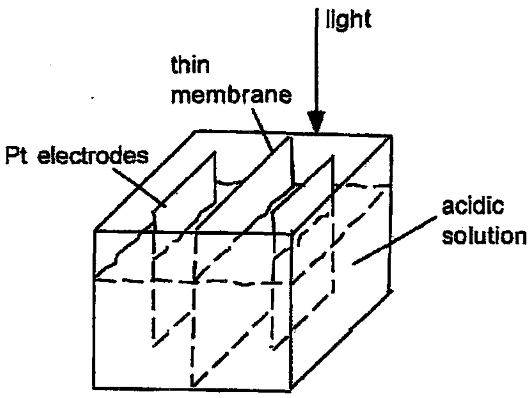

Figure 3.13 Diagram of apparatus described by Bequerel [23].

The next significant development arose when Adams and Day in 1876 were investigating the photoconductive effect in Se. They noted anomalies when Pt contacts were pushed into a Se bar. This led them to demonstrate that it was possible to start a current in selenium merely by the action of light.

This pioneered to the first thin film Se solar cells being fabricated by Fritts in 1883. Up until the 1940s, the most efficient photovoltaic devices used Se, Cu_2O or Tl_2S as the absorbing layer with a rectifying metal contact as in Figure 3.14, a structure very similar to that earlier demonstrated by Fritts [23].

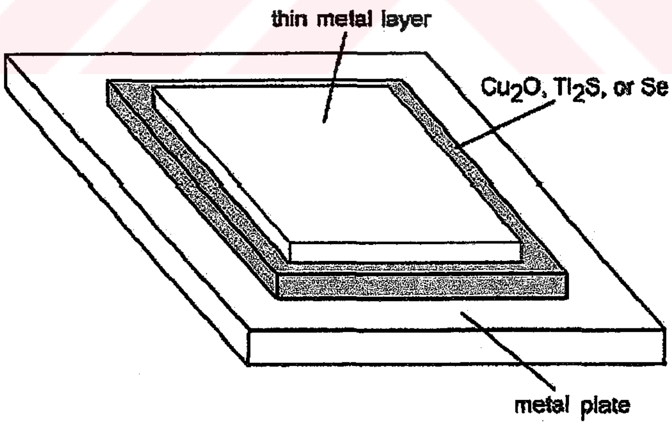

Figure 3.14 Structure of the most efficient photovoltaic devices developed during the 1930s [23].

Figure 3.15 is a schematic of a solar cell under illumination. Light entering the cell through the gaps between the top contact metal gives up its energy by temporarily releasing electrons from the covalent bonds holding the semiconductor together; at least this is what happens for those photons with sufficient energy. The p-n junction within the cell ensures that the now mobile charge carriers of the same polarity all move off in the same direction. If an electrical load, such as the lamp shown in Figure 3.15, is connected between the top and rear contacts to the cell, electrons will complete the circuit through this load, constituting an electrical current in it. Energy in the incoming sunlight is thereby converted into electrical energy consumed by this load.

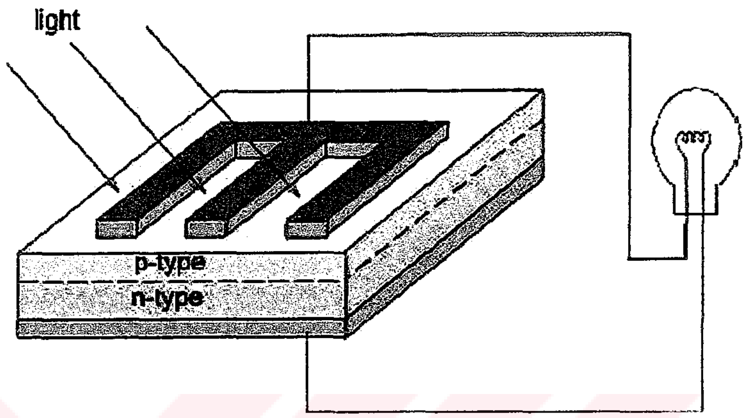

Figure 3.15 Simple p-n junction [24].

The first semiconductor p–n junction solar cells were described in 1941 by Russel Ohl of Bell Laboratories. These junctions formed naturally in slowly solidified melts of silicon. Exploration of their properties led to the understanding of the role of p- and n-type dopants in controlling semiconductor properties and hence to the microelectronics revolution. Most photovoltaic solar cells produced to date have been based on silicon p–n junctions, although now relying on junctions formed more controllably by diffusing one polarity dopant into a wafer substrate of opposite polarity. By the late 1970s, design had evolved to that of Figure 3.16. One new feature, introduced in 1974, was the use of crystallographic texturing on the top surface, to reduce reflection loss. Other features of the fabrication technology largely have been adapted from the standard or hybrid microelectronics areas [23].

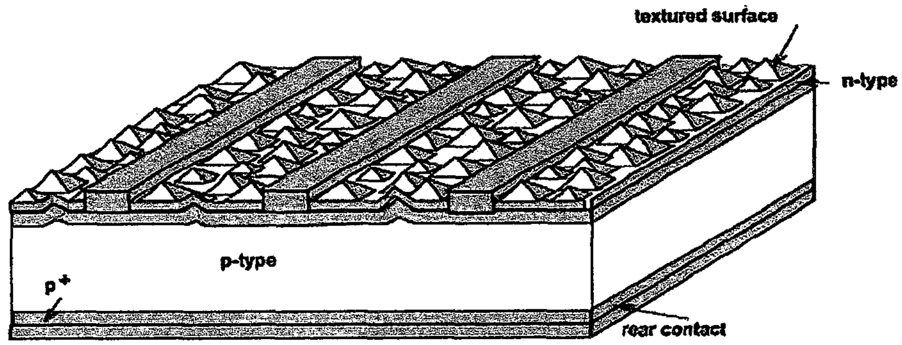

Figure 3.16 Standard silicon Photovoltaic cell structure developed in the 1970s [23].

3.2.1.1.2 Developments in PV Technologies

The photovoltaic market is increasing with over 30% per annum compounded growth over the last years. The government-subsidised urban-residential use of photovoltaics, particularly in Germany and Japan, is driving this sustained growth. Most of the solar cells being supplied to this market are **"First Generation"** devices based on crystalline or multicrystalline silicon wafers. **"Second Generation"** thin-film solar cells based on amorphous silicon/hydrogen alloys or polycrystalline compound semiconductors are starting to appear on the market in increasing volume [24].

3.2.1.1.2.1 First Generation Solar Cells

The technology based on the elemental semiconductor silicon, either single crystalline or multicrystalline, is the best-established photovoltaic technology at the present time. It has many points in common with the microelectronics industry, and benefits of those close links have helped to improve the performance of laboratory solar cells to nearly 25%, which is a level not far from the theoretical maximum [18]

A semiconductor only converts photons with the energy of the band-gap with good efficiency. Photons with lower energy are not absorbed and those with higher energy are reduced to gap energy by thermalization. Therefore, the curve of efficiency versus band-gap goes through a maximum, Figure 3.17. It can be seen that silicon is not at the maximum but relatively close to it. A much more serious point is that silicon is an indirect semiconductor, meaning that valence band maximum and conduction band minimum are not opposite to each other in *k*-space. Light absorption is much weaker in an indirect semiconductor than in a direct semiconductor. This has serious consequences from a materials point of view: for a 90% light absorption it takes only 1 μm for GaAs (a direct semiconductor) versus 100 μm for Si. The photo-generated carriers have to reach the p-n junction, which is near the front surface. The diffusion length of minority carriers has to be 200 μm or at least twice the silicon thickness. Thus the material has to be of very high purity and of high crystalline perfection. In view of these physical limitations it is quite surprising that silicon has played such a dominant role in the market. The main reason is that silicon technology has already been highly developed before the advent of photovoltaics and high quality material is being produced in large quantities for the semiconductor market [26].

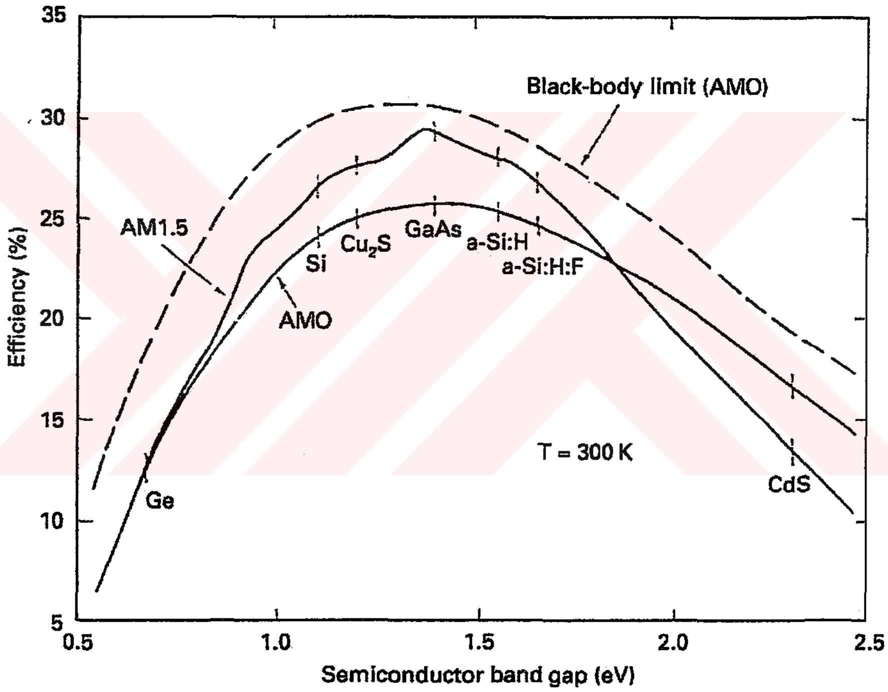

Figure 3.17 Conversion efficiency of solar cell materials versus band gap for single junction cells [26].

To make photovoltaic modules, four major stages are to be followed (the first one is not performed by the photovoltaic industry) [18],

- From sand to pure silicon
- From silicon feedstock to silicon crystals and wafers
- From silicon wafers to solar cells
- From cells to modules

The supply of silicon is practically endless. Although pure silicon does not occur in nature, 60% of the Earth's crust is sand, for the major part, quartzite or silicon dioxide (SiO_2). Silicon is produced in large amounts, more than 600,000 tones a year world wide, to make special steel and alloys. This Metallurgical-grade silicon (Mg-Si) is obtained by reducing quartzite with coke (coal) in electric-arc furnaces. Its purity is only 98-99%, which is insufficient for electronic applications but both the energy input and cost are relatively low. The semiconductor industry purifies this metallurgical-grade silicon until the impurity concentrations is less than 0.1 parts per million atomic (99.99999%) [18].

During the production of pure silicon no special attention is paid to its crystallographic structure, and specific crystallization techniques are usually required to obtain a material with appropriate semiconductor properties. The most common techniques produce silicon crystals or "ingots" with either a cylindrical or a square shape that need to be subsequently sliced into wafers, . There are techniques capable of directly producing thin sheets of crystalline silicon. Common techniques for the production of crystalline silicon include Czochralski (CZ) method and Float-zone (FZ) method, and other methods such as casting and die or wire pulling.

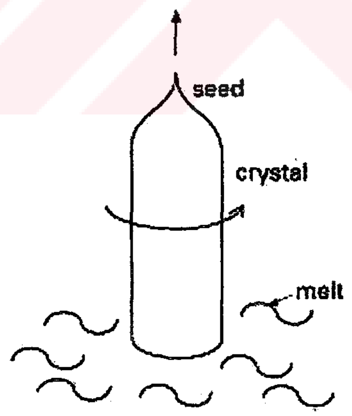

Figure 3.18 Growth of a cylindrical silicon crystal [24].

To transform a silicon wafer into a solar cell, the wafer is subjected to several chemical, thermal and deposition treatments. The cross section of a silicon cell shows the different that need to be formed, and points out the most essential layers: an n-type layer to form the p-n junction and two metal layers to form the electrical contacts. In a typical industrial fabrication sequence there are a number of additional steps as follows:

- Surface changing and etching (may include texturing)
- Phosphorus diffusion for p-n junction formation
- Front and back metal contacts
- Antireflection layer deposition

After testing the cells under standard test conditions and sorting them in different classes to match their current and voltage, about 36 cells are typically interconnected in series and encapsulated to for a module. Different module sizes are manufactured for different applications. The largest are for grid connected power plants and measure 2 m^2. The encapsulating materials must satisfy a number of very strict requirements, since the modules should last 20 years or more [18].

Single crystal silicon wafer based solar cells

- **Screen-printed cells**

Most of the monocrystalline and multicrystalline cells fabricated recently used the screen-printed solar cell shown schematically in Figure 3.19. The associated processing sequence was developed during the early 1970s, along with several alternative solar cell processing by the early 1980s, this approach had displaced the alternatives to emerge as the commercial standard. One advantage was that, as well as being based on silicon wafers developed for microelectronics, it was able to use the same screen-printers, drying and firing furnaces for applying cell for thick-film, hybrid microelectronics. The main cell processing steps consist of illumination, wafer cleaning and chemical etching, usually anisotropically to form the micron-sized, crystallographically defined pyramids apparent on the wafer surface in Figure 3.19, followed by p–n junction formation, either in the same dopant diffusion furnaces as used in microelectronics or using simpler approaches based on the spraying or spinning of dopant sources, followed by diffusion in the same type of belt furnaces used for contact firing [27].

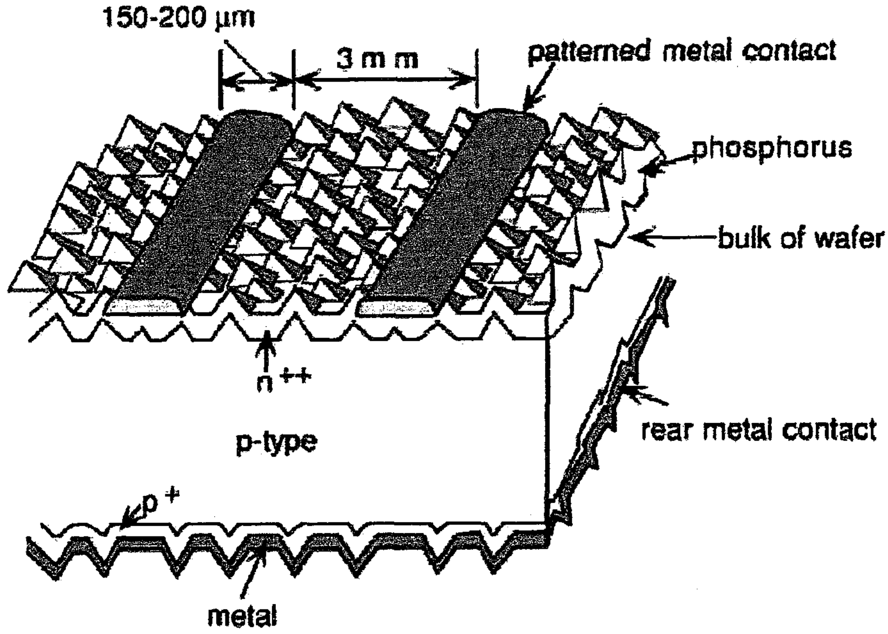

Figure 3.19 Screen-printed photovoltaic module [27].

- **Buried contact photovoltaics**

The buried-contact cell design of Figure 3.20 was developed in the early 1980s as a low-cost approach to incorporating some of the gains in laboratory to performance of this era into commercial sequences. The key feature of this approach is the use of a laser to form grooves into the top surface of the cell, through a previously lightly diffused layer and dielectric coating. These grooves expose fresh silicon that can be heavily doped during a second diffusion, confined by the dielectric to the grooved region. Similarly, the dielectric confines a subsequently electrolessly plated metal layer to this region [27].

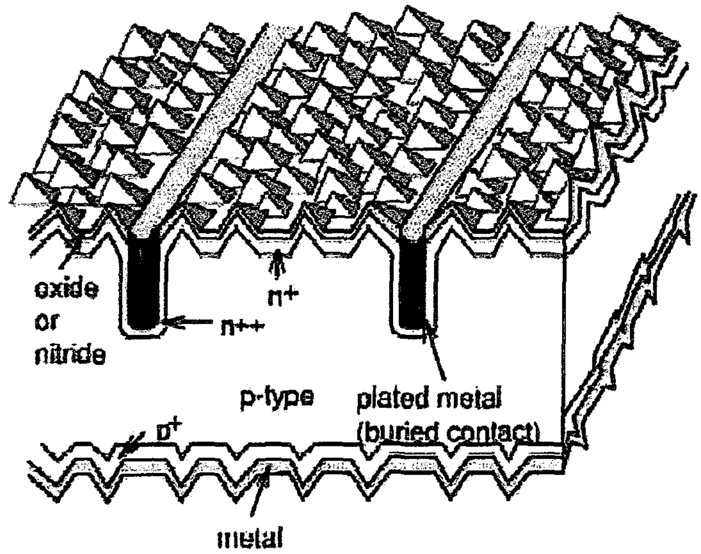

Figure 3.20 Buried contact photovoltaic cell [27].

- **HIT cell**

An alternative approach to a higher efficiency commercial solar cell is the HIT (heterojunction with thin intrinsic layers) cell of Figure 3.21. This cell combines both crystalline and amorphous silicon cell design features in the one structure [27].

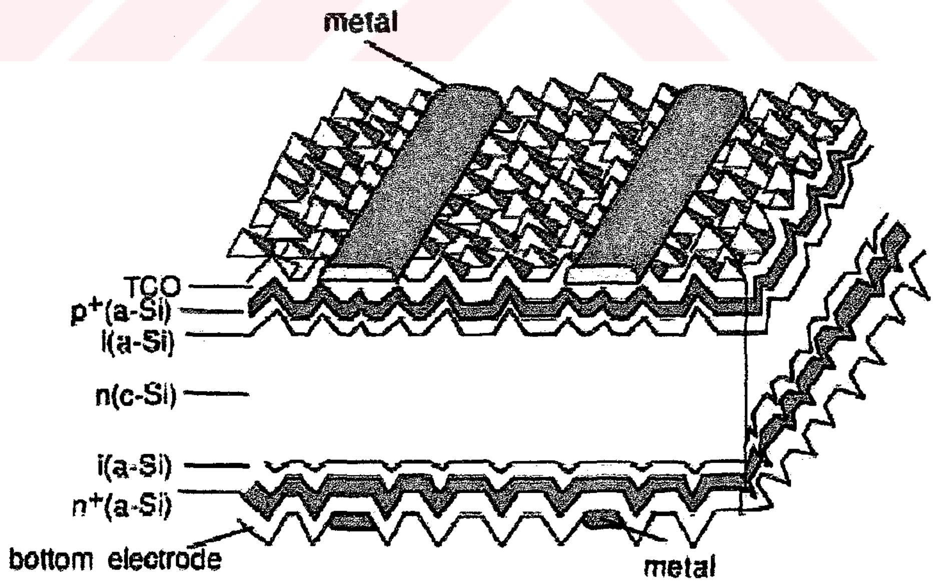

Figure 3.21 HIT cell [27].

Multicrystalline silicon wafer based solar cells

Most modules produced recently used multicrystalline silicon wafers rather than monocrystalline. These wafers are sliced from large-grained polycrystalline ingots produced more simply than the crystalline ingots which monocrystalline wafers are sliced. The starting ingot is formed simply by solidifying the molten silicon slowly in its container Figure 3.22(a) [24]. This ingot can be massive, weighing several hundreds of kilograms. It is sawn into pieces of a more manageable size Figure 3.22 (b) and then sliced into wafers. Grains are generally much larger than the wafer thickness (0.3 mm) and hence extend through the wafer as in Figure 3.23 [27]

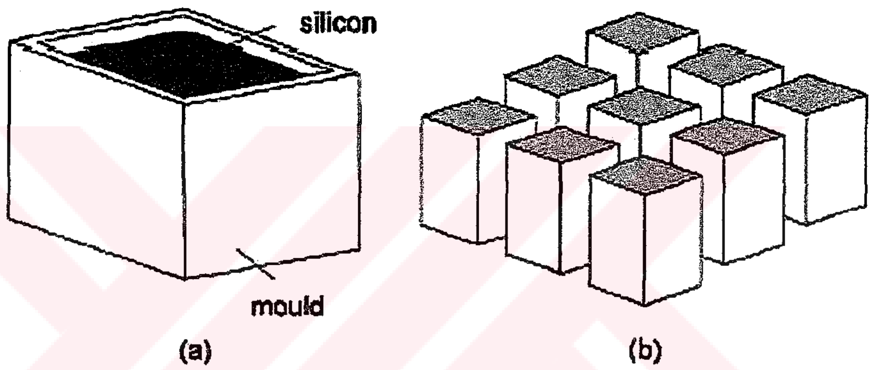

Figure 3.22 a) Directional solidification of a large block of multicrystalline silicon from a melt b) Sawing of large block into smaller ingots prior to slicing into multicrystalline wafers [24].

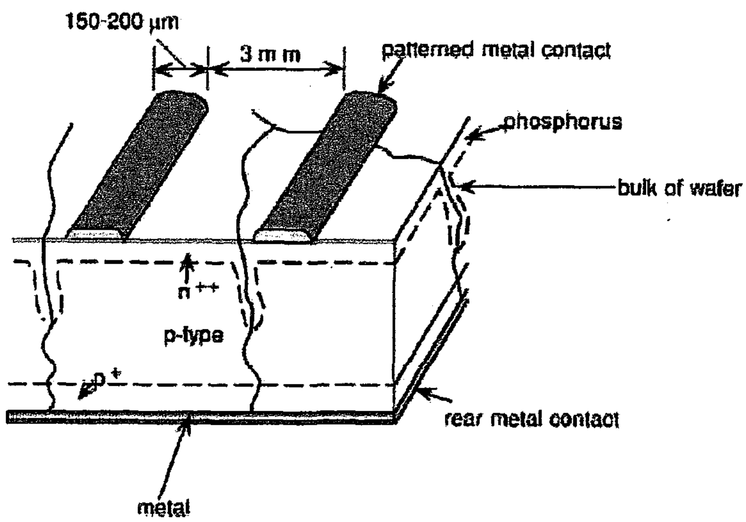

Figure 3.23 Screen-printed multicrystalline silicon cell [27].

3.2.1.1.2.2 Second Generation Solar Cells

In comparison with the crystalline silicon cells, second generation "thin film" technology holds the promise of reducing the module costs through lower material and energy requirements of the manufacturing process. In addition, integrally connected modules are produced directly without the costly individual cell handling and interconnections.

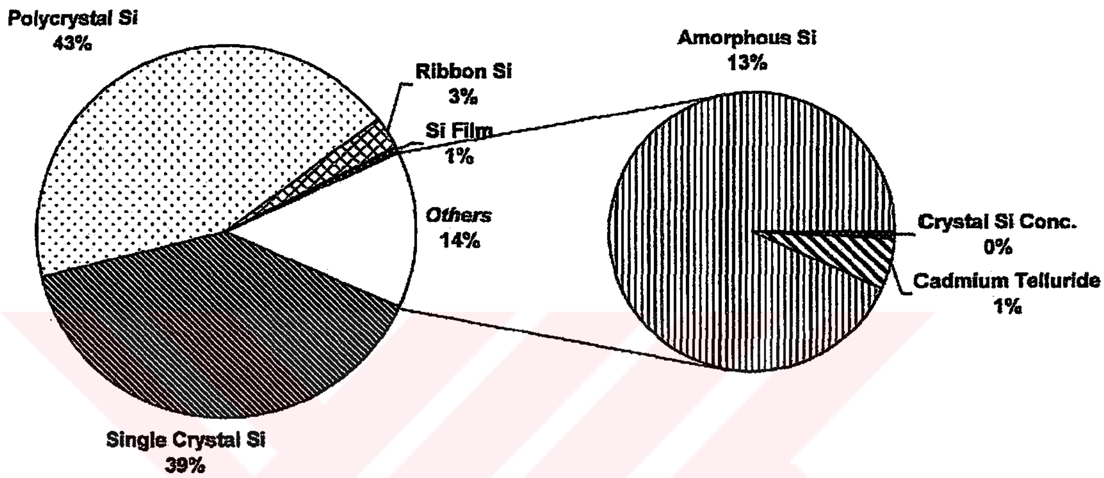

Figure 3.24 World market shares of different materials in 1998 [26].

Amorphous Silicon

Amorphous silicon (a-Si) differs from crystalline silicon in that the silicon atoms are not located at very precise distances from each other and the angles between the Si-Si bonds do not have a unique value. The interatomic distances and the bond angles have a range of values with any particular Si-Si distance or bond angle being randomly located within that range. This randomness in the atomic arrangement has a powerful impact on the electronic properties of the material [18].

The best-known thin film material is amorphous silicon (a-Si), which has been in production since many years. Like crystalline silicon, amorphous silicon can profit from other uses in the electronic industry in particular widespread use of thin film transistors in display applications. a-Si is actually a Si-hydrogen alloy containing 20-30% hydrogen. The films are deposited by decomposition of silane (SiH_4) in plasma. Deposition occurs at relatively low temperature but deposition rates are also low.

Amorphous cells show initially some degradation of efficiency because of the Staebler-Wronski effect (increase of recombination centers in the space charge region) but ways have been found to reduce this effect considerably. It has been found that thinner cells exhibit higher stability; so stacked cells have been designed that utilize this effect. Since the band gap of a-Si can be tailored with addition of carbon or germanium, such cells will also have higher efficiency due to the tandem effect [18].

There are two different types of *a*-Si multi-junction PV devices that are being scaled up to large areas. Solarex is commercializing a tandem structure that is shown schematically in Figure 3.25 while USSC and Canon are building facilities that will manufacture the triple-junction structure shown in Figure 3.26. There are several significant differences between the two approaches. The Solarex tandem structure is deposited on a glass substrate while the USSC/Canon triple-junction device is grown on a stainless steel substrate. Thus, the Solarex tandem PV modules are relatively rigid while the USSC/Canon triple-junction modules can be easily bent due to the flexibility of the stainless steel foil [28].

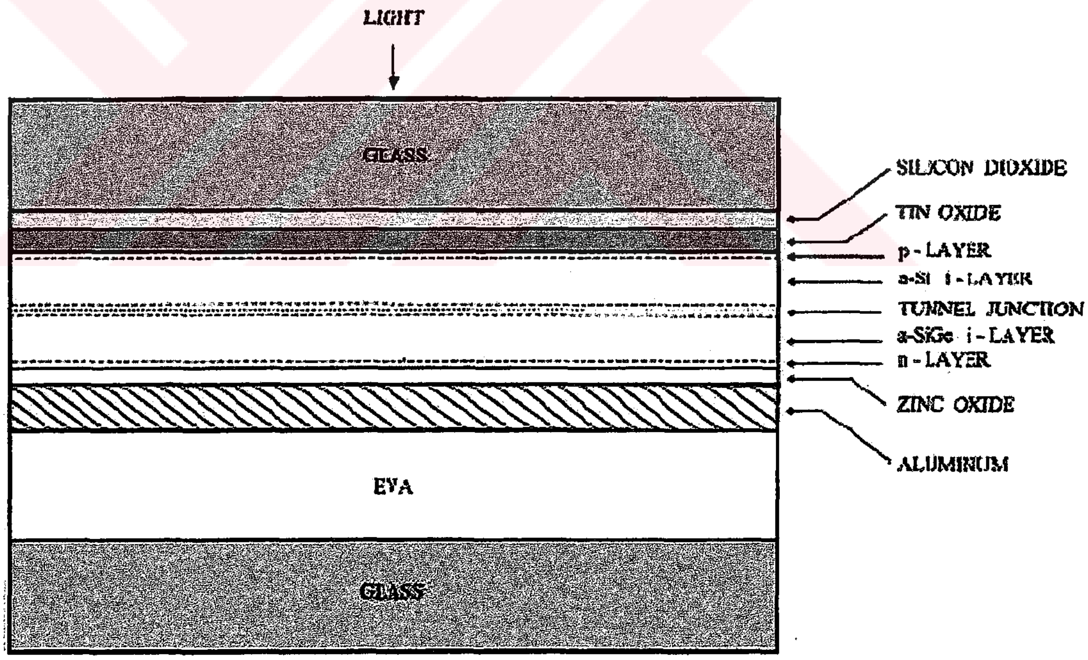

Figure 3.25 A schematic of the Solarex amorphous silicon tandem structure [28].

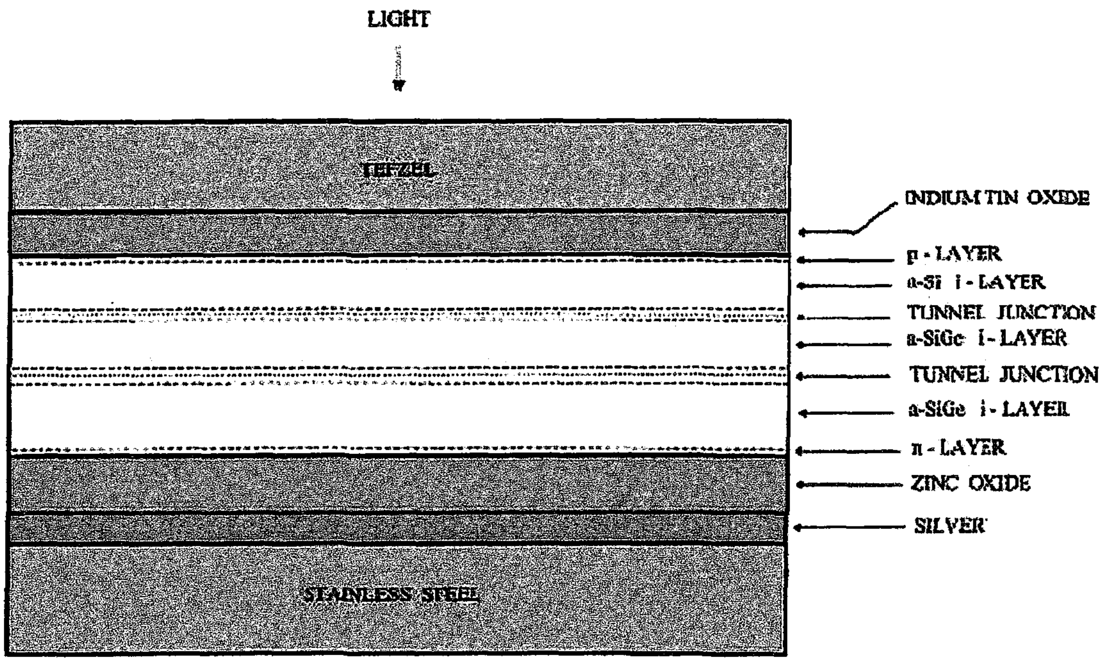

Figure 3.26 A schematic of the USSC/Canon amorphous silicon triple-junction structure [28].

Among the approaches followed in thin-film photovoltaics, solar cells based on amorphous hydrogenated silicon (a-Si:H) offer specific advantages: Amorphous silicon solar cells are fabricated from extremely abundant raw materials and involve almost no ecological risk during manufacturing, operation, and disposal. Low process temperatures facilitate the use of a variety of low-cost substrate materials such as float-glass, metal- or plastic-foils. The moderate energy demand for the whole module fabrication process leads to short energy payback times. The low material cost and proven manufacturability of a-Si:H solar modules make them ideally suited for low-cost terrestrial applications. Typically a-Si:H-based solar cells have a p-i-n or n-i-p diode structure depending on the deposition sequence of doped and intrinsic layers. For both structures the light is entering through the p-layer, which efficiently supports hole collection in the device. The reason for this is the smaller mobility of holes compared to electrons. A transparent conductive oxide (TCO) film contacts the a-Si:H diode from the front side and, in the most simplest case, a metal film serves both as rear contact and back reflector. The very thin (10–30 nm) p- and n-doped layers build up an electric field over the intrinsic (i) layer (typical thickness: 200–500 nm). Electrons and holes generated in doped layers do not (or only partly) contribute to the photo-current due to their short lifetime in highly doped a-Si:H. Therefore, wide-band-gap a-SiC:H and a-

SiO:H alloys for microcrystalline Si films are applied as p-doped window layers to reduce absorption losses. Electrons and holes generated in the i-layer are driven to the n- and p-layer, respectively, by the internal electric field. The material quality of the intrinsic layer and the strength and distribution of the electric field are responsible for the charge carrier collection and mainly determine the solar cell performance [28].

Depending on the deposition sequence of the doped and intrinsic a-Si:H layers (p-i-n or n-i-p) principally two cell structures exist Figure 3.27. In the p-i-n structure, also called superstrate configuration, the light is entering through the glass=TCO substrate. This structure is fully compatible with laser scribing techniques to form a monolytically integrated series connection of individual cells to an efficient thin-film module. The glass substrate already provides an effective encapsulation of the cell from the front side; the encapsulation materials "behind" the cell layers do not necessarily have to be transparent. In addition, the superstrate configuration offers a variety of cost-effective means for module protection [29].

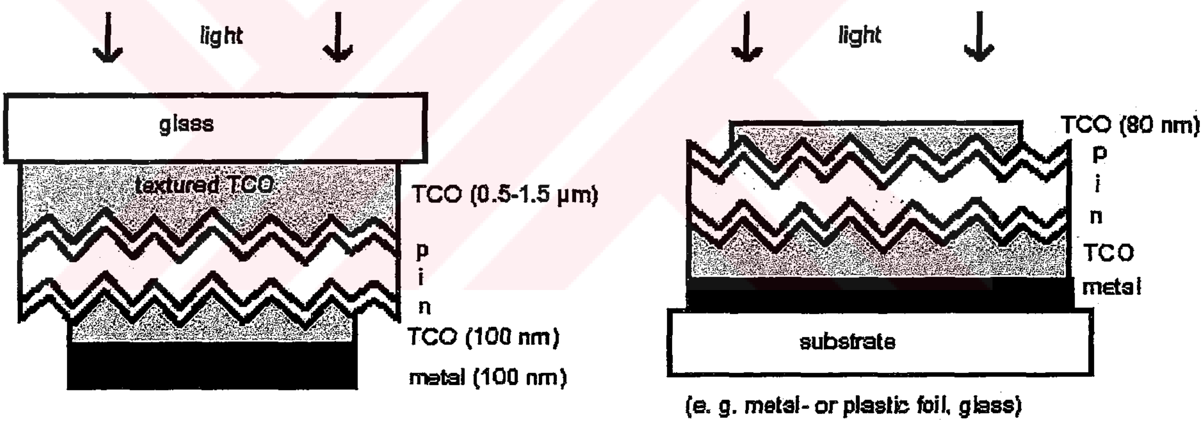

Figure 3.27 a) superstrate (p-i-n) structure b) substrate (n-i-p) structure [29].

The potential for on-going cost reductions is the key reason for confidence in a significant role for photovoltaics in the future. Rather than the wafer-based technology of the previous section, the future belongs to thin-film technology. In this approach, thin layers of semiconductor material are deposited onto a supporting substrate, or superstrate, such as a large sheet of glass. Typically, less than a micron thickness of semiconductor material is required, 100-1000 times less than the thickness of a silicon wafer. Reduced material use with associated reduced costs is a key advantage. Another is that the unit of production, instead of being a relatively small silicon wafer, becomes much larger, for example, as large as a conveniently handled sheet of glass might be. This reduces manufacturing costs. Silicon is one of the few semiconductors inexpensive enough to be used to make solar cells from self-supporting wafers. However, in thin-"lm form, due to the reduced material requirements, virtually any semiconductor can be used. At present, solar cells made from four different thin-film technologies are either available commercially, or close to being so. These are:

- Amorphous silicon alloy cells
- Thin film, polycrystalline compound semiconductors
- Thin film polycrystalline silicon cells
- Nanocrystalline dye cells

Amorphous silicon alloy cells

Given its success in wafer form, silicon is an obvious choice for development as a thin-film cell. Early attempts to make thin-film polycrystalline silicon cells did not meet with much success. However, starting from the mid-1970s, very rapid progress was made with silicon in amorphous form. In amorphous silicon, the atoms are connected to neighbors in much the same way as in the crystalline material but accumulation of small deviations from perfection means that the perfect ordering over large distances is no longer possible. Amorphous material has much lower electronic quality, as a consequence, and originally was not thought suitable for solar cells. However, producing amorphous silicon by decomposing the gas, silane (SiH_4), at low temperature, changed this opinion. It was found that hydrogen from the source was incorporated into the cell in large quantities (about 10% by volume), improving the material quality. Hydrogenated amorphous silicon cells very quickly found use in small consumer products such as solar calculators and digital watches, their main use so far [24].

Since the amorphous silicon quality is much poorer than crystalline silicon, a different cell design approach is required. The most active part of a p-n junction solar cell is right at the junction between the p- and n-type region of the cell. This is due to the presence of an electric field at this junction. With amorphous silicon cell design, the aim is to stretch out the extent of this junction region as far as possible so almost all the cell is junction. This is done by having the p- and n-type doped regions very thin, with an undoped region between them. The strength of the electric field established in this undoped region is nearly constant and depends on this region's width. The poorer the quality of amorphous silicon, the stronger the field needs to be for the device to work well and hence the thinner the device needs to be [24].

Thin-film, polycrystalline compound semiconductors

Many semiconductors made from compounds can absorb light more strongly than the elemental semiconductors, silicon and germanium, for reasons that are well understood but quite subtle (silicon and germanium are indirect rather than direct band-gap materials). This means compound semiconductor cells can be thin but still operate efficiently. Most compound semiconductors, when formed in polycrystalline form, have poor electronic properties due to highly deleterious activity at grain boundaries between individual crystalline grains in the material. A small number maintain good performance in polycrystalline form for reasons that are not usually well understood. These are the candidates for thin-film polycrystalline compound semiconductor solar cells. One such semiconductor is the compound cadmium telluride (CdTe). Technically, it is an ideal material, giving properties suitable for making reasonable solar cells even with relatively crude material deposition approaches (such as electro deposition, chemical spraying, and so on). The junction in these cells is again between p and n-type material, but for the latter, a different compound semiconductor, cadmium sulphide, gives best results. CdTe cells have been used mainly in pocket calculators to date, but large area, moderate performance modules have also been demonstrated. The main concern with this technology is the toxicity of the materials involved, even though very small amounts mean that modules would have to be carefully disposed of or, preferably, recycled after their useful life was finished. However, there may be some problems in gaining market acceptance in what is likely to be mainly a green market over coming years [24].

Thin-film polycrystalline silicon cells

Silicon is a weak absorber of sunlight compared to some compound semiconductors and even to hydrogenated amorphous silicon. Early attempts to develop thin film solar cells based on the polycrystalline silicon did not give encouraging results since the silicon layers had to be quite thick to absorb most of the available light. However, in early 1980s, understanding of how effectively a semiconductor can trap weakly absorbed light into its volume greatly increased. Due to the optical properties of semiconductors, particularly their high refractive index, cells can trap light very effectively if the light direction is randomized, such as by striking a rough surface, once it is inside the cell. Optically a cell can appear about 50 times thicker than its actual thickness if this occurs. Such light trapping removes the weak absorption disadvantage of silicon [24].

Nanocrystalline dye cells

A completely different thin-film approach is based on the use of ruthenium-based organic dyes. Dye molecules are coated onto a porous network to titanium dioxide particles and immersed in an electrolyte, Figure 3.28. In a process bearing some relationship to photosynthesis, light absorbed by the dye photo excites an electron into the titanium dioxide, which completes the circuit through the external load and the electrolyte [24].

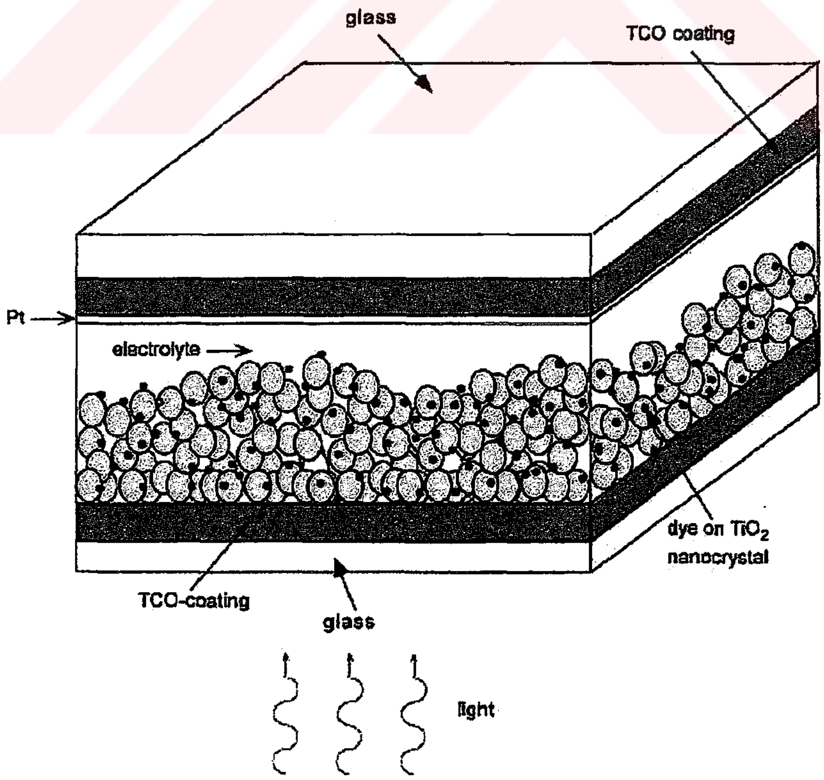

Figure 3.28 Nanocrystalline dye sensitized solar cell [24].

The only major disadvantage of silicon is that it is an indirect band gap semiconductor and, therefore, requires a relatively thick active layer of up to 1.5mm to absorb the full solar spectrum. Direct band gap semiconductors like amorphous silicon, cadmium telluride or copper indium diselenide require only 1 mm of material to be effective. Nevertheless, despite their potential for lower cost, these thin film technologies have struggled with the problems of low efficiency, light degradation, end of life disposal problems and a lack of manufacturing infrastructure. The market penetration, to date, for thin film technologies has been low and it is highly likely that for the next ten years crystalline silicon technology will remain the dominant PV technology [30].

3.2.1.1.3 Photovoltaic Module and Array

As mentioned, PV cells convert sunlight directly into electricity. This conversion is done without creating any air or water pollution. PV cells are made of at least two layers of semiconductor material. One layer has a positive charge, the other negative. When light enters the cell, some of the photons from the light are absorbed by the semiconductor atoms, freeing electrons from the cell's negative layer to flow through an external circuit and back into the positive layer. This flow of electrons produces electric current [31].

To increase the cell utility, dozens of individual PV cells are interconnected together in a sealed, weatherproof package called a module. When two modules are wired together in series, their voltage is doubled while the current stays constant. When two modules are wired in parallel, their current is doubled while the voltage stays constant [31].

To achieve the desired voltage and current, modules are wired in series and parallel into what is called a PV array. The flexibility of the modular PV system allows designers to create solar power systems that can meet a wide variety of electrical needs, no matter how large or small.

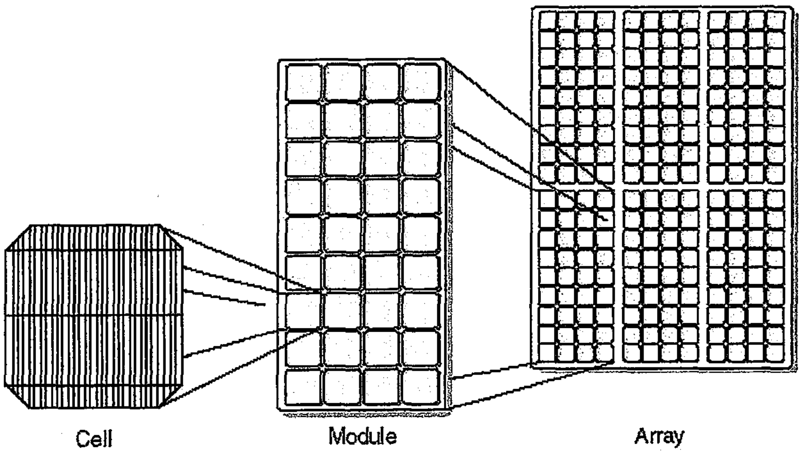

Figure 3.29 Photovoltaic cells, modules and arrays [31].

3.2.1.2 Inverter

Inverters change Direct Current (DC) to Alternating Current (AC). Stand-Alone inverters can be used to convert DC from a battery to AC to run electronic equipment, motors and appliances. Synchronous Inverters can be used to convert the DC output of a photovoltaic module, a wind generator or a fuel cell to AC power to be connected to the utility grid. Multifunction inverters perform both functions [18].

Synchronous inverters change DC power into AC power to be fed into the utility grid. A power system with this type of inverter uses the utility grid as a storage battery. When the Sun is shining, electricity comes from the PV array, via the inverter. If the PV array is making more power than needed, the excess is sold to the utility grid through a second electric meter. If more power than the PV array can supply is needed, the utility makes up the difference. There are no batteries to maintain or replace, but it has a very long payback period [31].

Stand-Alone inverters convert DC power stored in batteries to AC power that can be used as needed. Selecting an inverter for the power system based on the maximum load that will be powered, the maximum surge required, output voltage required, input battery voltage and optional features needed [18].

3.2.1.3 Batteries

All stand-alone systems require battery storage. Photovoltaic modules charge the batteries during daylight hours and the batteries supply the power when it is needed, often at night and during cloudy weather. Utility connected systems supply power directly to the utility grid; no battery storage is needed.

The two most common types of rechargeable batteries in use are lead-acid batteries and alkaline batteries. Lead-acid batteries have plates made of lead, mixed with other materials, submerged in a sulfuric acid solution. They are the most common in PV systems because their initial cost is lower and they are readily available nearly everywhere in the world. There are many different sizes and designs of lead-acid batteries, but the most important point is whether they are deep cycle batteries or shallow cycle batteries. Deep cycle batteries are designed to repeatedly discharged by as much as 80 percent of their capacity so they are a good choice for power systems [32].

Alkaline batteries can be either nickel-cadmium or nickel-iron batteries. They have plates made of nickel submerged in a solution of potassium hydroxide. Their usage is rare since they have high cost and environmental problems related to disposal [32].

3.2.1.4 Charge Controller

Charge controllers are included in most PV systems to protect the batteries from overcharge and/or excessive discharge. The minimum function of the controller is to disconnect the array when the battery is fully charged and keep the battery fully charged without damage. The charging routine is not the same for all batteries: a charge controller designed for lead-acid batteries should not be used to control NiCd batteries.

The basic criteria for selecting a controller include the operating voltage and the PV array current. Controllers are critical components in stand-alone PV systems because a controller failure can damage the batteries or load. The controller must be sized to handle the maximum current produced by the PV array.

There are two types of controllers: series and shunt. Series controllers stop the flow of current by opening the circuit between the battery and the PV array. Shunt controllers divert the PV array current from the battery. Both types use solid-state battery voltage measurement devices and shunt controllers are 100% solid state [31].

3.2.2 Types of Photovoltaic Systems

There are several combinations and alternatives that can be made by the photovoltaic system components. Each type has an advantage or disadvantage according to the requirements. A brief summary of the photovoltaic system types is listed.

3.2.2.1 Small "Stand-Alone" Systems

The small "Stand-Alone" system is an excellent system for providing electricity economically. These systems are used primarily for rural area power, lighting, cabins, backup and portable power systems. The size of the photovoltaic array (number of solar panels) and battery will depend upon individual power requirements.

The solar panels charge the battery during daylight hours and the battery supplies power to the inverter as needed. The inverter changes the 12-volt batteries DC power into 120-volt AC power, which is the most useful type of current for most applications. The charge controller terminates the charging when the battery reaches full charge, to keep the batteries from "gassing-out", which prolongs battery longevity.

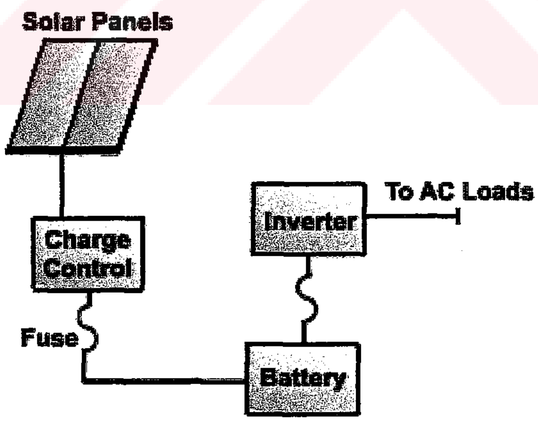

Figure 3.30 Small Stand-Alone System [32].

3.2.2.2 Grid Connected Photovoltaic Systems

A "Grid Connected" system is useful for homes that are already connected to the utility grid. The advantage of this type of system is the price reduction of utility.

The system has to be wired with an inverter that produces pure-sine-wave AC electricity, which is necessary for connecting to the utility grid. Most of these systems typically do not have the battery storage that allows for power when the utility fails. Grid connected system can be installed with battery backup power to keep critical loads operating in the event of a power failure.

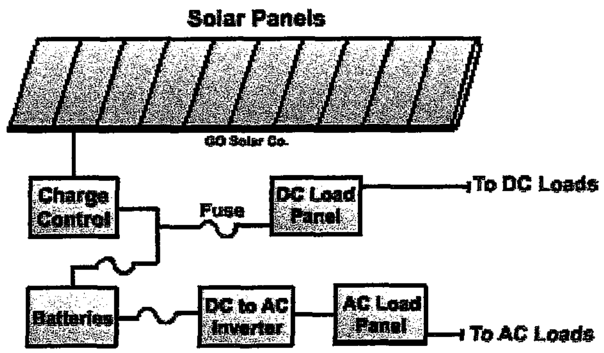

Figure 3.31 Grid Connected Photovoltaic System [32].

3.2.2.3 Complete "Stand-Alone" Systems

A Complete "Stand-Alone" solar system is useful for complete independence from fossil fuels and electric utility companies. The advantage to this type of system is its ability to provide power away from the utility grid, and to create a measure of self-independence.

These self-contained systems need a sizable battery storage capacity to provide electricity when solar power is unavailable due to prolonged adverse weather conditions. Typically this type of system is most cost effective when the system is located away from the utility grid.

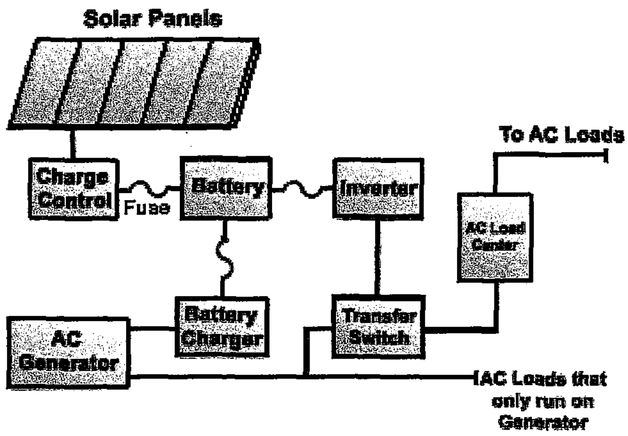

Figure 3.32 Complete Stand-Alone System [32].

3.2.2.4 "Hybrid" – Photovoltaic and Generator Combination System

The "Hybrid" - Solar Electric and Generator Combination provides a reliable power source, and produces electricity even when the Sun is not providing solar power. These "hybrid" systems have the ability to charge the battery bank and provide electricity when weather conditions are unfavorable for solar power production.

An advantage to this type of system is the reduction of photovoltaic panels (PV array) necessary to supply power, which makes this system an economical alternative to a larger "Stand-Alone" system. When more power is needed than the solar panels are producing, a gasoline, propane or diesel generator is activated. The generator will provide enough power to overcome the difference between solar power available and the electricity required. This type of system is used for cabins, remote homes and is a common system used to provide power for small medical facilities.

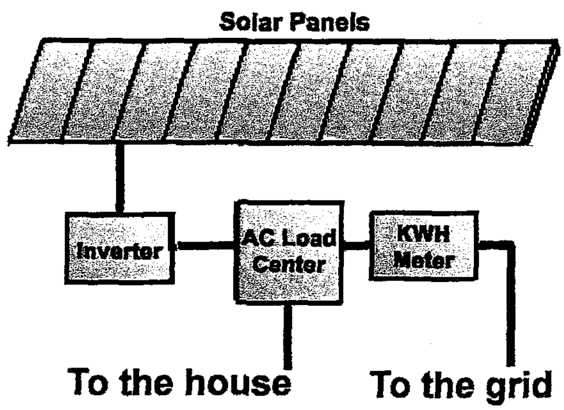

Figure3.33 Hybrid System [32].

PV is used worldwide in many applications, from niche markets in developed countries to primary village power in rural economies and developing countries. Many people are familiar with PV-powered calculators and watches, the most common small-scale applications of PV. However, there are numerous large-scale, cost-effective PV applications, including [26]:

- **Water pumping** for small-scale remote irrigation, stock watering, residential uses, remote villages, and marine sump pumps;

- **Lighting** for residential needs, billboards, security, highway signs, streets and parking lots, pathways, recreational vehicles, remote villages and schools, and marine navigational buoys;

- **Communications** by remote relay stations, emergency radios, orbiting satellites, and cellular telephones;

- **Refrigeration** for medical and recreational uses;

- **Corrosion protection** for pipelines and docks, petroleum and water wells, and underground tanks;

- **Utility grids** that produce utility- or commercial-scale electricity;

- **Household appliances** such as ventilation fans, swamp coolers, televisions, blenders, stereos, and others.

Another application of photovoltaic systems is ***transportation***, which has an important role to reduce the greenhouse gas emissions. ***Electro Vehicles*** that use electricity is the topic of the following part, Section 2.3.

There are some considerations that will be made when selecting photovoltaic systems including [31]:

- **Cost**—When the cost is high for extending the utility power line or using another electricity-generating system in a remote location, a PV system is often the most cost-effective source of electricity.

- **Reliability**—PV modules have no moving parts and require little maintenance compared to other electricity-generating systems.

- **Modularity**—PV systems can be expanded to meet increased power requirements by adding more modules to an existing system.

- **Environment**—PV systems generate electricity without polluting the environment and without creating noise.

- **Ability to combine systems**—PV systems can be combined with other types of electric generators (wind, hydro, and diesel, for example) to charge batteries and provide power on demand.

3.3 Electric Vehicles

An electric vehicle is a motor vehicle, such as an automobile, truck, or bus that uses a rechargeable battery for fuel, replacing gasoline, diesel or other types of combustible fuels. Electric vehicles are similar in many aspects to vehicles powered with internal combustion engines. The chassis or body of many electric vehicles on the road today is from vehicles that once contained an internal combustion engine (ICE). In most electric vehicles, even the interior of the vehicle is unchanged and almost all electric vehicles contain the same accessories as internal combustion engines. Electric vehicles (EVs) offer an attractive alternative to vehicles powered by internal combustion engines because they produce no harmful emissions and would reduce reliance on oil. An electric vehicle produces zero emissions [33].

Two kinds of electric vehicles (EVs) are currently in use: battery-operated EVs and hybrid electric vehicles (HEVs). EVs run on electricity stored in batteries, electricity that ultimately comes from utility power plants. With HEVs, small onboard generating plants driven by internal combustion engines produce most electricity. HEVs can be designed to run on gasoline, diesel, or alternative fuels [34].

Electric vehicles are more than 90% cleaner than the cleanest conventional gasoline-powered vehicle when the electricity running them comes from clean energy sources such as solar energy or other renewable energy sources. Electric vehicles remain cleaner than comparable gasoline-powered vehicles even when the electricity they use derives from polluting fuels like coal. The reasons are their high-efficiency electric power trains and the fact that modern coal-burning generating plants produce electricity more efficiently and with fewer emissions than they did in the past.

Electric vehicles are very simplistic. The propulsion system in an ICE vehicle has hundreds of moving parts. An electric vehicle's propulsion system has only one: the electric motor. In addition to reducing maintenance costs and saving on lubricants and oils, the reduction in friction losses contributes to the energy efficiency of electric vehicles [33].

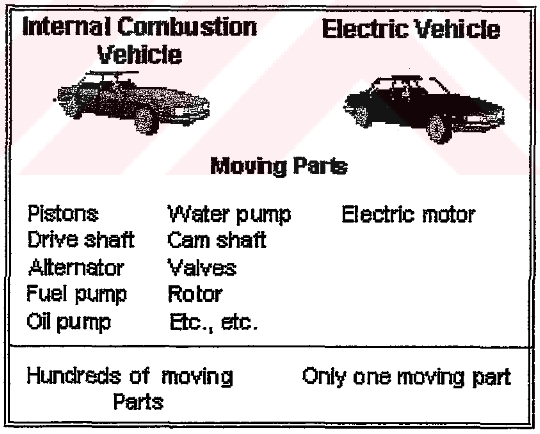

Figure 3.34 Internal combustion vehicle versus electric vehicle.

Testing has demonstrated that EV acceleration, speed, and handling can equal or exceed that of conventional vehicles. EVs are also more energy efficient and produce less noise than gasoline- or diesel-powered vehicles, particularly in stop-and-go traffic, because the engine does not run if the car is not moving.

EVs do not require tune-ups or oil changes associated with conventional vehicles. In addition, EVs do not have timing belts, water pumps, radiators, fuel injectors, or tailpipes to replace. Battery recharging can be a frequent and lengthy process, however, taking 4 to 14 hours depending on the battery type and the voltage level used in recharging [33]. An electric vehicle's battery defines the range, acceleration ability and recharge time for the vehicle. Because the battery contains the energy to fuel an electric vehicle, and because today's batteries do not provide electric vehicles with the same range potential as Internal Combustion Engine (ICE) vehicles, batteries, and alternative options such as flywheels and ultra capacitors, are the most heavily studied areas in electric vehicle technology [33].

Chapter 4

METHOD

Chapter 4 is divided into two parts, which are theoretical calculations and experimental calculations. Theoretical calculations are done with a program so-called MATHCAD. It is also used to analyze the raw data taken from the experimental station.

The screen view of the program is shown in the Figure 4.1 .

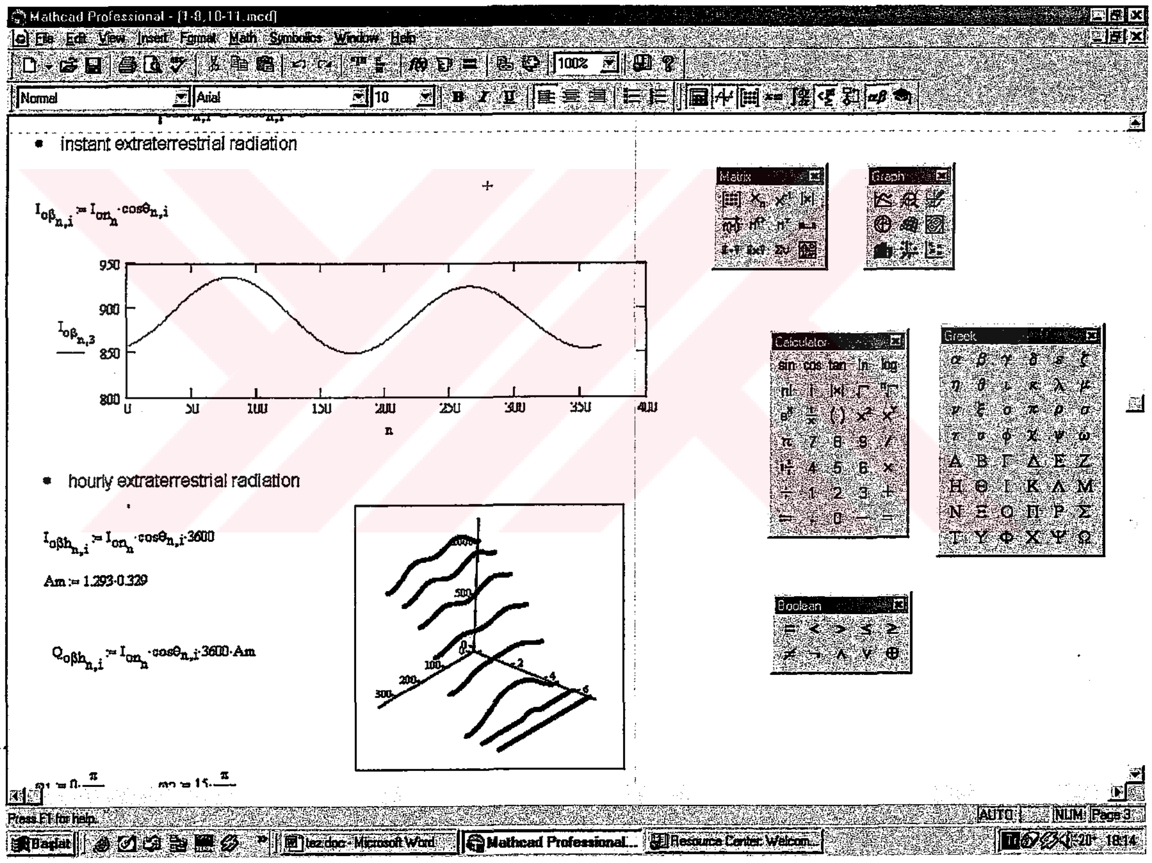

Figure 4.1 A screen view from MATHCAD [22].

4.1 Theoretical Calculations

The calculations of the surface orientation of the photovoltaic modules and the total solar energy received by the modules and the extra solar energy gained through reflectors will be given in Theoretical Calculations Section. The solar energy gain caused by the vertical and tilted reflectors will be calculated after so called ***"Fictive Sun Method"*** of Atagündüz [1].

4.1.1 Energy Collected by Photovoltaic Station

According to the orientation and the slope of the modules given in Table 4.1 and Figure 4.2, the angles of incidence for İzmir-Turkiye with a latitude of **ϕ=38.46°** can be calculated with Equation (3.9).

Table 4.1 Orientation and inclination angles of the photovoltaic modules and reflectors.

Module No.	γ(°)	β(°)	Vertical R_1 (°)	Tilted R_2 (°)	Tilted R_3 (°)
1	7.5	30	90	30	45
2	22.5	36	90	36	36
3	37.5	42	90	42	30
4	52.5	48	90	48	30
5	67.5	54	-	-	-
6	82.5	60	-	-	-
7	97.5	66	-	-	-
8	112.5	72	-	-	-
9	-7.5	30	90	30	45
10	-22.5	36	90	36	36
11	-37.5	42	90	42	30
12	-52.5	48	90	48	30
13	-67.5	54	-	-	-
14	-82.5	60	-	-	-
15	-97.5	66	-	-	-
16	-112.5	72	-	-	-

After having the angles of incidence, the solar energy falling into the whole solar charge station can be calculated. In order to demonstrate the function of the developed station and compare with another concept, e.g., south facing photovoltaic modules, first of all, the extraterrestrial solar radiation will be taken into account for the calculation of solar radiation. Hourly extraterrestrial solar radiation, Q_{ohm} will be calculated after Atagündüz [3]. From Equation (3.14)the zenith angle, θ_z, and from Equation (3.10) the solar azimuth angle, γ_s, can be calculated.

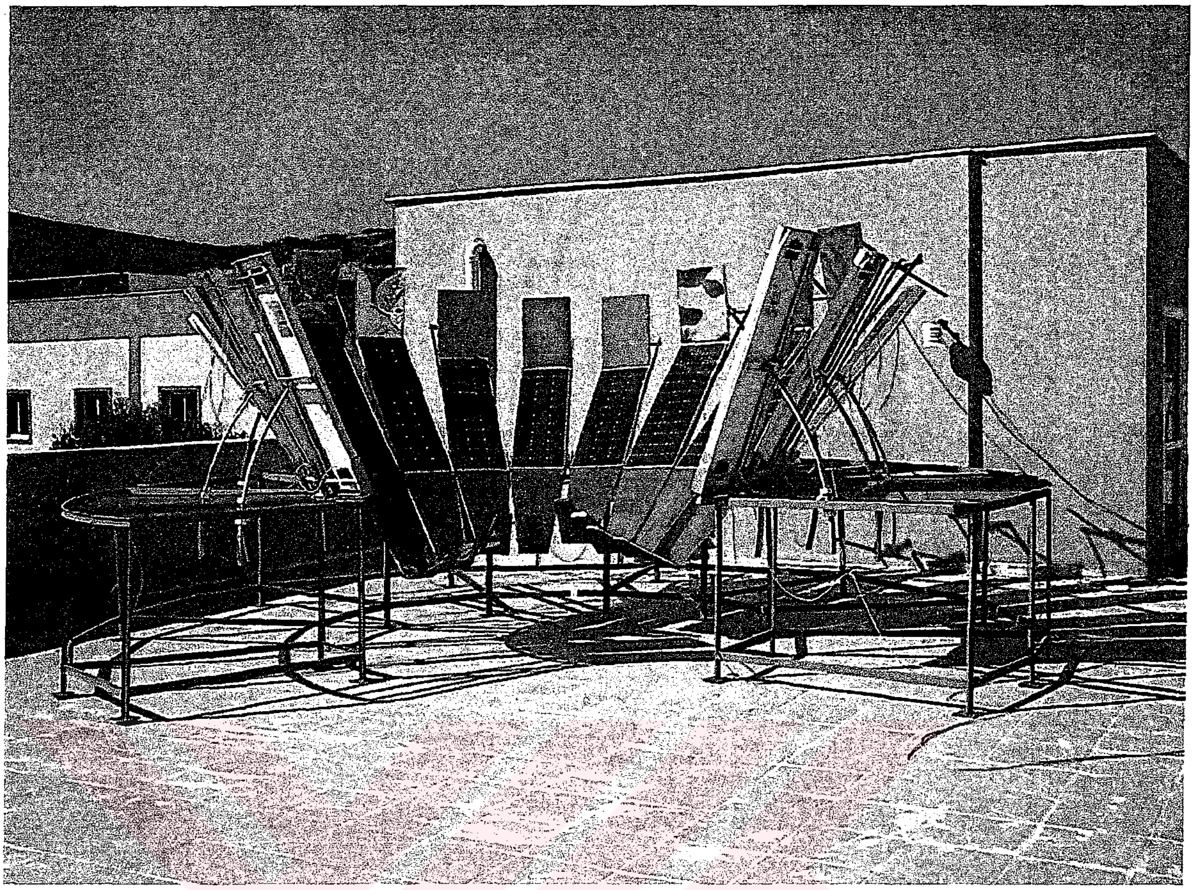

Figure 4.2 Omega Type Solar Charge Station on Classroom's Building rooftop.

Hourly solar radiation can be calculated with the Equations (3.35) for inclined surfaces and (3.36) for horizontal surfaces. These equations are obtained with the integration of incident solar radiation on inclined and horizontal surfaces for an hour period. If this integration is done between the sunrise and sunset hours than integrated daily solar radiation is obtained [19].

The hourly extraterrestrial radiation can also be approximated by writing Equations (3.29) and (3.30), by evaluating ω at the midpoint of the hour (instead of calculating hourly extraterrestrial radiation between -15° and 0°, calculating instantaneous extraterrestrial radiation for –7.5°). The demonstration of this rule is given is shown by Figure 4.3. Differences between the hourly radiations calculated by these two methods are slightly larger at times near sunrise and sunset but are still small [2]. The difference is given in Results and Discussions chapter as an example.

As mentioned in the Sections 4.1.2 and 4.2.2, extra energy gain by vertical and tilted reflectors, the calculation is done with evaluating ω at the midpoint of the hour since effective shaded area must be calculated in order to calculate total solar energy reflected by the reflectors. The integration procedure is slightly difficult for area calculations so instant values are considered for both energy collections by the modules and extra energy gain by the reflectors.

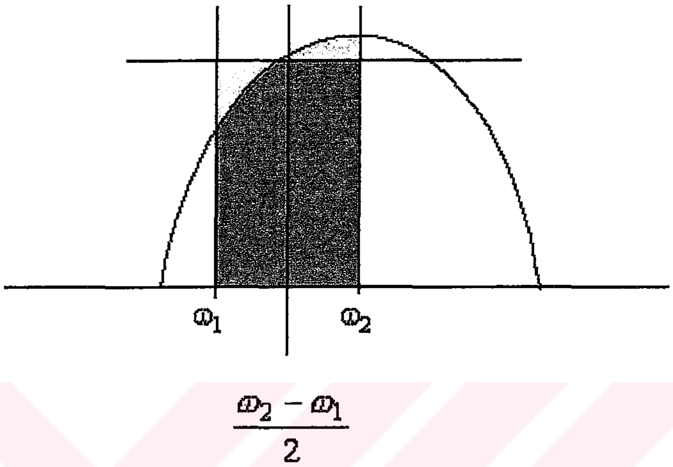

Figure 4.3 Midpoint Rule.

When hourly solar radiation is found from Equation (3.29) for an inclined surface or from Equation (3.30) for a horizontal surface, extraterrestrial solar radiation falling on the surface is found from Equation (4.1) by midpoint rule.

$$Q^*_{ohm} = I^*_s \cdot \cos\theta \cdot A_m \cdot t \tag{4.1}$$

If hourly extraterrestrial radiation is found from Equation (3.35) for an inclined surface and from Equation (3.36) for a horizontal surface, than hourly extraterrestrial solar radiation falling on the surface is

$$Q_{ohm} = I_{oh\beta} \cdot A_m \tag{4.2}$$

where m stands for module.

4.1.2 Extra Energy Gain by Vertical Reflectors

In order to calculate the extra energy gain caused by the reflectors, a method called "fictive Sun" is developed. Illustration of the method is shown in Figure 4.4

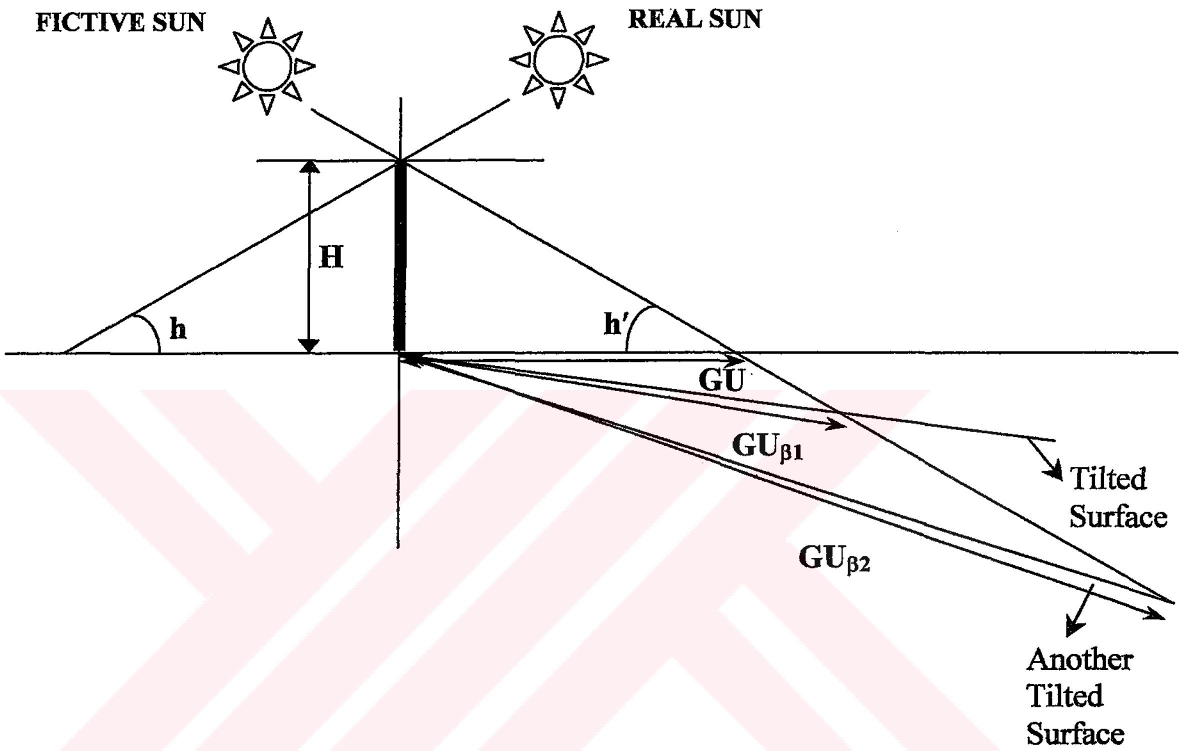

Figure 4.4 Illustration of the Fictive Sun Method [1].

The amount of the solar energy of the reflected beams can be calculated as follows: First of all, the angle of incidence can be calculated by giving the hour angle, Equation (3.9). Afterwards the zenith angle will be determined using the Equation (3.14).

As the relation between the zenith angle and the solar altitude angle, h is:

$$\theta_z + h = 90° \tag{4.3}$$

The solar altitude angle can be calculated, Figure 4.4. According to the idea of Atagündüz [6], the solar altitude angle of the reflected beam, h′, is equal to the solar altitude angle h.

Now, the angle of incidence of the reflected beam can be calculated as follows:

$$\cos\theta' = \cos\theta_z \cos\beta + \sin\theta_z \sin\beta \cos(\gamma_s' - \gamma) \tag{4.4}$$

the solar azimuth angle of the reflected beam can be determined through Equation (4.5):

$$\cos\gamma_s' = \frac{-\cos\phi\sin\delta + \sin\phi\cos\delta\cos\omega}{\sin\theta_z} \tag{4.5}$$

The shade of the reflector on the tilted surface will be calculated using the beams coming from the fictive Sun, Figure 4.4.The length of the shaded area of a horizontal surface is [1]:

$$GU = \frac{H}{\tan h'} \tag{4.6}$$

where H is the height of the reflector.

According to the law of sinus, the length of the shaded area on the tilted surface will be [1]:

$$GU_\beta = \frac{GU}{\cos\beta} \tag{4.7}$$

In Equation (4.7), two cases should be taken into consideration:

- ($\beta = h'$) reflected beams are parallel to the tilted surface,
- ($\beta > h'$) reflected beams do not fall onto the tilted surface.

Now the shaded area on the tilted surface can be calculated as follows [1]:

$$A_{sh} = GU_{\beta} \cdot W_R \tag{4.8}$$

where W_R is the width of the reflector.

This shaded area is not yet the area on the photovoltaic module; Figure 4.5.The true area of the tilted photovoltaic module must be compared with the shaded area on it, in order to get effective A_{she} area covered by the reflected beam. γ_s' must be plotted in the shading diagram and the length of the shaded area. GU_β must be marked on it. Afterwards at the end of GU_β a parallel line to the reflector bottom line must be plotted, Figure 4.5. Thus the shaded area on the module can be compared with the real area of the corresponding photovoltaic module. This procedure is repeated for each hour angle from the sunrise till to the sunset on an inclined surface [3], and for each module. For a better understanding of the effective shaded area change with time, an illustration for a south facing module, γ=0°, for solar noon

Now the extra solar energy gain through reflected beams can be calculated as follows: First of all, the energy of the beams falling onto the reflector must be calculated [1].

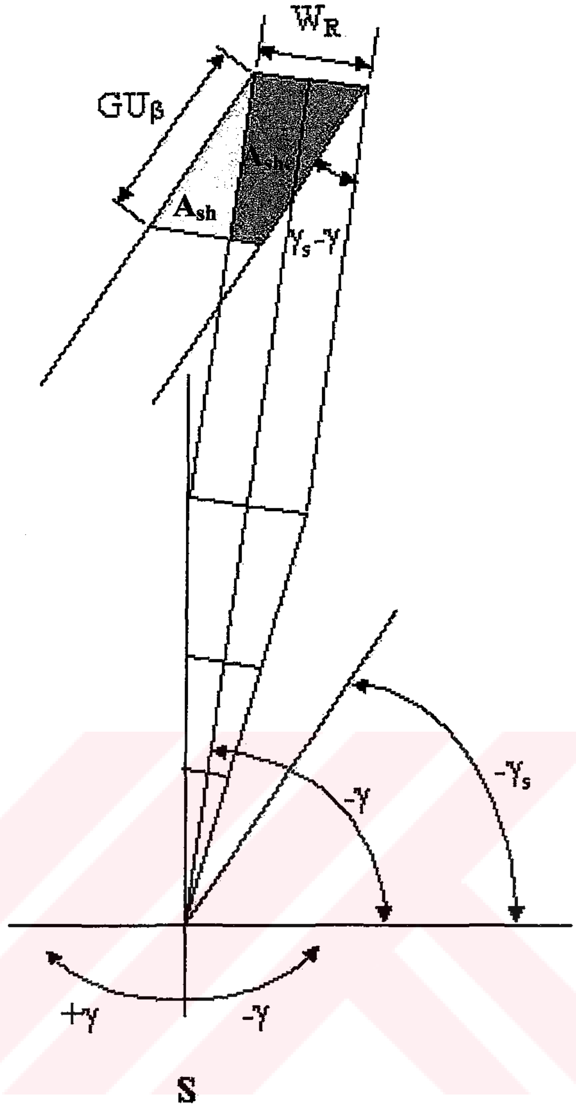

Figure 4.5 Illustration of shaded areas, A_{sh}, and A_{she} for the 1st module.

Afterwards, taking into account the reflectance of the reflector, r_R, the amount of the reflected solar energy will be calculated. If the extraterrestrial solar radiation is taken just to give an example, the reflected solar energy per unit time and area will be [1]:

$$I_{oR}^{*\,'} = I_o^* \cdot r_R \cdot \cos\theta' \text{ (W/m}^2\text{)} \tag{4.9}$$

And the total energy per unit time is [1]:

$$Q_{oR}^{*'} = A_{she} \cdot I_{oR}^{*'} \cdot a_m \text{ (W)} \tag{4.10}$$

where a_m is the absorbance of the photovoltaic module.

After integrating for one hour, the amount of the hourly solar energy desired, will be [1]:

$$Q_{ohR}^{*'} = A_{she} \cdot I_{oh} \cdot \cos\theta' \cdot r_R \cdot a_m \text{ (J)} \tag{4.11}$$

As the hourly solar energy falling onto the photovoltaic module is known, Q_{ohm}, the hourly total extraterrestrial solar beam energy received by the photovoltaic module will be [1]:

$$Q_{oht} = Q_{ohm} + Q_{ohR}^{*'} \text{ (J)} \tag{4.12}$$

In general the reflectance of the reflector can be taken as r_R = 0.86, and the absorbance of the photovoltaic module has been taken as, a_m = 0.86 [1].

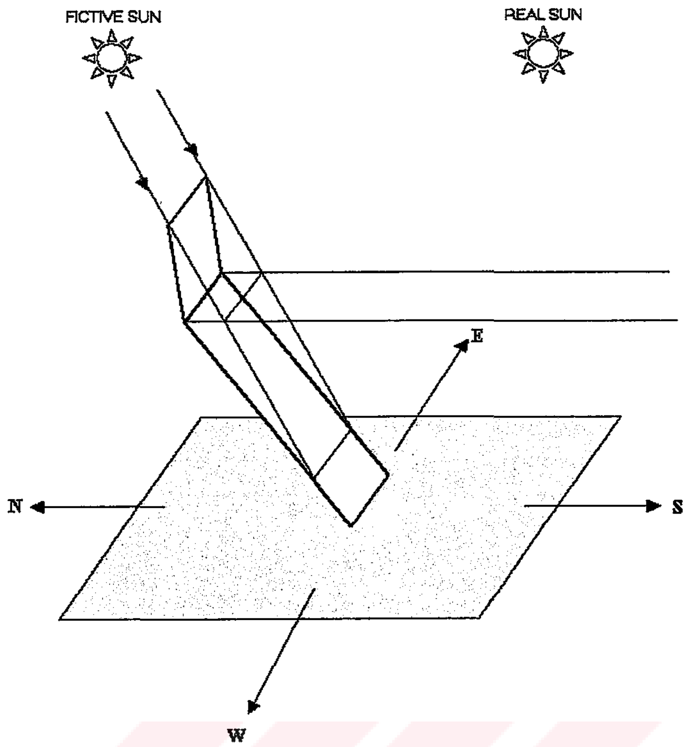

Figure 4.6 Shadow length and effective shaded area on a south facing module at solar noon, ω=0°.

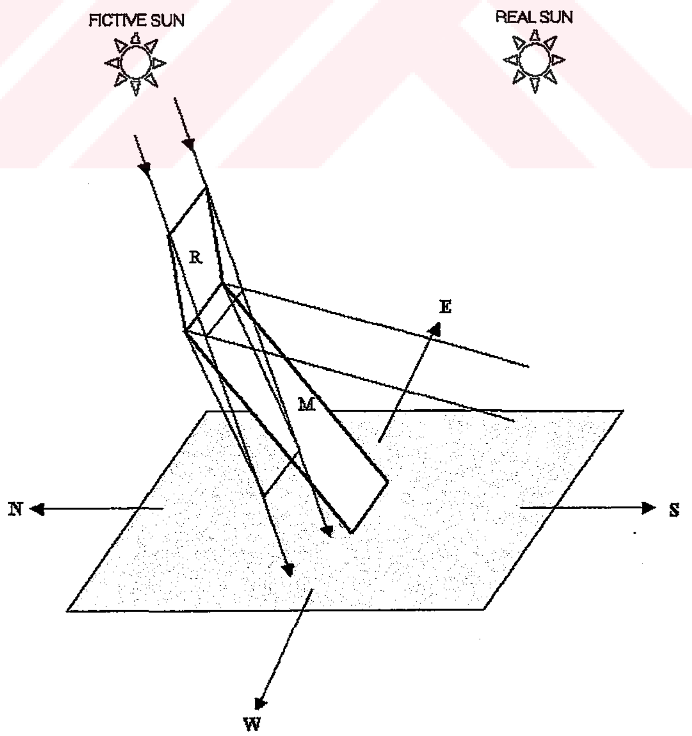

Figure 4.7 Shadow length and effective shaded area on a south-facing module at a time except solar noon, ω≠0°.

4.1.3 Extra Energy Gain by Tilted Reflectors

The tilted reflectors of the modules 1 to 4 and 9 to 12, Figure 5.2, also add some solar energy to their photovoltaic modules. This amount of energy can be calculated as follows [1]:

Giving the hour angle ω, the angle of incidence can be calculated from Equation (3.9). Afterwards, using Figure 4.8 the angle of incidence of the reflected beam, θ', can be determined $\theta' = 180 -(\beta m + \beta r + \theta)$. The combination of the Equation (3.14) in Chapter 2 and Equation (4.5) gives the solar azimuth angle of the reflected beam, $\gamma s'$ [1].

Using the dimensions and slopes of the tilted reflectors of the modules 1 to 4 and 9 to 12, Table 4.1 and the law of sinus, the length of the reflected beam a will be, Figure 5.2 and Figure 4.8 [1]:

$$a = b \cdot \frac{\sin[180° - (\beta_m - \beta r)]}{\sin(90° - \theta)} \tag{4.13}$$

and

$$c = b \cdot \frac{\sin(90° - \theta)}{\sin(90° - \theta')} \tag{4.14}$$

where b chosen.

From Figure 4.8 and using fictive Sun definition, the height of the solar beam at the reflector, H_{Rb}, and the height of the reflected beam at the module, H_{mc} are given below [1]:

$$H_{Rb} = b \cdot \sin \beta_R \qquad H_{mc} = c \cdot \sin \beta_m \tag{4.15}$$

Using the solar altitude angle for the fictive Sun, $h' = 90 - \theta_z$, Fig. (5) the "shade lengths" GU_b and GU_c will be [1]:

$$GU_b = \frac{H_{Rb}}{\tan h'} \qquad GU_c = \frac{H_{mc}}{\tan h'} \tag{4.16}$$

where θ_z can be calculated using the Equation (3.14).

As the solar azimuth angle of the reflected beam is known, $\gamma s'$, the length, GUb and GUc can be plotted on Figure 4.8. First of all, the distance between the points z and p. Lp, can be calculated as follows [1]:

$$L_P = b \cdot \cos \beta_R \tag{4.17}$$

Afterwards stating from the point z taking the length L = Lp + GUb the reference point RI can be fixed. Later on, from this reference point RI the length GUc can be shown. The reference point RI can be fixed also in the horizontal plane on the solar azimuth angle, γs', line starting from the point z, taking any arbitrary position on the bottom line of the reflector is equal to zero. All points z on the bottom line of the reflector can be plotted in the horizontal plane, Figure 4.8. Thus taking into account all the reflected beams at the same hour angle ω, the area covered by the reflected beams, active area can be plotted in the horizontal plane, where the real area of the module is given as well. Now, the effective area for the reflected beams is the intersection area of the both areas in horizontal plane, Figure 4.8 [1].

The effective area should be calculated for the module height between HRm and Hm [1],

$$H_{Rm} < H_{mc} < H_m \tag{4.18}$$

$$(\gamma - \arctan(0.125/1)) \leq \gamma'_s \leq (\gamma + \arctan(0.125/1)) \tag{4.19}$$

Figure 4.8 and for the azimuth angles of the reflected beams between the azimuth angles (γ + arctan(0.125 / 1)) and (γ - arctan(0.125 / 1)). By given step by step, the width of the reflector must be calculated in order to able to plot the active area in the horizontal plane [1].

The extra solar energy gain through tilted reflectors can be calculated by the same method used for the vertical reflectors [1].

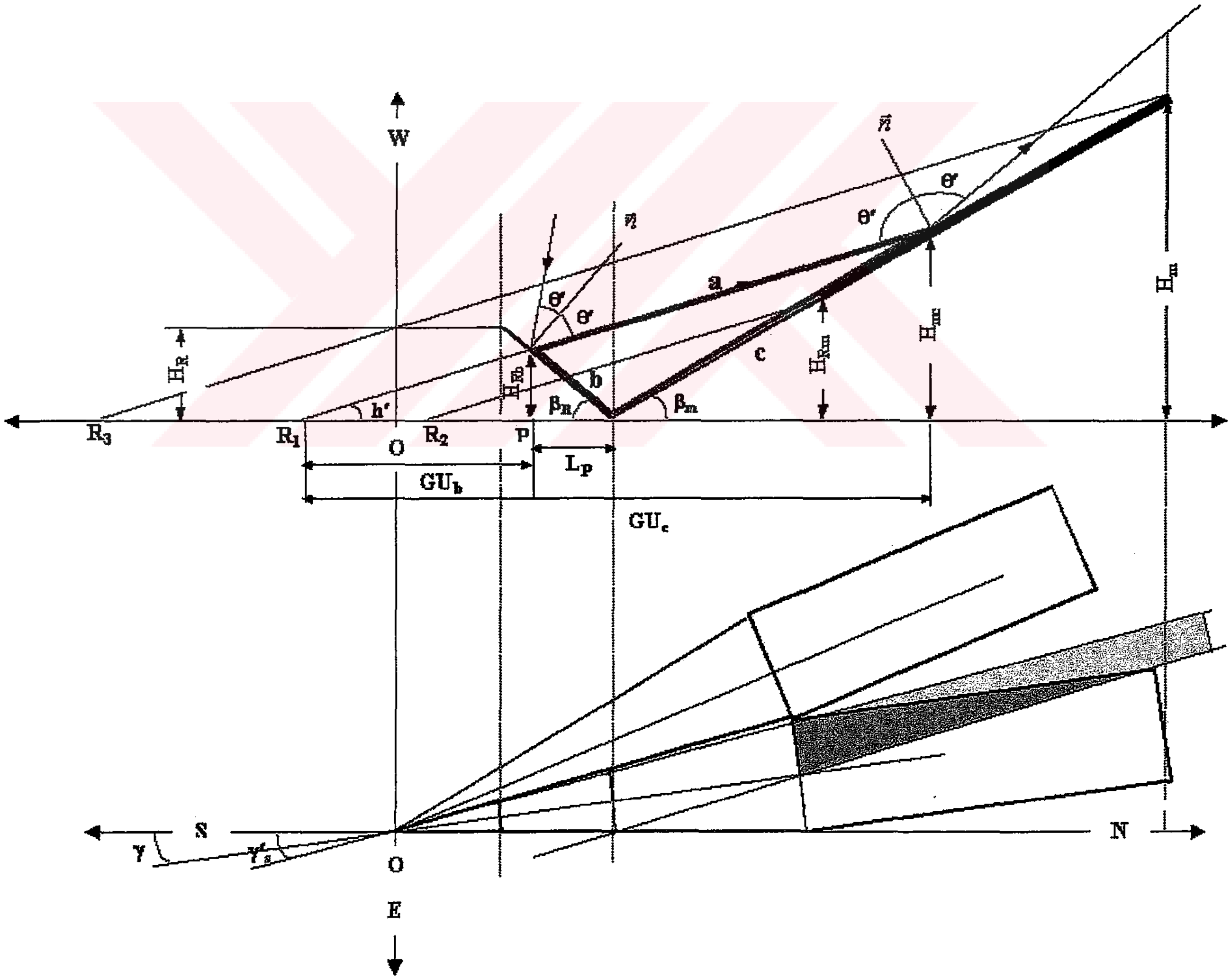

Figure 4.8 Illustration of the calculation of the effective solar energy gain by the tilted reflectors for the modules 1 to 4 and 9 to 12.

4.2 Experimental Calculations

The methods used for calculating theoretical solar radiation values (extraterrestrial and terrestrial), calculation of direct and diffuse components of the total solar radiation and the conversion of direct solar radiation to an inclined surface are explained in Chapter 3. Using the solar radiation data and the measured current intensity (A) and potential difference (V) values, the efficiency of the whole Solar Charge Station can be calculated.

The power obtained from the photovoltaic generator is calculated by the famous formula

$$P = I \times V \tag{4.20}$$

where P is power in Watts (J/s), I is Current intensity in Amperes and V is potential difference in Volts, measured during the experiments at the mid hours. This instantaneous power value gives the total energy that the solar charge station collects in one hour assuming the energy stays constant during the hour.

$$Energy_{Collected} = P \times 3600 \tag{4.21}$$

The I-V characteristic of a solar cell can be obtained by droving an equivalent circuit of the device is shown in Figure 4.9. The generation of current I_l by light is represented by a current generator in parallel with a diode, which represents the p-n junction. The output current is then equal to the difference between the light-generated current I_l and the diode current I_D.

In mathematical terms, the I-V characteristic of a diode is given by the Shockley equation

$$I = I_0[\exp(\frac{qV}{kT}) - 1] \tag{4.22}$$

Where I is the current, V is the voltage, k is the Boltzmann constant, q is the magnitude of the electron charge, and T is the absolute temperature. Equation (4.22) then gives

$$I = I_l - I_0[\exp(\frac{qV}{kT}) - 1] \tag{4.23}$$

for a photovoltaic module.

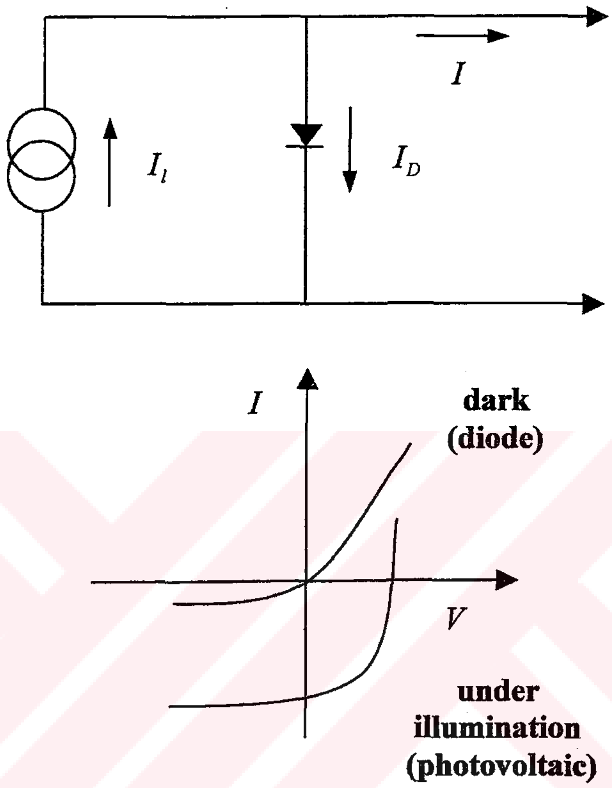

Figure 4.9 The equivalent circuit and I-V characteristic of a photovoltaic module compared to a diode [18].

Under open circuit when I=0, all the light-generated current passes through the diode. Under short circuit (V=0) on the other hand, all this current passes through the external load. Both I_l and I_0 depend on the structure of the device. No power is generated under short or open circuit. The maximum power P_{max} produced by the device is reached at a point on the characteristic where the product IV is maximum. This is shown graphically for the photovoltaic module used in this study, SM55, in Figure 4.10

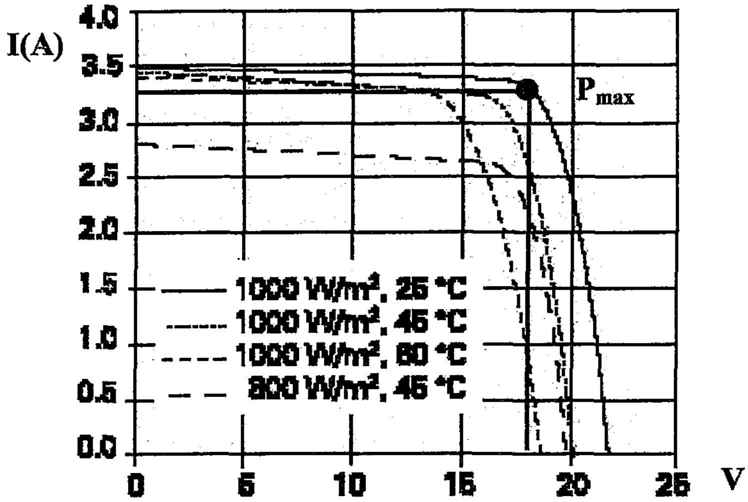

Figure 4.10 The I-V characteristic of SM55 with maximum power point for 1000 W/m^2, 25 °C.

The *efficiency,* η, of a photovoltaic module is defined as the power P_{max} produced by the cell at the maximum power point under standard test conditions, divided by irradiance $1000 W/m^2$, standard reference AM 1.5 spectrum, and temperature 25 °C. the irradiance is the total solar radiation on horizontal surface.

Since photovoltaic devices convert direct solar radiation to electricity, the efficiency of a photovoltaic module can be calculated by using direct solar radiation value. So in this study another efficiency is defined as η_I, collected energy by the photovoltaic generator divided by direct solar radiation on the inclined surface.

$$\eta = \frac{Energy_{Collected}}{I_{thz}} \tag{4.24}$$

$$\eta_I = \frac{Energy_{Collected}}{I_{th\beta}} \tag{4.25}$$

Where I_{thz} is the total solar radiation measured by the pyranometer and $I_{th\beta}$ is the estimated direct solar radiation using the total solar radiation data, which explained in Chapter 3.

Chapter 5

EXPERIMENTAL WORK

5.1 Experimental Set-up

The investigation station of the "Omega Type Solar Charge Station" consists of photovoltaic generator, batteries, charge controller, DC lamps, the measurement unit including voltmeter, amperemeter, pyranometer, data logger which also collects the ambient temperature and relative humidity values, for the data analysis a computer and wiring.

5.1.1 Photovoltaic Generator

Omega, Ω, Type Solar Charge Station's photovoltaic generator has been set up on the roof of the Classrooms Building of Faculty of Engineering in Gülbahçe-Campus of the İzmir Institute of Technology. Sixteen Siemens Model SM55 photovoltaic modules are used as the generator, which are composed of 36 PowerMax® single-crystalline solar cells, having the dimensions $1.293m \times 0.329m \times 0.034m$. Technical specifications of the modules are shown in Figure 5.1.

After trying many angles of surface azimuth, γ, and slopes, β, of the modules in previous studies [6], the following angles for the 16 modules have been chosen for the photovoltaic charge stations generator. The modules numbered from 1 to 8 are located from North via East to South having the azimuth angles, γ, from -172.5° to –67.5° and having an angle difference 15° from each other. The rest 8 modules numbered from 9 to 16 are located symmetrically to the North-South-axis on the West side having the azimuth angles, γ, from +172.5° to +67.5°. The corresponding values for the photovoltaic modules are given in Table 5.1 and Figure 5.2.

The inclination angles,β, are given in Figure 5.2, marked on each module, for instance module 1 has an inclination angle β= 30° and module 8, β= 72°.

Table 5.1 Orientation and the slope of the photovoltaic modules: γ, azimuth angle; β, slope of the module; H, height; L, projected length.

Module No.	γ(°)	β(°)	H (m)	L (m)
1	7,5	30	0,65	1,12
2	22,5	36	0,76	1,05
3	37,5	42	0,87	0,96
4	52,5	48	0,96	0,87
5	67,5	54	1,05	0,76
6	82,5	60	1,12	0,65
7	97,5	66	1,18	0,53
8	112,5	72	1,23	0,40
9	-7,5	30	0,65	1,12
10	-22,5	36	0,76	1,05
11	-37,5	42	0,87	0,96
12	-52,5	48	0,96	0,87
13	-67,5	54	1,05	0,76
14	-82,5	60	1,12	0,65
15	-97,5	66	1,18	0,53
16	-112,5	72	1,23	0,40

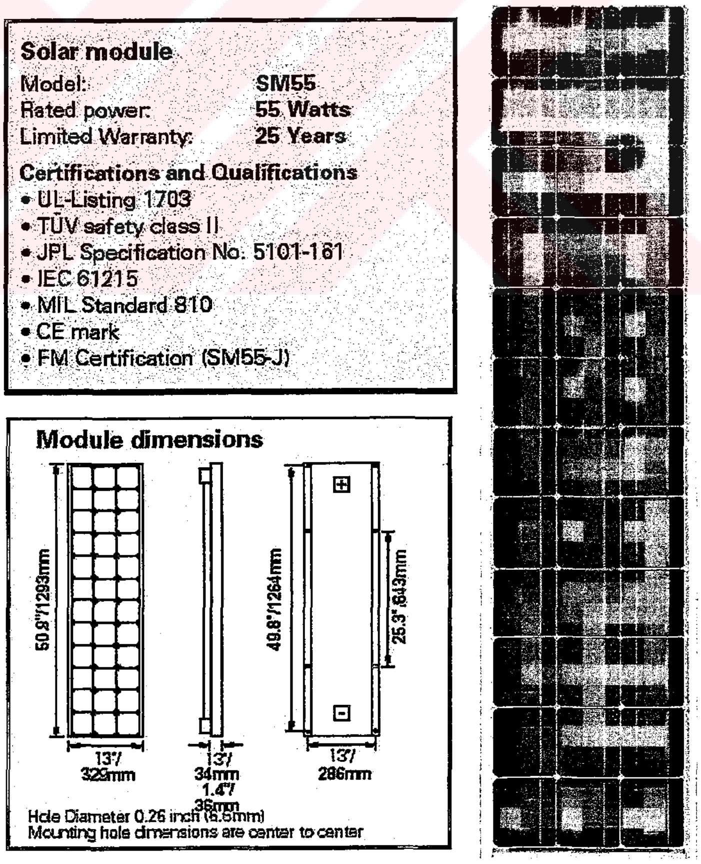

Figure 5.1 Technical specifications of Siemens SM55.

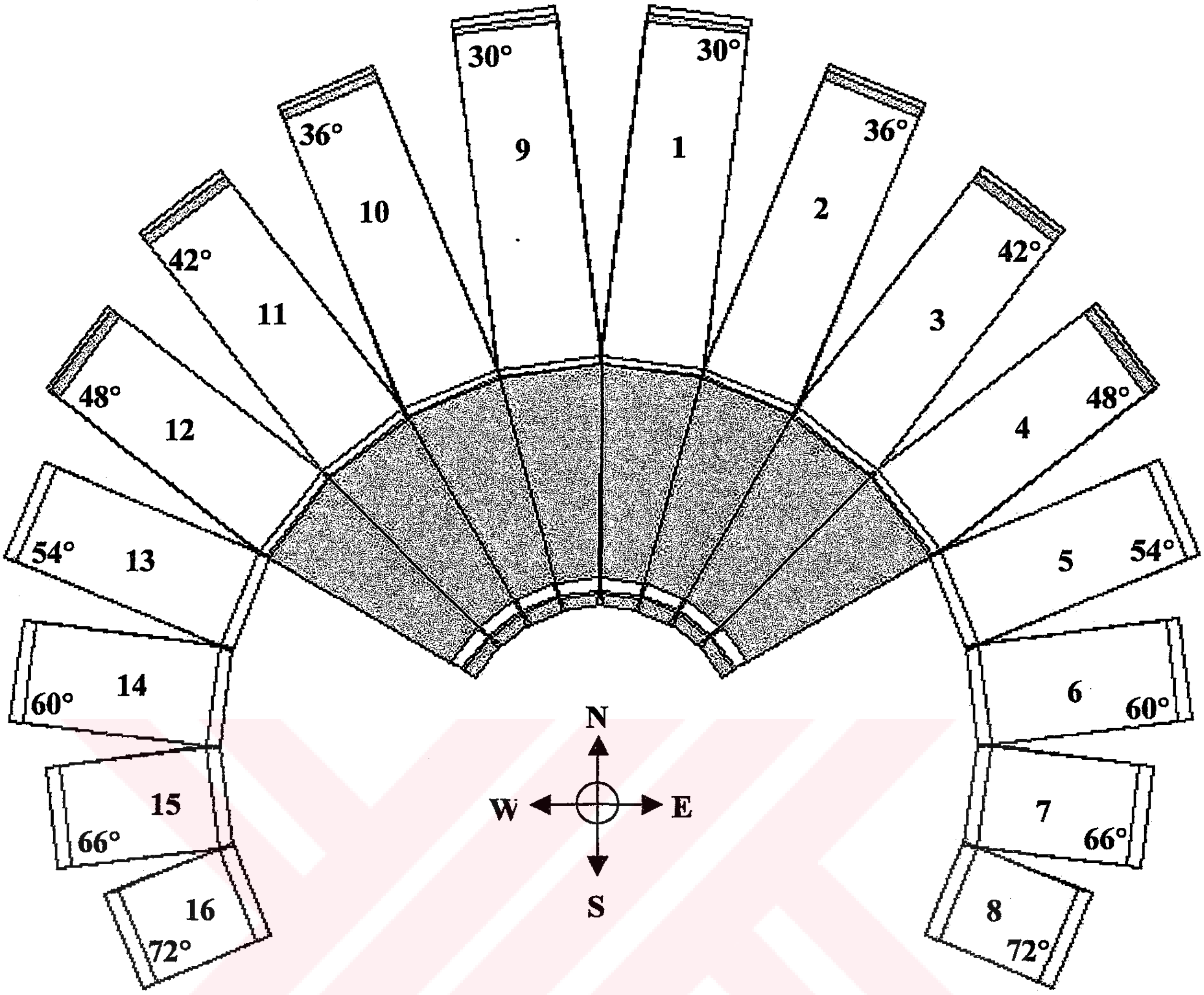

Figure 5.2 Schematic Representation of Omega Type Solar Charge Station.

The generator has two types of modules, the ones with reflectors, and the ones without reflectors. According to the previous design of the charge station by Atagündüz [6], optical analysis showed that the modules from 1 to 4 and 9 to 12 would have booster reflectors in order to increase the efficiency of the array. Mounting reflectors to other modules, 5 to 8 and 13 to 16, is calculated to be ineffective for increasing array efficiency.

Figure 5.2, Figure 5.3, and Figure 5.4 show the representations of top, front and left views of Omega Type Solar Charge Station, schematically.

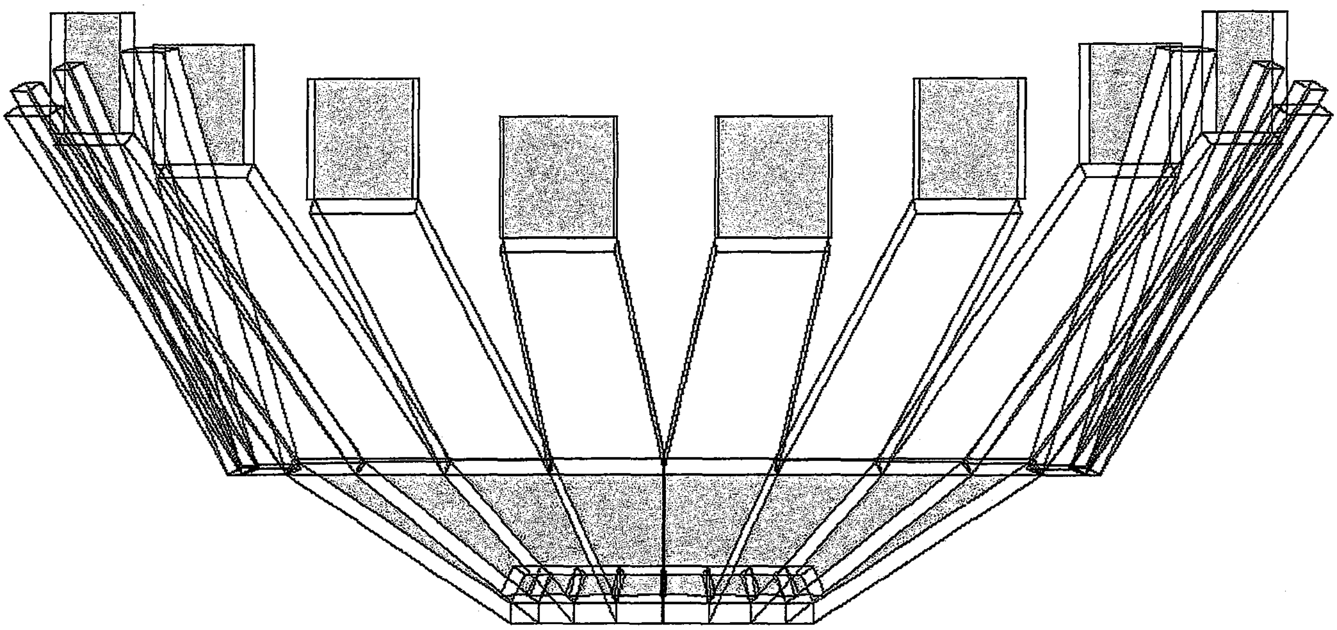

Figure 5.3 Front view of Omega Type Solar Charge Station.

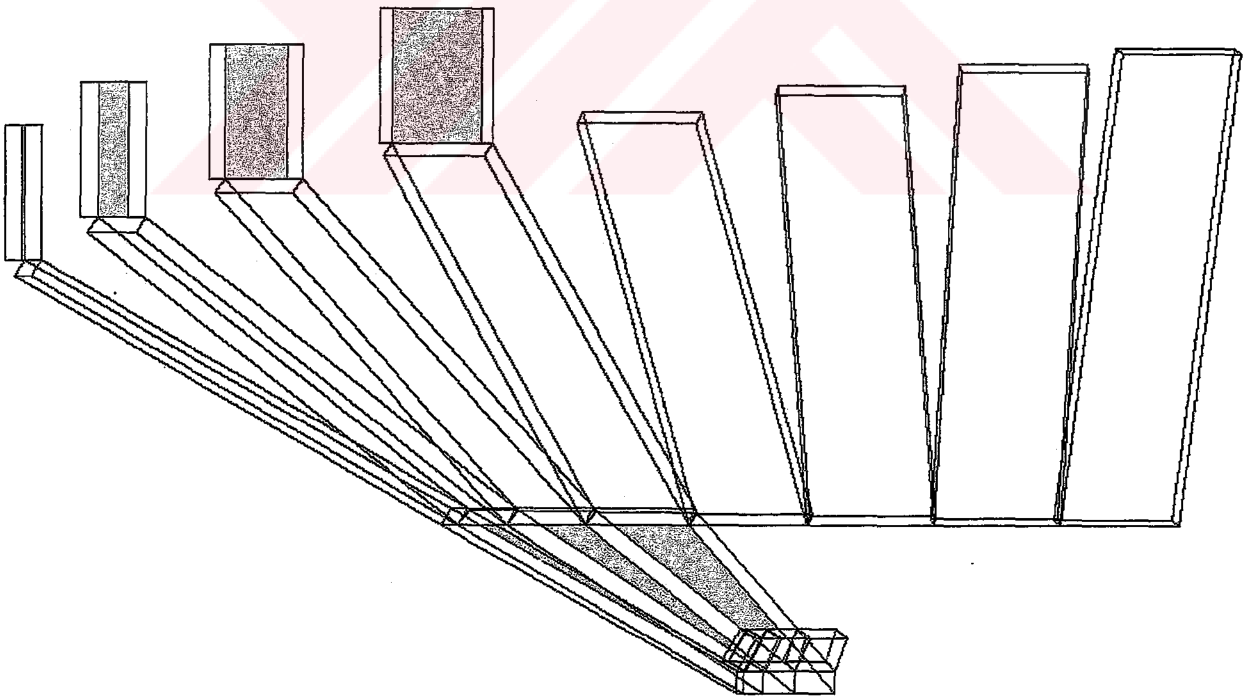

Figure 5.4 Left view of Omega Type Solar Charge Station.

It is decided to use three types of reflectors, one vertical reflector and two tilted reflectors on the module side. Schematic representation of a module with reflector and the dimensions of the reflectors are shown in Figure 5.5.

The material of the reflectors is stainless steel. It is chosen because of its high reflectance and its resistance to the effects of Sun.

The mounting construction of the whole photovoltaic generator including stainless steel reflectors is done by TARTES.

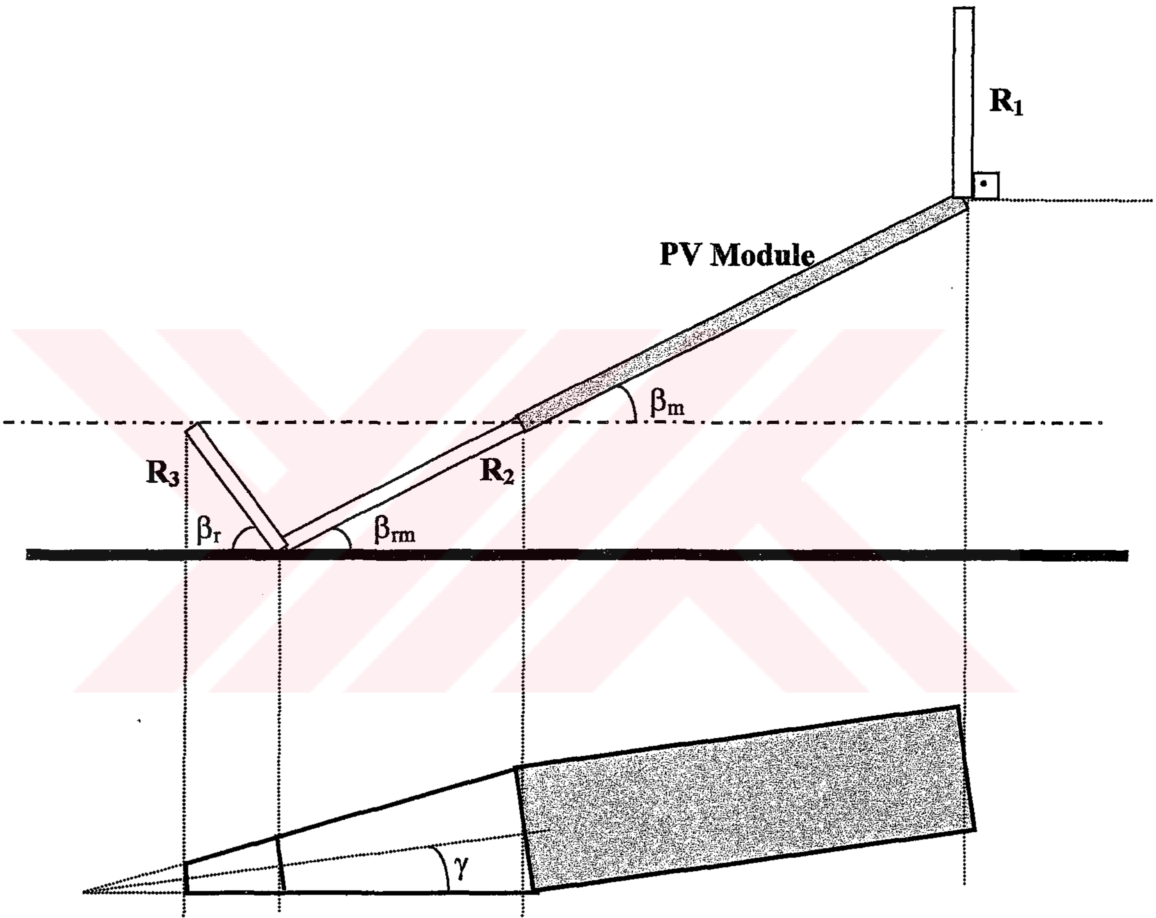

Figure 5.5 Schematic representation of a module with reflectors.

The front view of a module with reflectors is shown in Figure 5.8, construction sheet for the reflectors.

The area of each photovoltaic module is 0.4254 m^2 and the area of the 16 modules is 6.8064 m^2. The area of the reflectors that is mounted to one module is 0.3726 m^2 and total reflector area for 8 PV modules is 2.98 m^2.

The construction plan sheets of the Omega Type Solar Charge Station is given in Figure 5.6, Figure 5.7, Figure 5.8.

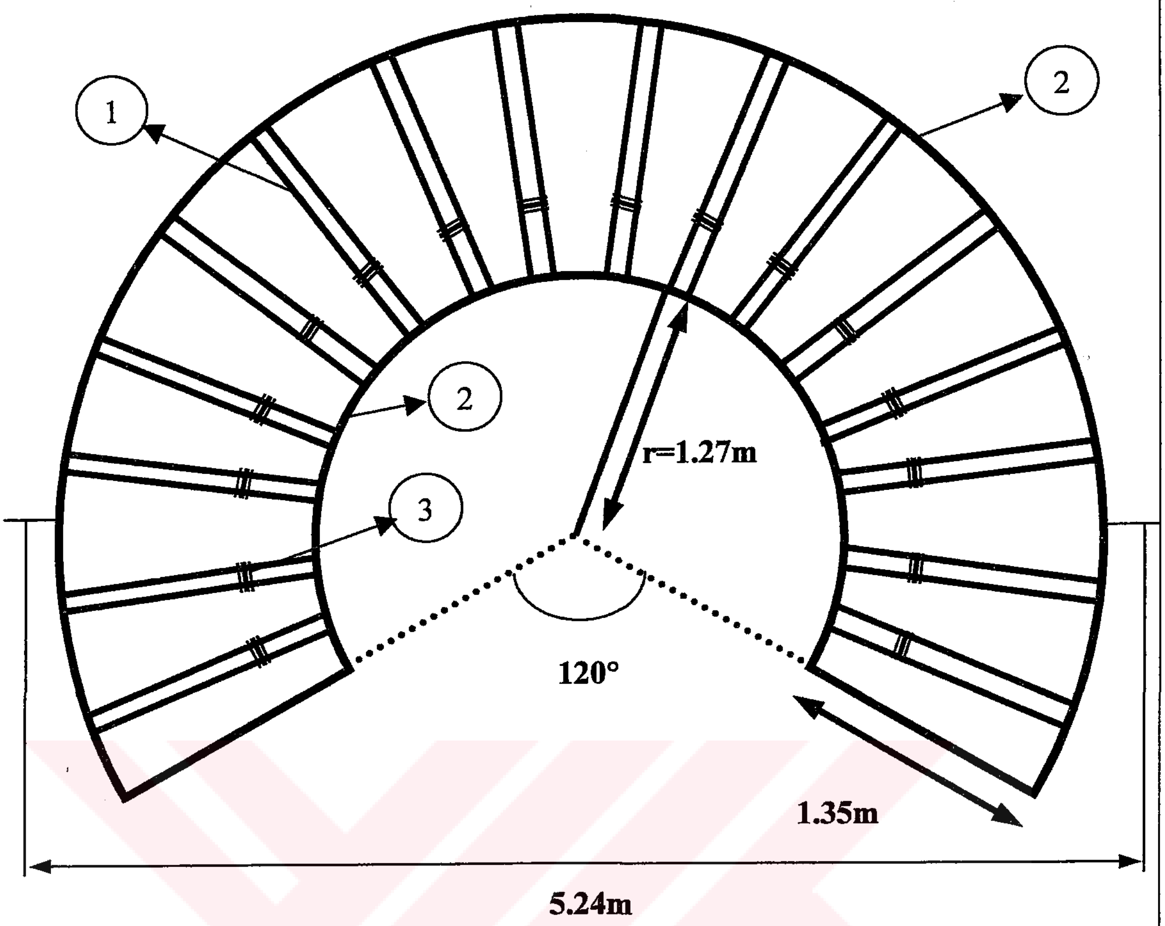

Materials used for steel mounting construction TOP SIDE
Section 1, U Profile: 1,35 m x 32 pieces
Section 2, Box Profile: 7,2 m x 1 piece 5,32 m x 1 piece
Section 3, Rotation Unit: 16 pieces

Figure 5.6 Construction Sheet for Omega Type Solar Charge Station, Top Side.

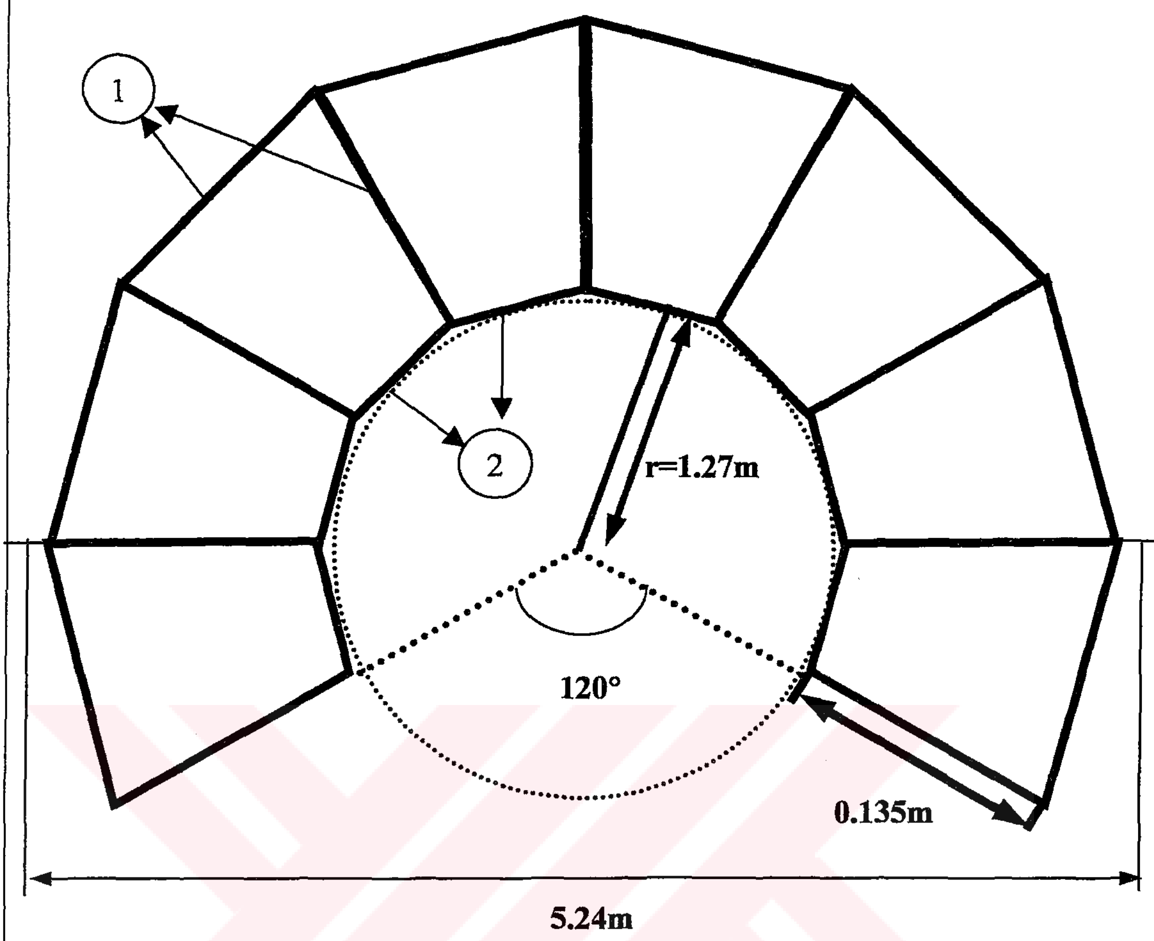

Materials used for steel mounting construction BOTTOM SIDE
Section 1, U Profile: 1,35 m x 9 pieces 1,4 m x 8 pieces
Section 2, Box Profile: 0,66 m x 8 pieces
U Profile: 1,50 m x 18 pieces for legs (not shown in figure)

Figure 5.7 Construction Sheet for Omega Type Solar Charge Station, Bottom Side.

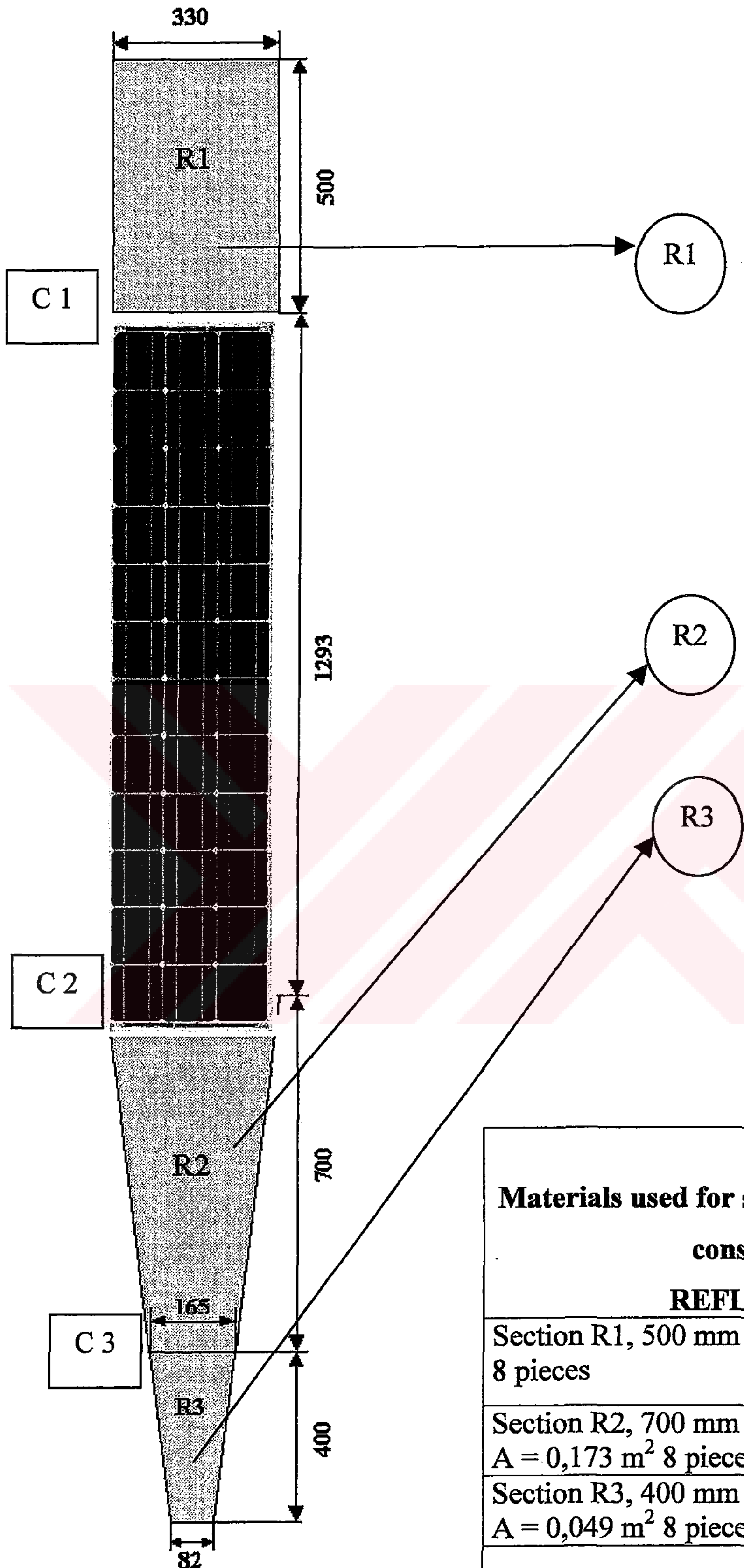

Materials used for stainless steel mounting construction REFLECTORS
Section R1, 500 mm x 330 mm A = 0,165 m^2 8 pieces
Section R2, 700 mm x (330 mm + 165 mm) A = 0,173 m^2 8 pieces
Section R3, 400 mm x (165 mm + 82 mm) A = 0,049 m^2 8 pieces

Figure 5.8 Construction Sheet for Omega Type Solar Charge Station, Reflectors.

In Figure 5.8 the points C1, C2 and C3 are the connection points of the reflectors and the module. In this figure, all the angles between the module and the reflectors are 180°.

Connection point C1, which is between the vertical reflector R1 and the module, moves when the inclination angle of the module changes. For every location of the point C1, the angle between the horizontal and the reflector R_1 is perpendicular (90°). For example, when the inclination of the module is 30°, the angle between reflector and module is 120°, when inclination of the module is 60° than the angle between reflector and module is 150°.

Connection point C2 that is between the module and the tilted reflector R_2 is stationary and angle between the module and the reflector is always 180°.

Connection point C3, similar to point C1, changes location due to the inclination of the module and R_2. The angle between R_2 and R_3 is chosen according to the inclination angle of the module.

5.1.2 Batteries and Charge Regulators

Solar energy is discontinues, it is available during the day but not at night, but it is also true that we need energy continuously, through night and day. We need to store solar energy during the day in order to use it when we cannot obtain it. Batteries are chosen to store energy in Omega Type Solar Charge Station.

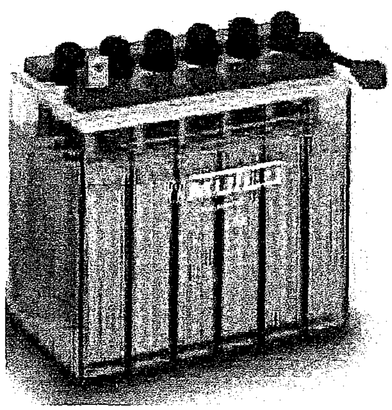

Figure 5.9 Lead-Acid Battery from Mutlu Akü.

The most common battery type that is used in PV system applications is Lead-acid Batteries as mentioned in Section 2.2.1.3. A prominent feature of their operation is cycling affecting the battery life and maintenance. The average life of a PV is 20 years (25 years for Siemens SM55) so we need a long lasting battery.

For the photovoltaic station, OGI Type Lead-acid battery from MUTLU AKÜ is chosen. It is a 150-Ampere deep cycle battery specially used for PV applications.

Various electronic devices are used to accommodate the variable nature of power output from the PV generator to avoid the malfunction of the system.

A photovoltaic cell in the dark behaves as a diode. Similarly the array of Photovoltaic Station also will provide a discharge path of the battery during the nighttime operation. The solution for the problem is to separate the generator and battery by a **blocking diode**. Many photovoltaic cells, including Siemens SM55, have this feature.

When solar intensity is high, another problem, excessive overcharge of batteries occurs. This is the function of the **charge regulator**. Monitoring the battery voltage and disconnecting the load from the battery when the voltage falls below or rise over a pre-set value avoid excessive discharge and overcharge.

SOLSUM and SOLARIX charge regulators are chosen for Omega Type Solar Charge Station.

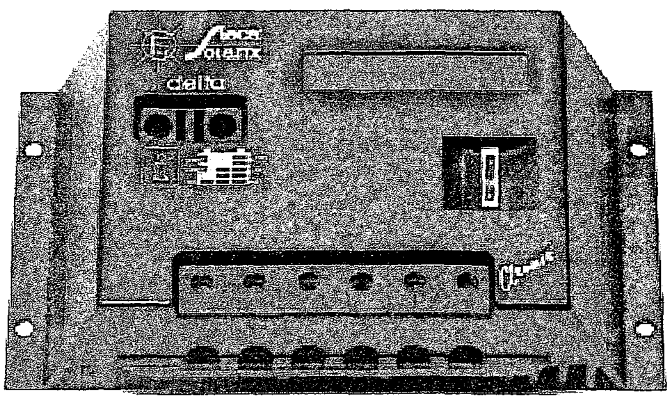

Figure 5.10 Solarix Charge Regulator.

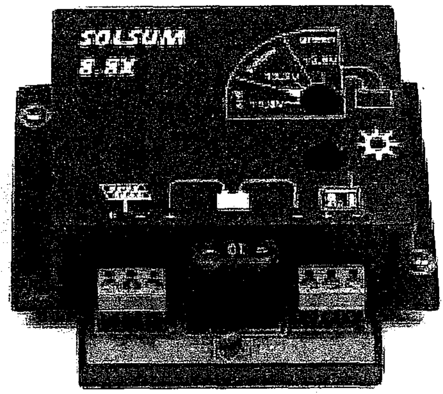

Figure 5.11 Solsum Charge Regulator.

5.1.3 Measuring Solar Radiation and Data loggers

Solar radiation measurement has an important role in an investigation of a photovoltaic array. Since all the calculations and approximations in the world cannot yield exact predictions of the amount of sunlight that will fall on a given surface at a given angle at a given time at a given day in a given place, the design of photovoltaic system is dependent upon the use of data based on measurements averaged over a long time [4]. In order to collect solar radiation data pyranometers are used and data loggers to log these measurements.

5.1.3.1 Pyranometer

It is better to consider radiation in two wavelength ranges. **Solar**, or **short wave**, radiation is radiation originating from the sun. It is in the wavelength range of 0.3 to 3μm. **Long-wave radiation** is originating from sources at temperatures near ordinary ambient temperatures and thus at wavelengths higher than 3μm.

Instruments for measuring solar radiation are of two basic types.

A **pyrheliometer** is an instrument using a collimated detector for measuring solar radiation from the sun and from a small portion of the sky around the sun at normal incidence.

Pyranometers are designed to measure total (direct and diffuse) radiation. They are normally mounted horizontally to collect general data for global radiation on a horizontal surface. However, it is also often mounted in the plane of a photovoltaic collector in order to measure the global radiation incident on the inclined surface. When shaded from direct radiation by shade ring or disc, a pyranometer measures diffuse radiation. For Omega Type Solar Charge Station, the plane of array is not stationary. Every photovoltaic module has different surface azimuth angle and a different inclination angle, so it is decided to use the measurements of a horizontally mounted pyranometer to determine the system performance parameters. The measured values are than converted to inclined values by using the necessary equations given in the Theory, Section 2.1.5.1.

Two types of measured values are used for the photovoltaic station system performance investigations that are

- *IZTECH Measurements and*
- *Omega Type Solar Charge Station Measurements.*

The pyranometer in Iztech is a first class thermopile pyranometer from Kipp & Zonen, CM6B. The CM6B Pyranometer is suitable for the routine measurement of incoming global solar radiation (0.3 to 2.8 μm spectral range), diffuse sky irradiance measurements, and surface reflected solar radiation measurement research [9]. The image of the pyranometer is shown in Figure 5.12.

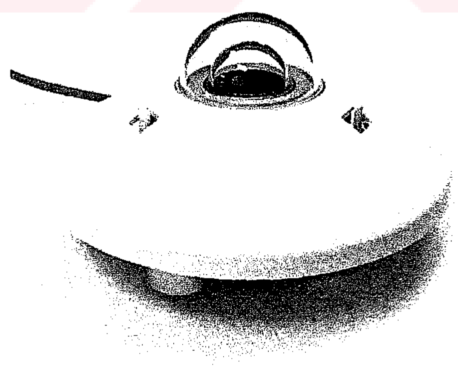

Figure 5.12 Kipp & Zonen Pyranometer used in IZTECH solar radiation measurements [36].

In Omega Type Solar Charge Station Measurements a pyranometer from Apogee Instruments is used, namely Silicon Pyranometer Sensor (model PYR). This sensor measures the radiation between 300 and 1100 nanometers, which includes most of the shortwave radiation reaching the Earth's surface. The Pyranometer is calibrated to provide an output of about 0.25 mV per W m^{-2}. This results in a full-scale output of about 0.25 volts in full sunlight (1000 W m^{-2}). A calibration certificate is provided with the sensor, Figure 5.13 [10].

Figure 5.13 Silicon Pyranometer Sensor used in Photovoltaic Station solar radiation measurements [37].

This sensor offers good accuracy at a low cost, but potential sources of error can occur. The biggest error is often caused by small changes in the position of the sensor. The sensor must be exactly horizontal for the most accurate measurement. A comparison between an Eppley pyranometer and the silicon pyranometer is shown in Figure 5.14.

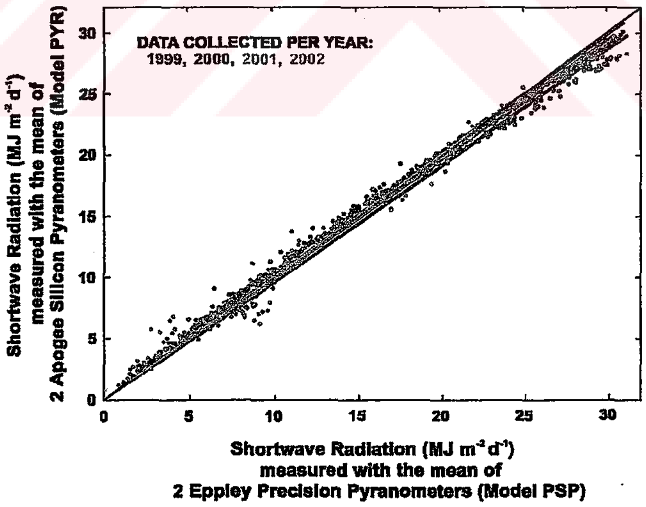

Figure 5.14 Comparison between an Eppley pyranometer and the silicon pyranometer [37].

5.1.3.2 Data logger

Solar Radiation measurements are to be done periodically to be meaningful. In order to collect the data from the measuring devices like amperemeters, voltmeters or pyranometers **data loggers** are used. In Omega Type Solar Charge Station two HOBO H8 data loggers are used, one with a 4 external entry and one with a temperature and humidity sensor and 2 external entry, Figure 5.15 [29].

Figure 5.15 Humidity and temperature plus 2 external entry data logger [35].

In order to launch the data logger and take the readings from it a program software called Boxcar is used. A screen view from the program is shown in Figure 5.16.

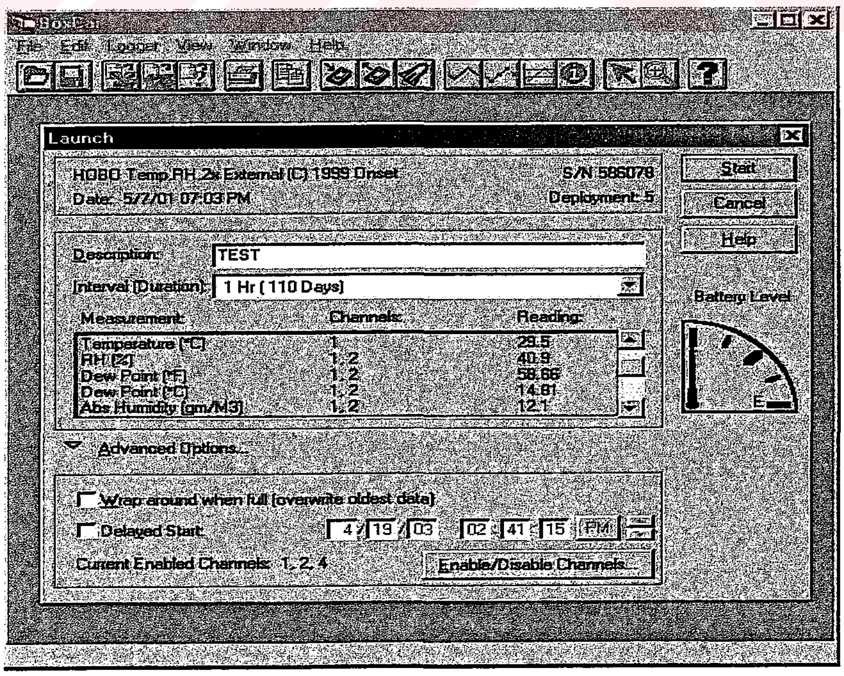

Figure 5.16 Screen view from the Boxcar Software for the Hobo data logger [38].

Important specifications for the data logger are listed below.

- Capacity: 7943 measurements total
- User-selectable sampling interval: 0.5 seconds to 9 hours, recording times up to 1 year
- Internal temperature sensor on 4" wire can extend from case
- Eternal inputs accept external sensors for temperature, AC current, 4-20 mA and 0-2.5 Volts DC [35].

5.1.4 Multimeters, Loads and Wring

To measure the incident voltage and the current through the array and a single photovoltaic module digital multimeters are used.

Technicians in Iztech Campus had done all the necessary connections and wiring of the experiment station. 6mm^2 wire is used to prevent voltage drops and the distance between the photovoltaic modules and the measurement devices is kept short.

12 Volt 50 Watt halogen lamps are used as the load. Photovoltaic modules create DC current and if loads that work with AC current (TVs, radios, refrigerators, etc.) will be used in an application, an inverter must be added to the system to convert DC to AC current.

5.2 Experimental Procedure

The experiment station to investigate the behavior of Omega Type Solar Charge Station is given in Figure 5.17. The experiment station includes photovoltaic generator having sixteen photovoltaic modules oriented as if they create an omega shape as explained in Chapter 5.1.1, a lead-acid battery to store the electricity generated by the generator, which is 150Ah, five charge regulators protecting the battery from overcharging and discharging, halogen lamps to spend the dc electricity generated by the photovoltaics during day and also night.

The station constructed on the Classrooms Building on Engineering Faculty in late July 2003. The electrical connections took 3 weeks and the measurements started at 20.08.2003 after some trials of the system.

For the measurements, which are used to investigate the charge station, two data loggers and four digital multimeters are used. The measurements carried out by both manually using four digital multimeters and using two data loggers. One data logger having temperature and humidity sensor measures solar radiation by a pyranometer as shown in the Figure 5.17. The other one measures the current intensities reaching to five charge controllers. The voltage values are read from digital multimeters manually.

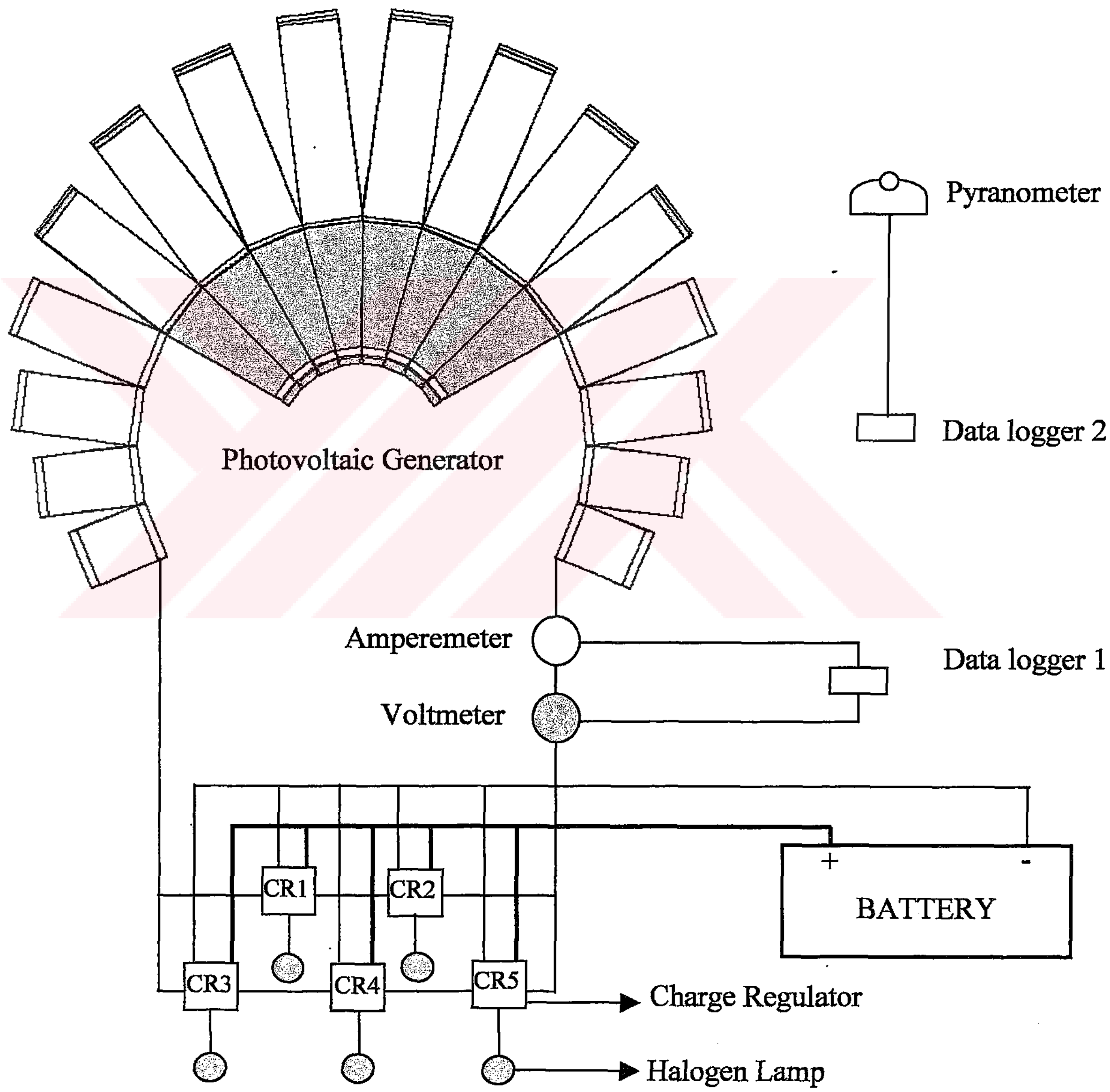

Figure 5.17 Experiment Station.

When the photovoltaic panels are connected in series the system current stays constant and voltage increases. If the opposite is done, the modules are connected in parallel, then system current increases and voltage stays constant.

In Omega Type Solar Charge Station the photovoltaic modules of the generator are connected parallel since the regulators and battery work with 12 V. This caused an increase in current. After several measurements of the system voltage it is seen that the voltage varies slightly which can be considered as constant

The connections of the generator, charge regulator, battery and loads are shown in Figure 5.18.

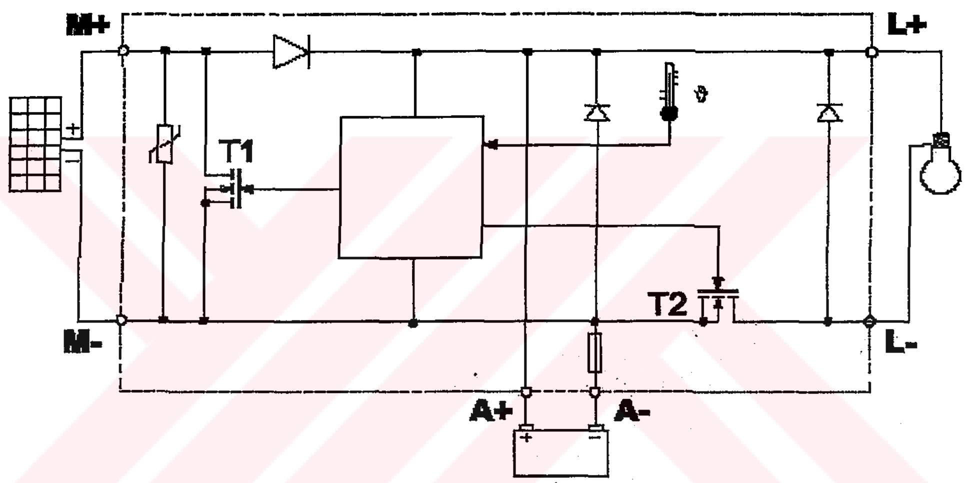

Figure 5.18 Generator, Charge Regulator, Battery and Load connections of the system.

As mentioned, when photovoltaic modules are connected in parallel than the system current increases. Considering the maximum current which can occur from sixteen photovoltaic modules, it is realized that one charge regulator cannot be enough to handle the system, since one of them has a 10A fuse. With five of them, the system can handle a 50A maximum current.

Chapter 6

RESULTS AND DISCUSSIONS

6.1 Theoretical Evaluation

In order to demonstrate the behavior of Omega Type Solar Charge Station, comparisons with different stations are done theoretically for a year period. The results are followed.

Figure 6.1 shows the difference between midpoint rule and hourly and daily integration methods used to calculate extraterrestrial radiation that falls on the solar charge stations.

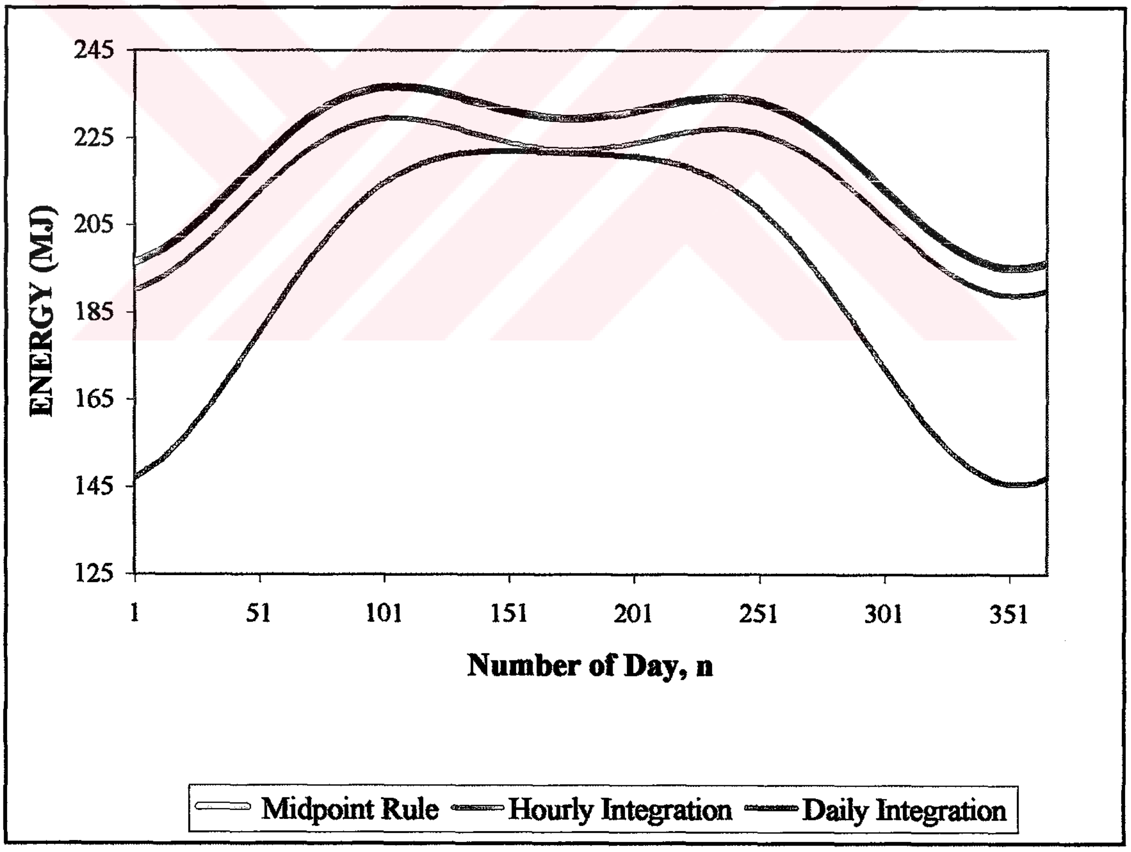

Figure 6.1 Comparison of Extraterrestrial Solar Radiation Calculation Methods; Midpoint Rule, Hourly Integration, Daily Integration.

The figure is based on the values calculated for Omega Type Solar Charge Station. Although we obtain more accurate results from integration, we have to use midpoint results explained with Figure 4.3 in order to calculate total radiation including extraterrestrial solar radiation collected by the modules and radiation reflected by the reflectors to the modules since instantaneous reflected energy is calculated. From Figure 4.3 we understand that the results from three methods are close in summer and far in winter.

Extraterrestrial solar radiation for the modules and reflected energy calculations are done for every day of the year but only the data for the days, which are given in Table 3.1 are used to plot the necessary graphs to prevent data crowd.

6.1.1 Omega Type Solar Charge Station; First Combination

Energy falling on to the whole Omega Type Solar Charge Station with inclination angles, β, and surface azimuth angles, γ, given in Table 5.1 and Figure 5.2 is shown in Figure 6.1.

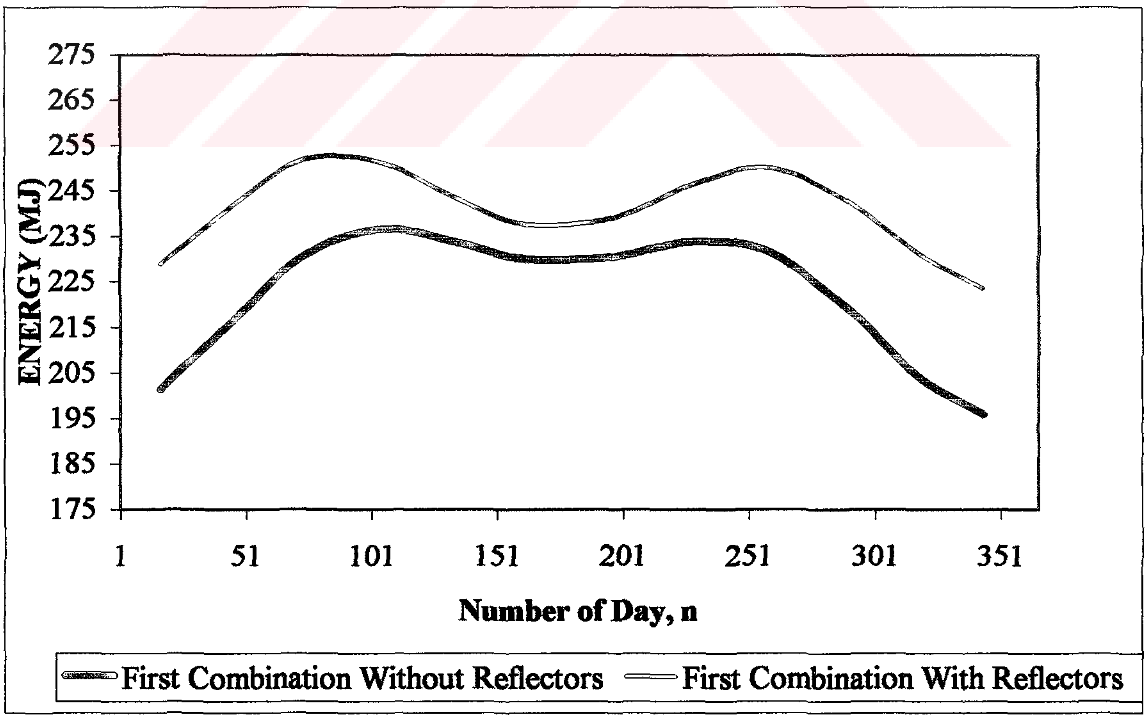

Figure 6.2 Theoretical hourly average daily extraterrestrial solar radiation for a year period for Omega Type Solar Charge Station with and without reflectors.

The effect of reflectors is high during winter and less in summer. According to the design of the station more energy is obtained during summer. The usage of reflectors affects our linear energy desire in a positive manner.

6.1.2 South Facing Solar Charge Station with Different Inclination Angles; Second Combination

Energy falling on to the whole south facing solar charge station with different inclination angles, β, and surface azimuth angles, γ, given in Table 6.1 is shown in Figure 6.3.

Table 6.1 Orientation and the slope of the photovoltaic modules for south facing solar charge station with different inclination angles: γ, azimuth angle; β, slope of the module.

Module No.	γ(°)	β(°)
1	0	30
2	0	36
3	0	42
4	0	48
5	0	54
6	0	60
7	0	66
8	0	72
9	0	30
10	0	36
11	0	42
12	0	48
13	0	54
14	0	60
15	0	66
16	0	72

South facing stations are most commercial stations since the Sun continues its path from East via South to West. Facing all the modules to South has some problems including shading affect and more area requirement. Second Combination's modules have the same inclination angles with the Omega Type Solar Charge Station so we can understand the affect of surface azimuth angle. Figure 6.4 is the comparison of First and Second combination solar charge stations.

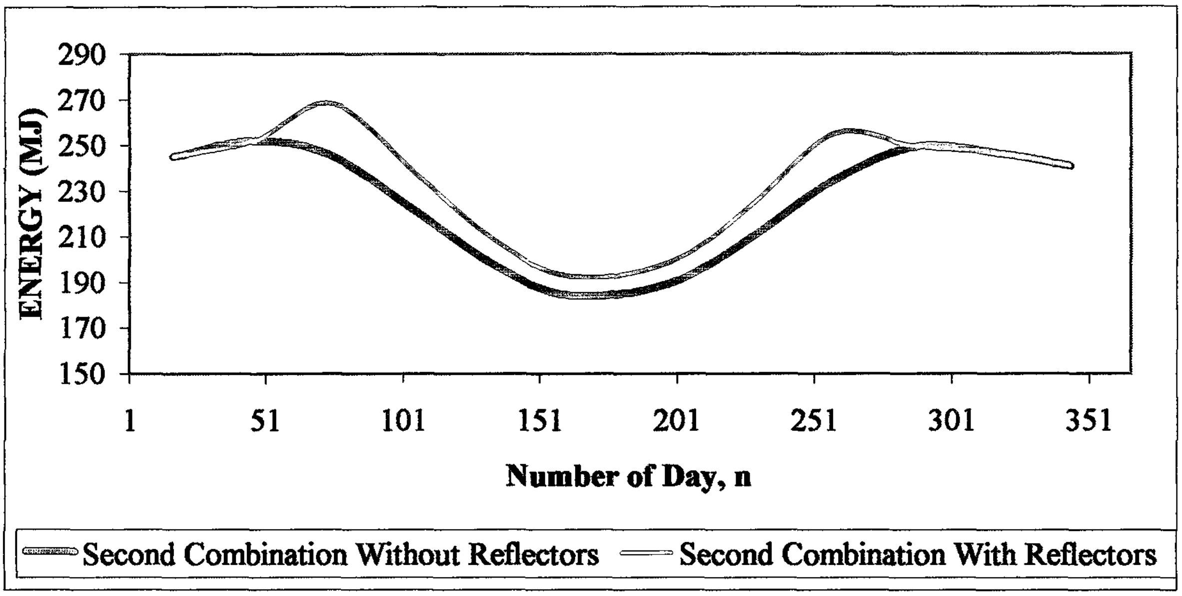

Figure 6.3 Theoretical hourly average daily extraterrestrial solar radiation for a year period for south facing solar charge station with different inclination angles with and without reflectors.

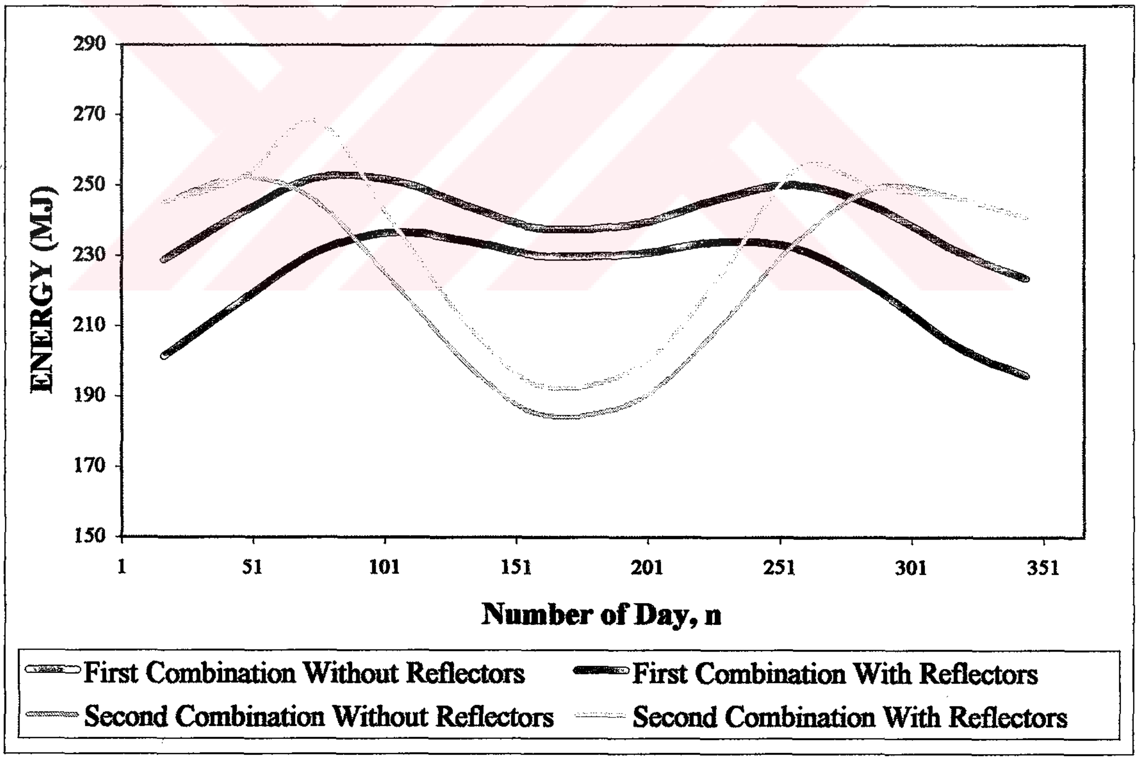

Figure 6.4 Comparison of hourly average daily extraterrestrial solar radiation for a year period for First and Second Combinations with and without reflectors.

Second Combination's advantage is more energy collection during winter compared to first combination but in summer it is very low. The affect of reflectors to the second combination is very low in summer and it has no affect in winter. It is useless to use reflectors for this combination. The oscillation of energy in year is very high so it is not suitable for a commercial application.

6.1.3 South Facing Solar Charge Station with Fixed Inclination Angles; Third Combination

Energy falling on the whole south facing solar charge station with fixed inclination angles, β, and surface azimuth angles, γ, given in Table 6.2 is shown in Figure 6.5.

Table 6.2 Orientation and the slope of the photovoltaic modules for south facing solar charge station with different inclination angles: γ, azimuth angle; β, slope of the module.

Module No.	γ(°)	β(°)
1	0	38,46
2	0	38,46
3	0	38,46
4	0	38,46
5	0	38,46
6	0	38,46
7	0	38,46
8	0	38,46
9	0	38,46
10	0	38,46
11	0	38,46
12	0	38,46
13	0	38,46
14	0	38,46
15	0	38,46
16	0	38,46

In solar energy applications South-facing surfaces with the inclination angles same as the latitude of the application place are mostly used. According to Figure 6.5 we can understand the reason since the energy collected by the third combination solar charge station is considerably high. Although it is high, we need to compare it with Omega Type Solar Charge Station.

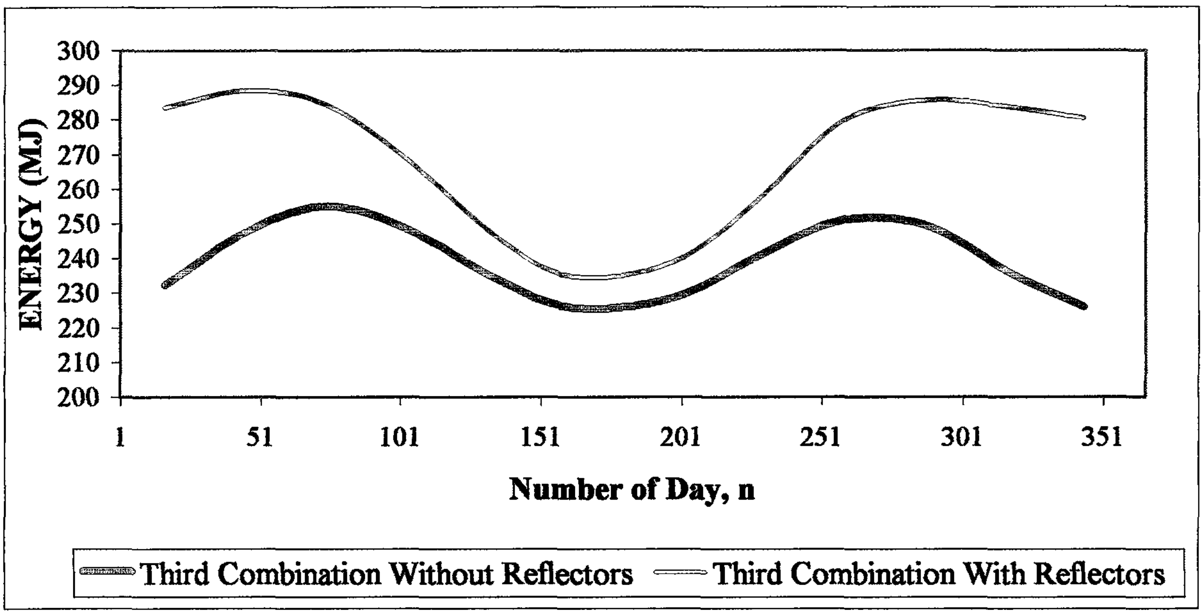

Figure 6.5 Theoretical hourly average daily extraterrestrial solar radiation for a year period for south facing solar charge station with different inclination angles with and without reflectors.

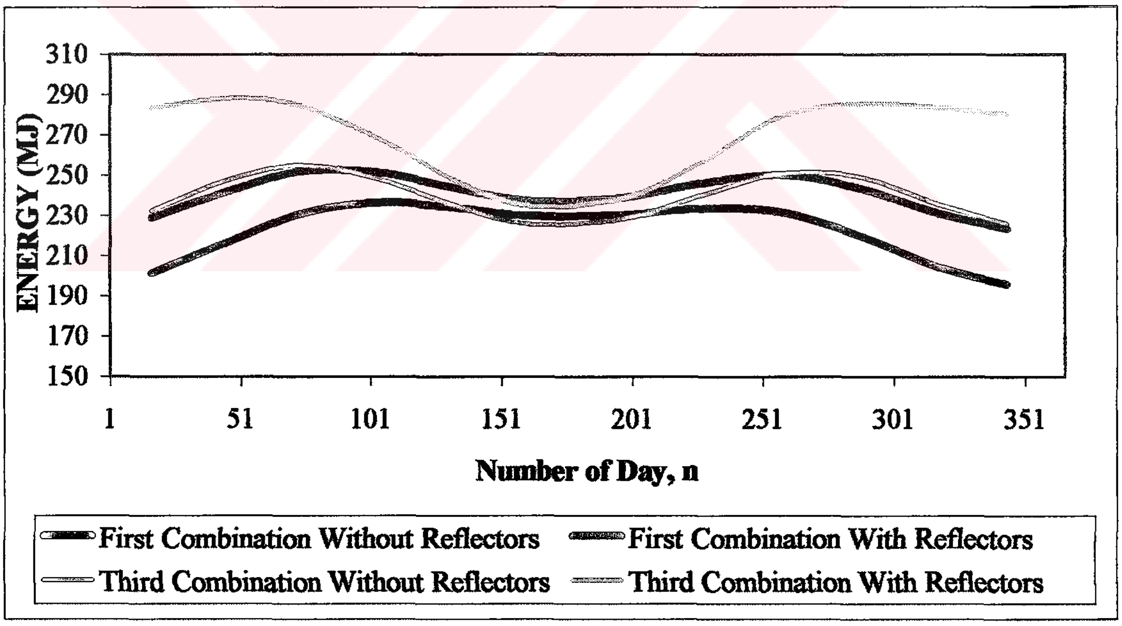

Figure 6.6 Comparison of hourly average daily extraterrestrial solar radiation for a year period for First and Third Combinations with and without reflectors.

From Figure 6.6 it is seen that South Facing charge station with fixed inclination angles without reflectors has higher energy collection compared to Omega Type Charge Station without reflectors. If we consider the stations with reflectors we see that Omega

Type Station with reflectors has a very close energy collection value to South Facing without reflectors. Considering the need for a linear energy through a year period Omega Type Station with reflectors is more efficient than South Facing with reflectors.

6.1.4 Inverse of Omega Type Solar Charge Station; Fourth Combination

Energy falling on to the whole inverse of Omega Type Solar Charge Station with inclination angles, β, and surface azimuth angles, γ, given in Table 6.3 and is shown in Figure 6.7.

Table 6.3 Orientation and the slope of the photovoltaic modules for inverse of omega type solar charge station: γ, azimuth angle; β, slope of the module.

Module No.	γ(°)	β(°)
1	7,5	72
2	22,5	66
3	37,5	60
4	52,5	54
5	67,5	48
6	82,5	42
7	97,5	36
8	112,5	30
9	-7,5	72
10	-22,5	66
11	-37,5	60
12	-52,5	54
13	-67,5	48
14	-82,5	42
15	-97,5	36
16	-112,5	30

Inverse of Omega Type Station has the same characteristic energy plot through a year period. The reflected energy is high during winter and less in summer, Figure 6.7.

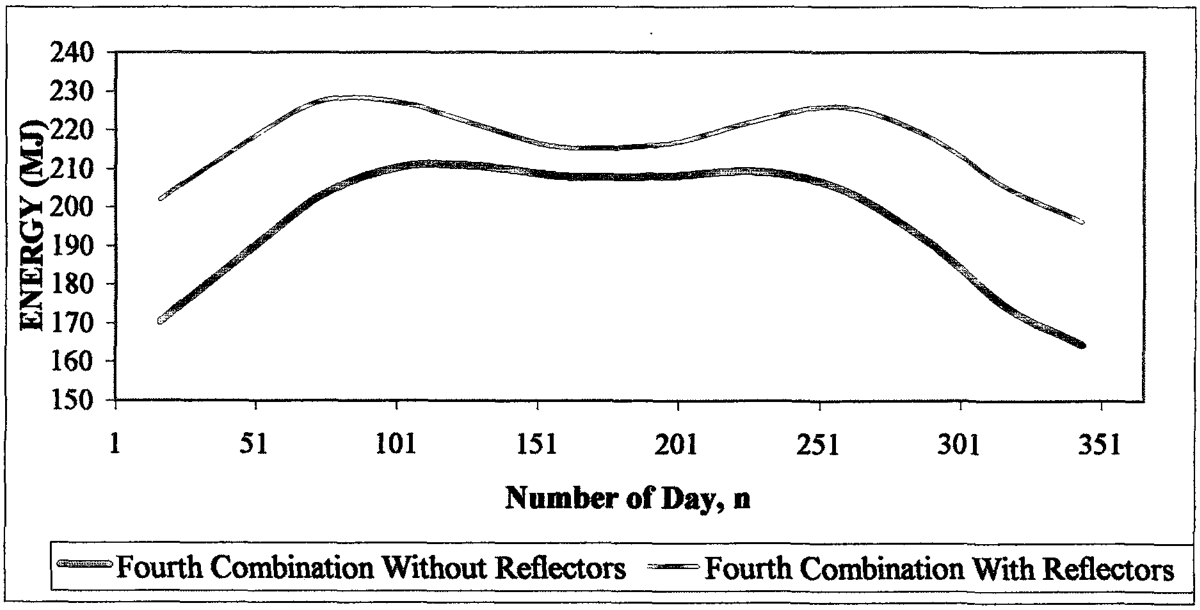

Figure 6.7 Theoretical hourly average daily extraterrestrial solar radiation for a year period for inverse of omega type solar charge station with and without reflectors.

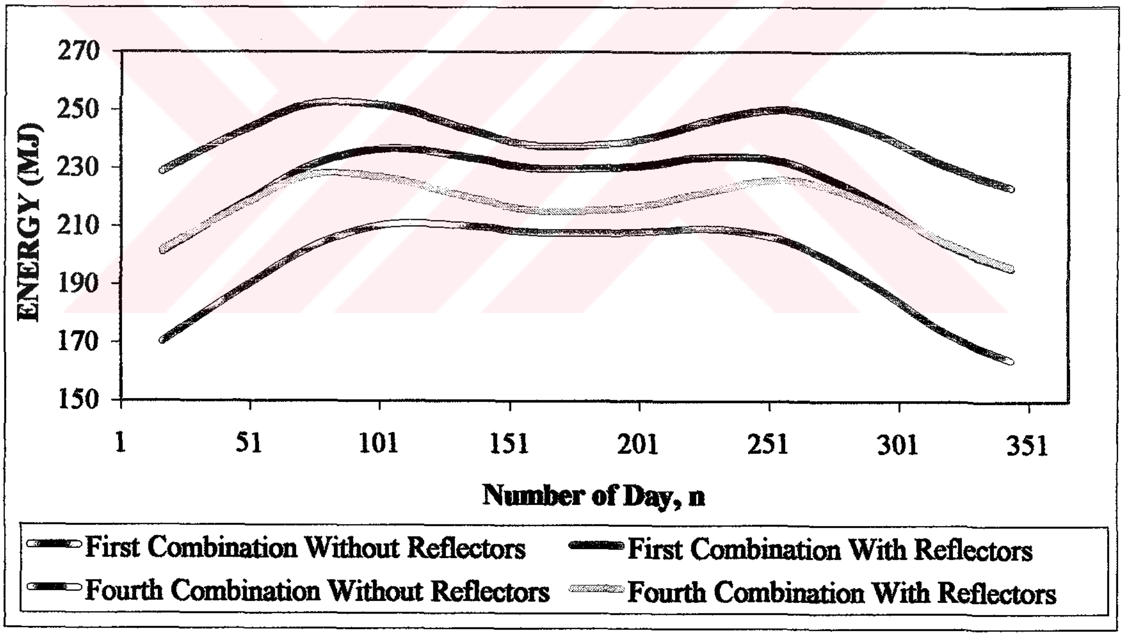

Figure 6.8 Comparison of hourly average daily extraterrestrial solar radiation for a year period for First and Fourth Combinations with and without reflectors.

If the station is compared with Omega Type Station it is seen that it has a quite less energy collection. The surface azimuth angles of the stations are same. Thinking the first modules of the both stations, having a surface azimuth angle of 7.5° and β=30° for Omega Type Station and β=72° for Inverse of Omega Type Station we understand the reason of "less energy collection" seen in Figure 6.8. From Equation (3.29) we know that extraterrestrial solar radiation falling an inclined surface is directly proportional to the cosine of incidence angle. At solar noon (where (γs-γ) value is smaller for the module) the incidence angle is high and cosine of the incidence angle reaches to 1. If the inclination of the surface is increased than the incidence angle reduces so does the cosine of incidence angle. The result is less energy falling on the surface. This is also valid for the modules having higher surface azimuth angles. Inverse of Omega Type Solar Charge Station's eighth module has a surface azimuth of 112.5° and an inclination angle of 30°. For sunrise or sunset hour angles (where (γs-γ) value is smaller for the module) cosine of incidence angle is less for the surfaces having less inclination angles.

6.1.5 Comparison of First, Second Third and Fourth Combinations

Figure 6.9 is the plot of First, Second, Third and Fourth Combination solar charge stations without reflectors.

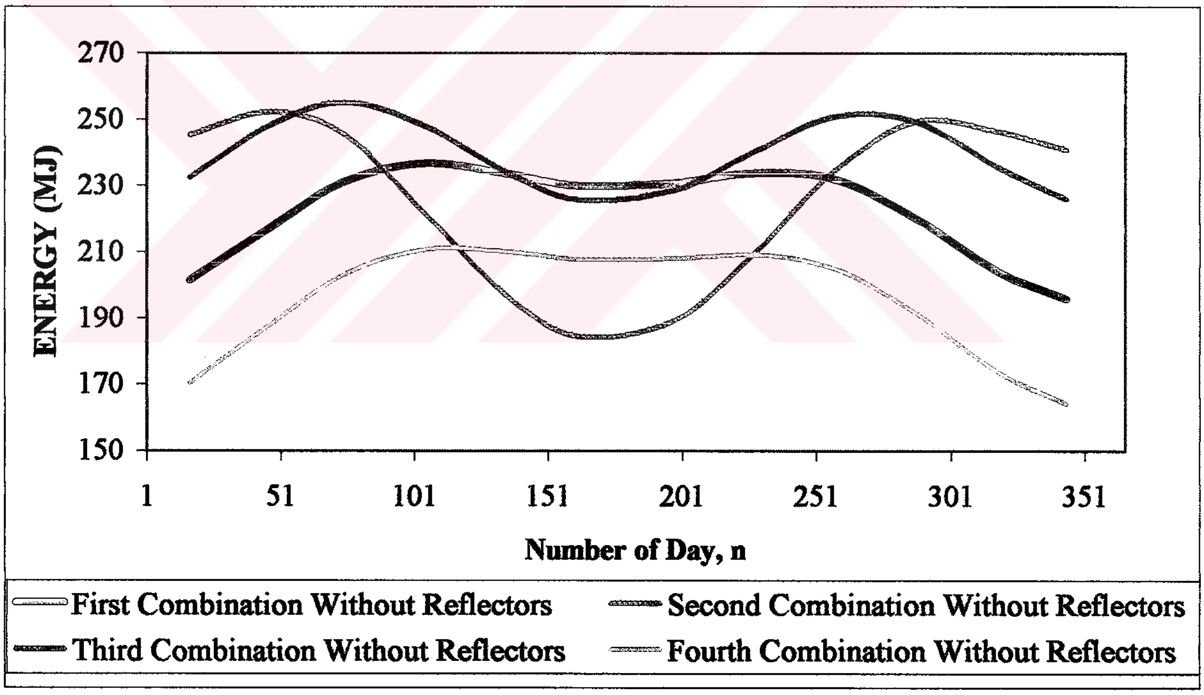

Figure 6.9 Comparison of theoretical hourly average daily extraterrestrial solar radiation falling to the solar charge stations, First, Second, Third and Fourth Combinations without reflectors for a year period.

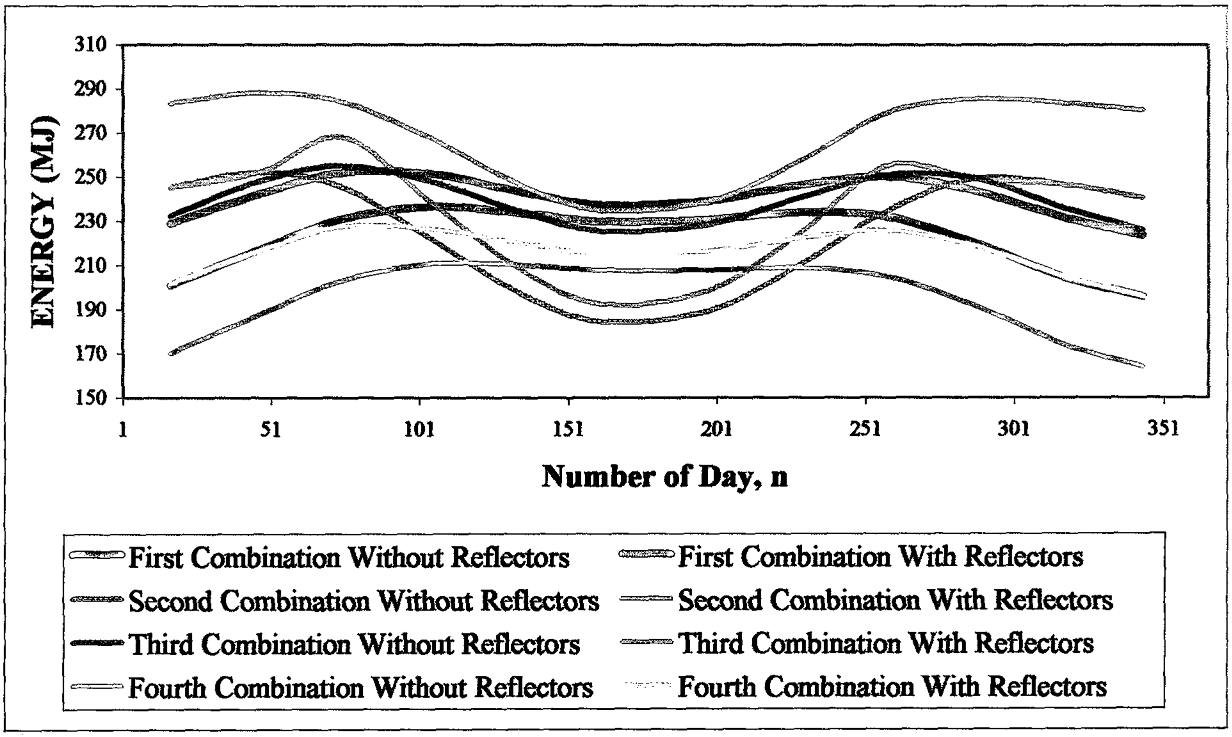

Figure 6.10 Comparison of theoretical hourly average daily extraterrestrial solar radiation falling to the solar charge stations, First, Second, Third and Fourth Combinations with and without reflectors for a year period.

Figure 6.10 includes four types of combinations with and without reflectors. Although the graph is complex, the curve representing Omega Type Solar Charge Station with reflectors can be noticed easily. The oscillation of the curve is very low and it is the most linear one. The curve for south facing station with fixed angles and reflectors, third combination, shows an increase in winter but it has a huge difference between summer and winter and it is not stable.

Figure 6.11 is a plot for the energy gain from reflectors through a year period. It is less in summer and higher in winter. This result is valuable since energy collection by the modules in winter is lower than summer. Reflectors can close this gap.

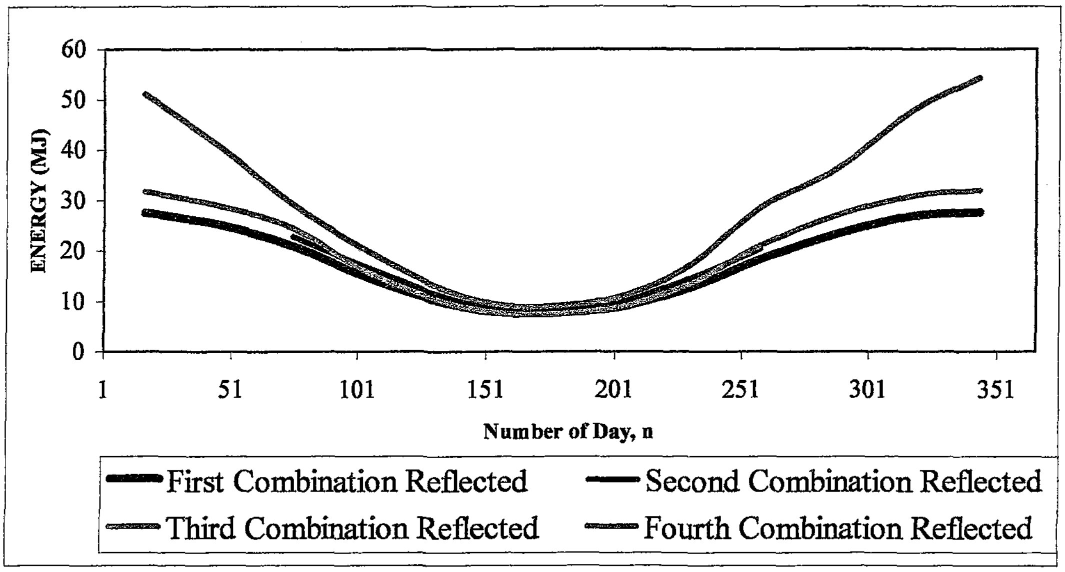

Figure 6.11 Comparison of hourly average daily extraterrestrial solar radiation falling to the solar charge stations, first, second, third and fourth combinations from the reflectors for a year period.

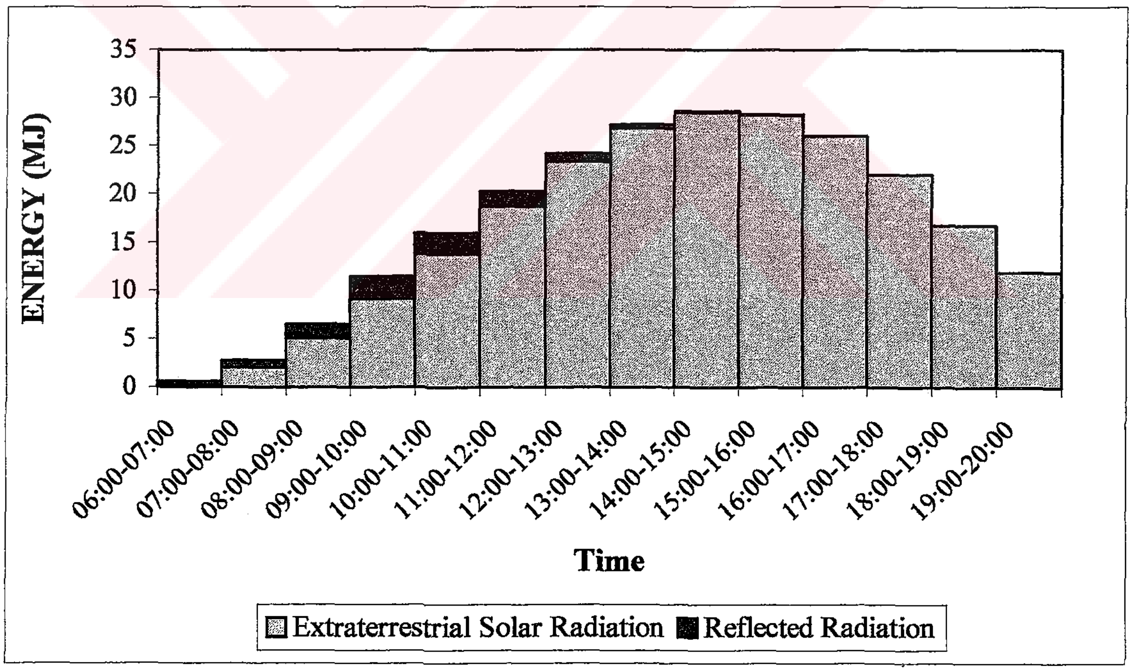

Figure 6.12 Daily Extraterrestrial Solar Radiation Falling on Omega Type Solar Charge Station and Reflected Energy from Reflectors for 20th of March, theoretically.

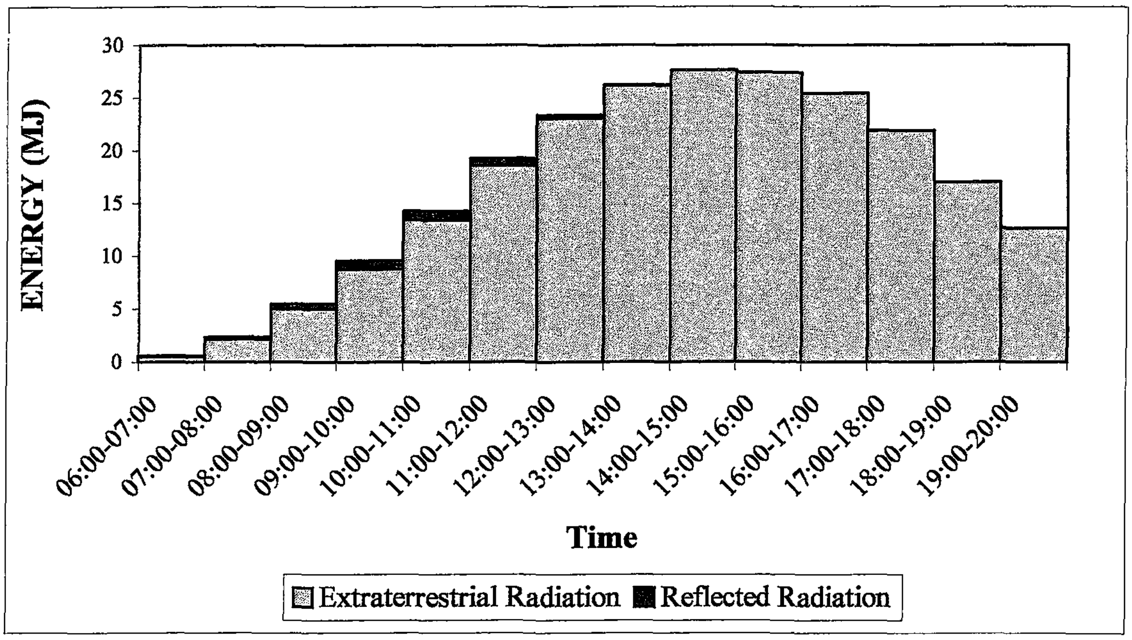

Figure 6.13 Daily Extraterrestrial Solar Radiation Falling on Omega Type Solar Charge Station and Reflected Energy from Reflectors for 22nd of September, theoretically.

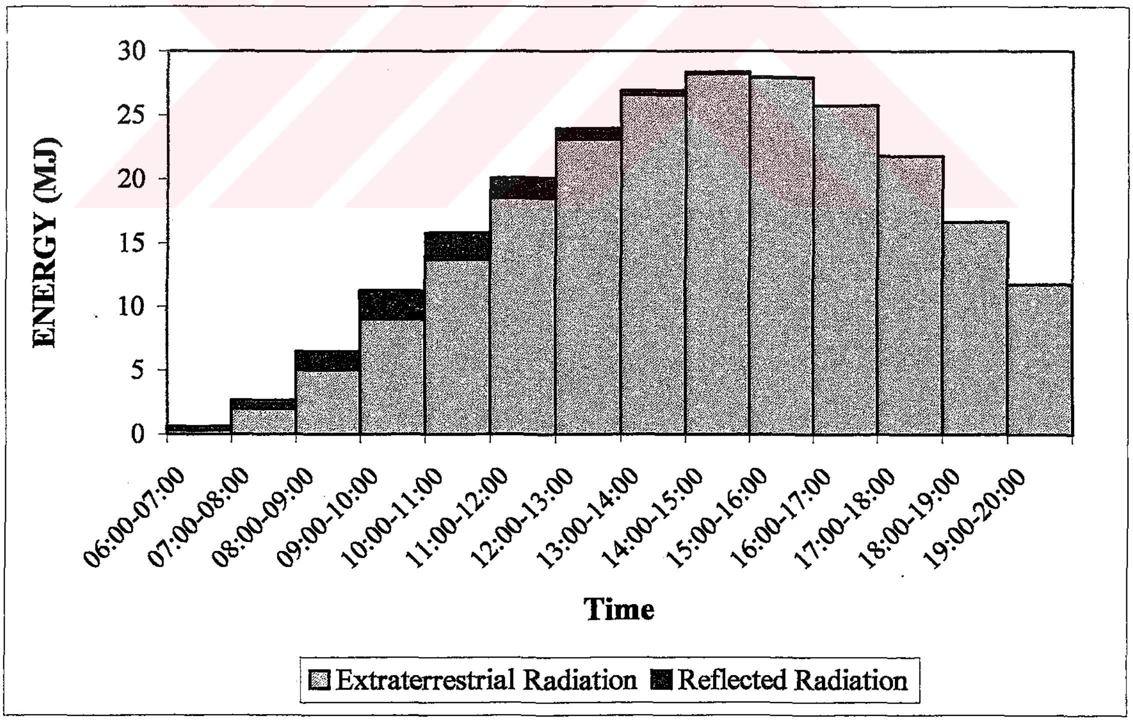

Figure 6.14 Daily Extraterrestrial Solar Radiation Falling on Omega Type Solar Charge Station and Reflected Energy from Reflectors for 21st of June, theoretically.

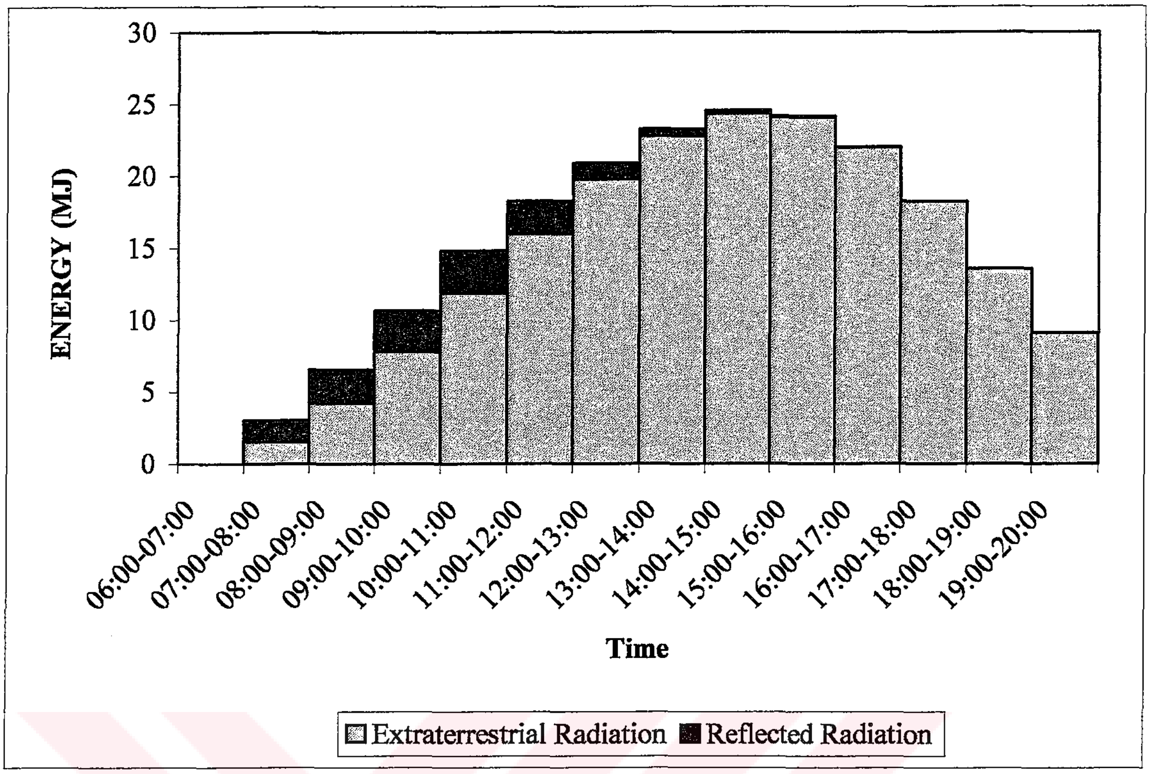

Figure 6.15 Daily Extraterrestrial Solar Radiation Falling on Omega Type Solar Charge Station and Reflected Energy from Reflectors for 21st of December, theoretically.

Figures 6.12, 6.13, 6.14 and 6.15 show the effect of reflectors during the day, which are chosen for theoretical calculations. According to the figures, again, we can say that energy collection during winter is high. The characteristics of all the graphs are same. They have their maximum on the time interval of 15:00 and 16:00. Reflectors affect the energy collection during morning and they balance the energy collection difference between morning and afternoon hours.

6.1.6 Omega Type Solar Charge Station with Optimum Inclination Angles; Fifth Combination

The angles, which daily average monthly extraterrestrial solar radiation values become higher are calculated and are shown in Table 6.4. by this new inclination angle combination an extra energy is obtained,

Table 6.4 Surface Azimuth and calculated optimum inclination angles for the Omega Type Solar Charge Station by using daily average monthly extraterrestrial solar radiation values.

		January	February	March	April	May	June
Module No	γ	β	β	β	β	β	β
1	7,5	65	56	42	24	7	0
2	22,5	64	55	42	25	7	0
3	37,5	61	53	41	25	8	0
4	52,5	57	50	39	25	8	0
5	67,5	53	46	36	21	6	0
6	82,5	45	36	24	10	2	0
7	97,5	0	0	0	0	0	0
8	112,5	0	0	0	0	0	0
9	-7,5	65	56	42	24	7	0
10	-22,5	64	55	42	25	7	0
11	-37,5	61	53	41	25	8	0
12	-52,5	57	50	39	25	8	0
13	-67,5	53	46	36	21	6	0
14	-82,5	45	36	24	10	2	0
15	-97,5	0	0	0	0	0	0
16	-112,5	0	0	0	0	0	0
		July	**August**	**September**	**October**	**November**	**December**
Module No	γ	β	β	β	β	β	β
1	7,5	65	56	42	24	7	0
2	22,5	64	55	42	25	7	0
3	37,5	61	53	41	25	8	0
4	52,5	57	50	39	25	8	0
5	67,5	53	46	36	21	6	0
6	82,5	45	36	24	10	2	0
7	97,5	0	0	0	0	0	0
8	112,5	0	0	0	0	0	0
9	-7,5	65	56	42	24	7	0
10	-22,5	64	55	42	25	7	0
11	-37,5	61	53	41	25	8	0
12	-52,5	57	50	39	25	8	0
13	-67,5	53	46	36	21	6	0
14	-82,5	45	36	24	10	2	0
15	-97,5	0	0	0	0	0	0
16	-112,5	0	0	0	0	0	0

6.2.1 Omega Type Solar Charge Station Experiments with Reflectors

Photovoltaic generator of the Omega Type Solar Charge Station with Reflectors is shown in Figure 6.17.

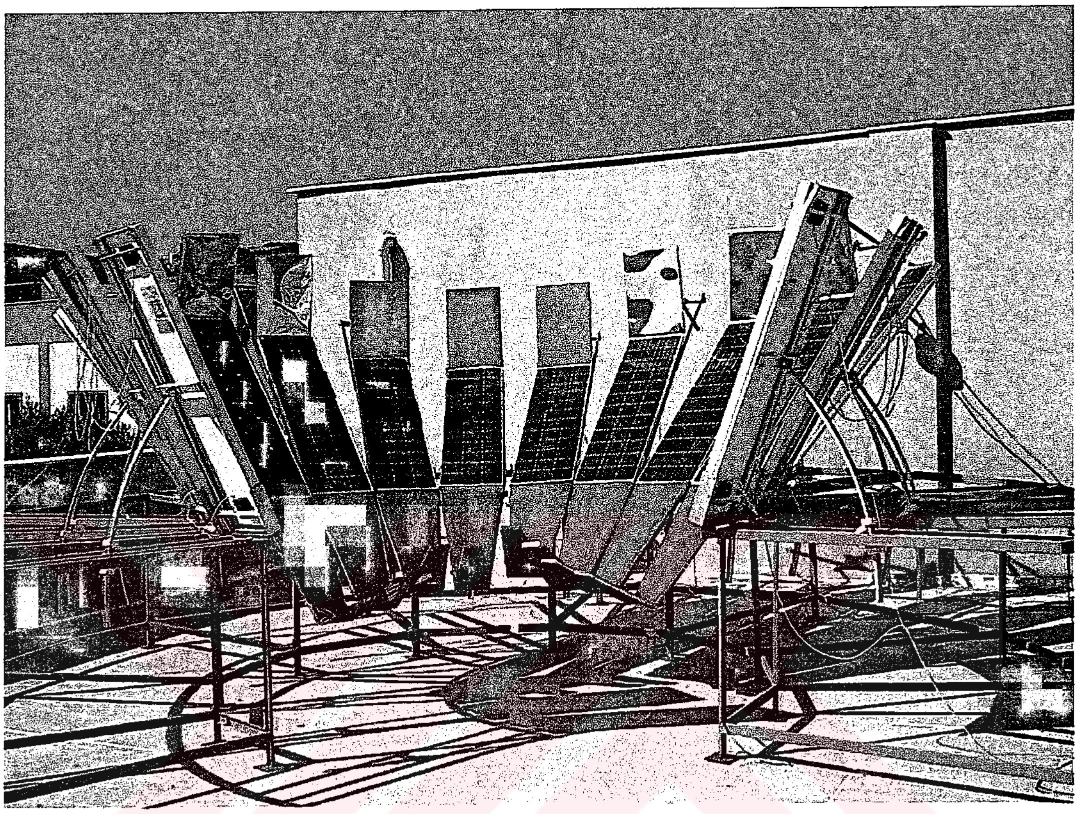

Figure 6.17 Omega Type Solar Charge Station Experiments with Reflectors.

6.2.1.1 Direct Radiation Data from Pyranometer Reading

Solar Radiation data taken from pyranometers are the instant total solar radiation data and direct and diffuse components of the total solar radiation must be calculated in order to know the photovoltaic systems efficiency. According to the procedure given in Section 3.1.6.1 hourly direct solar radiation is calculated by total solar radiation data taken from pyranometer measurements (Equations (3.53) (3.54) (3.55) (3.56)). Pyranometer measurements are given for 21.08.2003 in Table 6.5.

Table 6.5 Total Solar Radiation Data taken from Pyranometer, 21.08.2003.

Date/Time	Measured Values (V)	Measured Total Solar Radiation (W/m2)
21/08/03 06:30	0.005	19.85
21/08/03 07:30	0.015	59.55
21/08/03 08:30	0.024	95.28
21/08/03 09:30	0.151	599.47
21/08/03 10:30	0.21	833.7
21/08/03 11:30	0.249	988.53
21/08/03 12:30	0.269	1067.93
21/08/03 13:30	0.269	1067.93
21/08/03 14:30	0.259	1028.23
21/08/03 15:30	0.229	909.13
21/08/03 16:30	0.181	718.57
21/08/03 17:30	0.122	484.34
21/08/03 18:30	0.054	214.38
21/08/03 19:30	0.015	59.55
21/08/03 20:30	0.005	19.85

The pyranometer sensor gives a 0.25 mV signal for 1 W/m^2, which must be multiplied by 3.97 to obtain total solar radiation data.

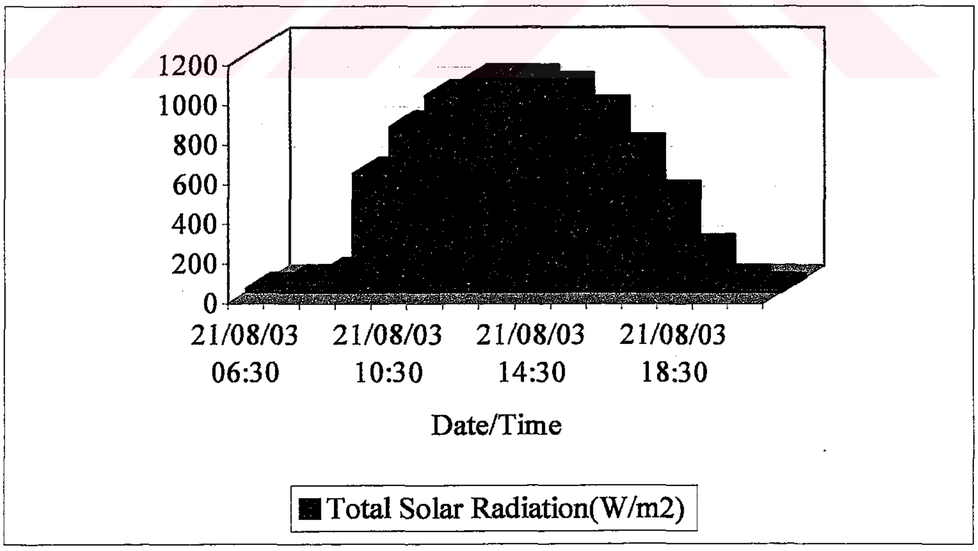

Figure 6.18 Total Solar Radiation, 21.08.2003.

Omega Type Solar Charge Station's photovoltaic generator has sixteen photovoltaic modules having different inclination and surface azimuth angles. So the direct hourly solar radiation calculated by pyranometer sensors total radiation measurements, must be converted to inclined surfaces of the photovoltaic modules. The conversion is done by Equation (3.29) given in Section 3.1.5.1. The results of the procedure explained are given for the day 21.08.2003, the 233rd (n) day of the year 2003 in Table 6.6 and Figure 6.19

Table 6.6 Direct Solar Radiation on Horizontal and Inclined Surfaces, Hourly, 21.08.2003.

Date/Time	Direct Solar Radiation on Horizontal Surface (MJ)	Direct Solar Radiation on Inclined Surface (MJ)
21/08/03 06:30	0.3891055	0.0867154
21/08/03 07:30	1.1673166	0.2865215
21/08/03 08:30	1.8677065	0.5026385
21/08/03 09:30	11.750987	3.3997417
21/08/03 10:30	16.342432	4.8681441
21/08/03 11:30	19.377455	5.8156507
21/08/03 12:30	20.933878	6.2827713
21/08/03 13:30	20.933878	6.2358608
21/08/03 14:30	20.155667	5.831345
21/08/03 15:30	17.821033	4.7960094
21/08/03 16:30	14.08562	3.4573596
21/08/03 17:30	9.494175	2.1158565
21/08/03 18:30	4.2023397	0.7821024
21/08/03 19:30	0	0
21/08/03 20:30	0	0

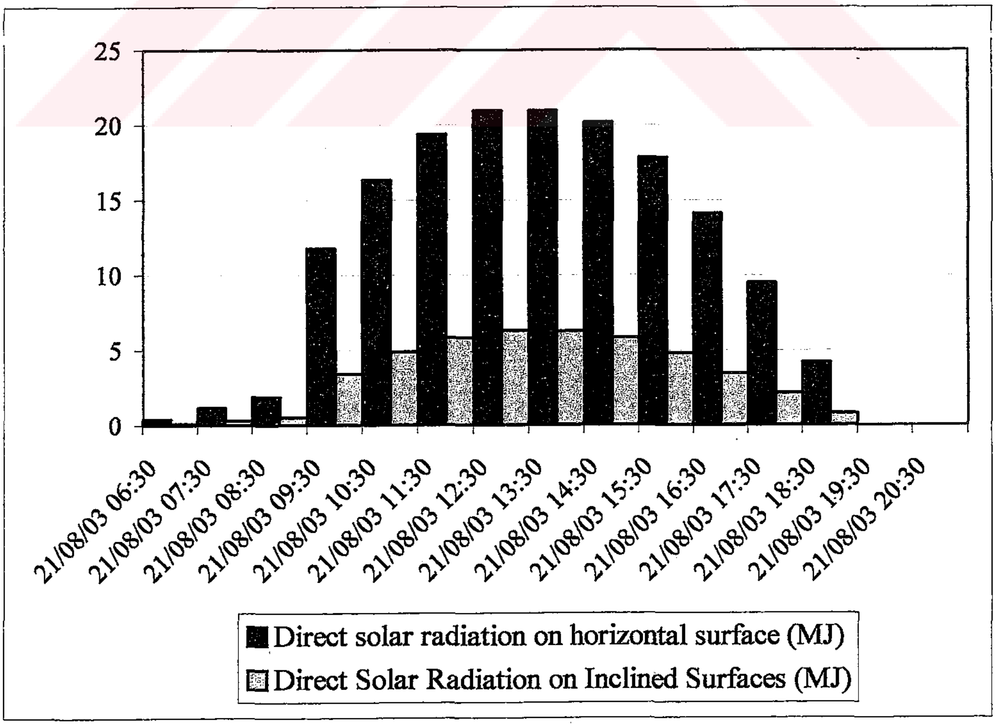

Figure 6.19 Direct Solar Radiation on Horizontal and Inclined Surfaces, Hourly.

6.2.1.2 Omega Type Solar Charge Station Efficiency

To calculate the efficiency of the Solar Charge Station, the current intensity and voltage values taken from the data loggers must be analyzed. As explained in Section 5.2 the voltage values are taken as 14 V.

As the direct solar radiation falling on the whole solar charge station and the energy taken from the station is known, the efficiency of the station can be calculated. The results are given in Table 6.8. The comparison of the calculated and measured results is shown in Figure 6.21.

By using the hourly direct solar radiation and hourly energy from charge station data, daily % efficiency of the solar charge station is calculated as 31.65315%. Calculated efficiency values for different days are given in Appendix C.

Table 6.7 Current Intensities and Power obtained from Photovoltaics on 21.08.2003.

Date/Time	Current Intensity (A)	Power (W)	Energy from photovoltaics (J), Hourly
21/08/03 06:30	0.833325	11.66655	41999.58
21/08/03 07:30	2.766639	38.732946	139438.6
21/08/03 08:30	14.499855	202.99797	730792.7
21/08/03 09:30	24.933084	349.063176	1256627
21/08/03 10:30	31.766349	444.728886	1601024
21/08/03 11:30	33.699663	471.795282	1698463
21/08/03 12:30	36.299637	508.194918	1829502
21/08/03 13:30	32.099679	449.395506	1617824
21/08/03 14:30	29.433039	412.062546	1483425
21/08/03 15:30	28.466382	398.529348	1434706
21/08/03 16:30	23.633097	330.863358	1191108
21/08/03 17:30	16.433169	230.064366	828231.7
21/08/03 18:30	4.366623	61.132722	220077.8
21/08/03 19:30	1.499985	20.99979	75599.24
21/08/03 20:30	0.833325	11.66655	41999.58

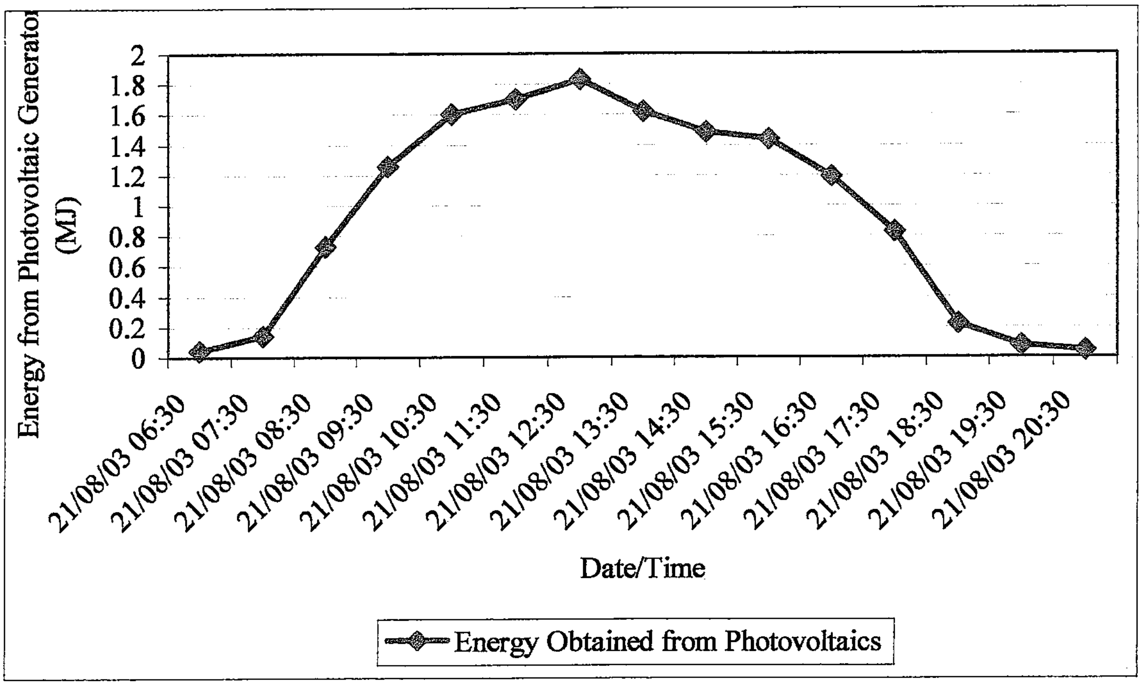

Figure 6.20 Energy Generated by Photovoltaic Generator, 21.08.2003.

Table 6.8 Solar Radiation and Efficiency, Hourly, 21.08.2003.

Date/Time	Total Solar Radiation (MJ)	Direct Solar Radiation on Horizontal Surface (MJ)	Direct Solar Radiation on Inclined Surfaces (MJ)	Energy Obtained from Photovoltaics (MJ)	%Efficiency, η_I
21/08/03 06:30	0.486381914	0.3891055	0.0867154	0.04199958	48.43380249
21/08/03 07:30	1.459145742	1.1673166	0.2865215	0.139438606	48.66601629
21/08/03 08:30	2.334633187	1.8677065	0.5026385	0.730792692	145.3912978
21/08/03 09:30	14.6887338	11.750987	3.3997417	1.256627434	36.96243862
21/08/03 10:30	20.42804038	16.342432	4.8681441	1.60102399	32.88776909
21/08/03 11:30	24.22181931	19.377455	5.8156507	1.698463015	29.20503824
21/08/03 12:30	26.16734697	20.933878	6.2827713	1.829501705	29.11934289
21/08/03 13:30	26.16734697	20.933878	6.2358608	1.617823822	25.94387336
21/08/03 14:30	25.19458314	20.155667	5.831345	1.483425166	25.43881665
21/08/03 15:30	22.27629166	17.821033	4.7960094	1.434705653	29.9145715
21/08/03 16:30	17.60702528	14.08562	3.4573596	1.191108089	34.4513801
21/08/03 17:30	11.8677187	9.494175	2.1158565	0.828231718	39.14404037
21/08/03 18:30	5.25292467	4.2023397	0.7821024	0.220077799	28.13925495
21/08/03 19:30	1.459145742	0	0	0	0
21/08/03 20:30	0.486381914	0	0	0	0

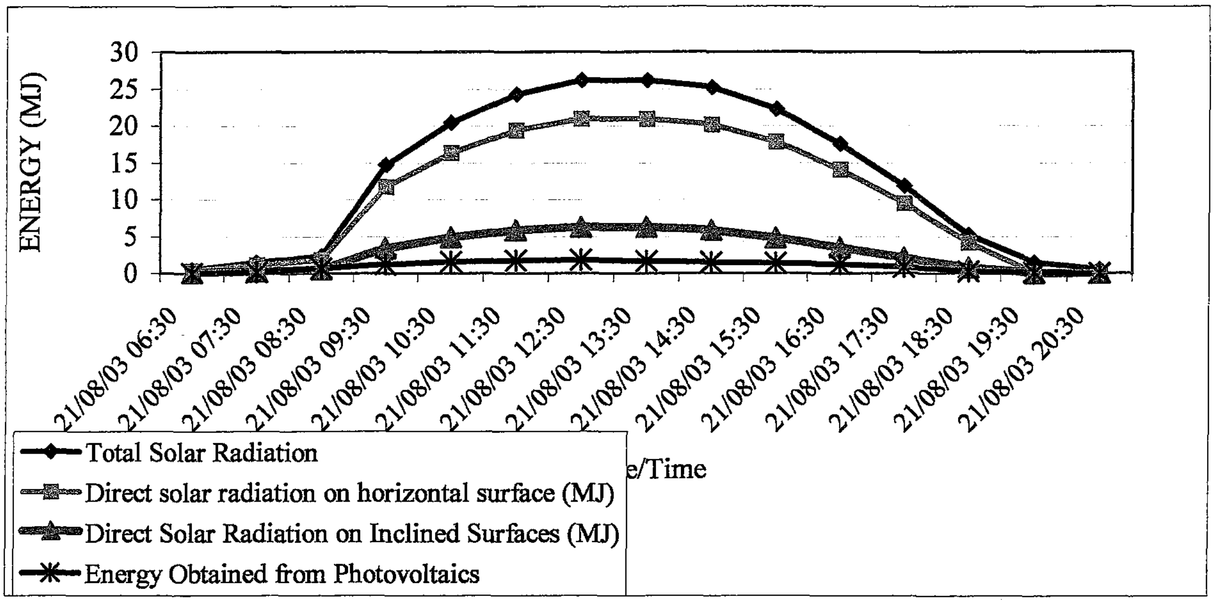

Figure 6.21 Comparison of Total Solar Radiation Data from Pyranometer, Direct Solar Radiation on horizontal and Inclined Surfaces and Energy Obtained from Solar Charge Station, 21.08.2003.

As explained in Section 4.2, Experimental Calculations, there are two different efficiency definitions that are used in this study, η and η_I. The difference is shown in Figure 6.22.

Table 6.9 Percentage Efficiencies of the Solar Charge Station, 21.08.2003.

Date/Time	% Efficiency, η_I	%Efficiency, η
21/08/03 06:30	48.43380249	8.635103156
21/08/03 07:30	48.66601629	9.556180826
21/08/03 08:30	145.3912978	31.30224894
21/08/03 09:30	36.96243862	8.555042597
21/08/03 10:30	32.88776909	7.837384103
21/08/03 11:30	29.20503824	7.012119912
21/08/03 12:30	29.11934289	6.991544489
21/08/03 13:30	25.94387336	6.182605457
21/08/03 14:30	25.43881665	5.887873426
21/08/03 15:30	29.9145715	6.440504887
21/08/03 16:30	34.4513801	6.764959268
21/08/03 17:30	39.14404037	6.978862059
21/08/03 18:30	28.13925495	4.189624124
21/08/03 19:30	0	5.181061894
21/08/03 20:30	0	8.635103156

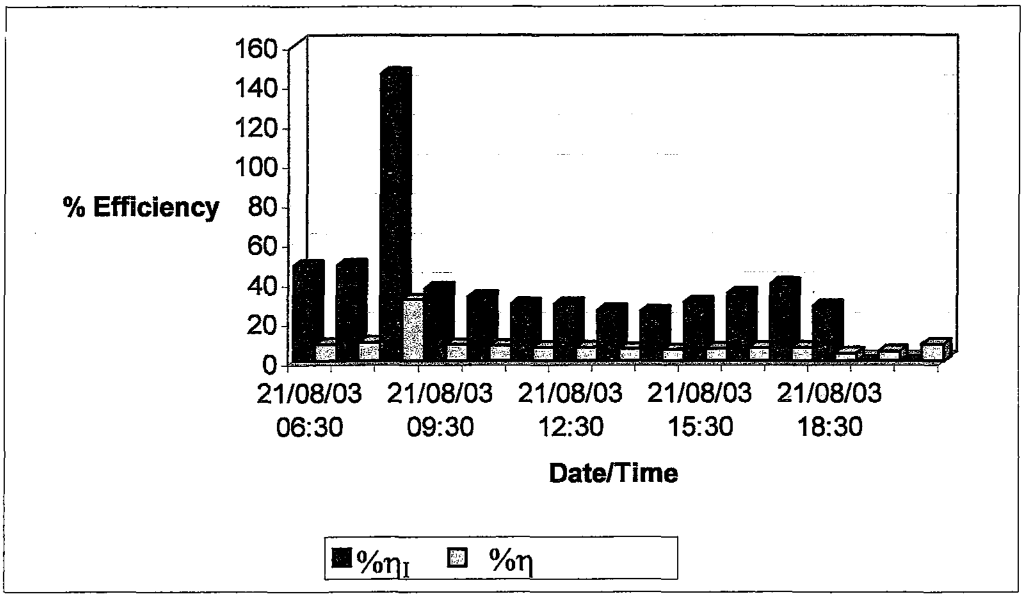

Figure 6.22 Solar Charge Station Efficiencies by using total solar radiation and direct solar radiation values, 21.08.2003.

Temperature and humidity values that are measured are given in Figure 6.23.

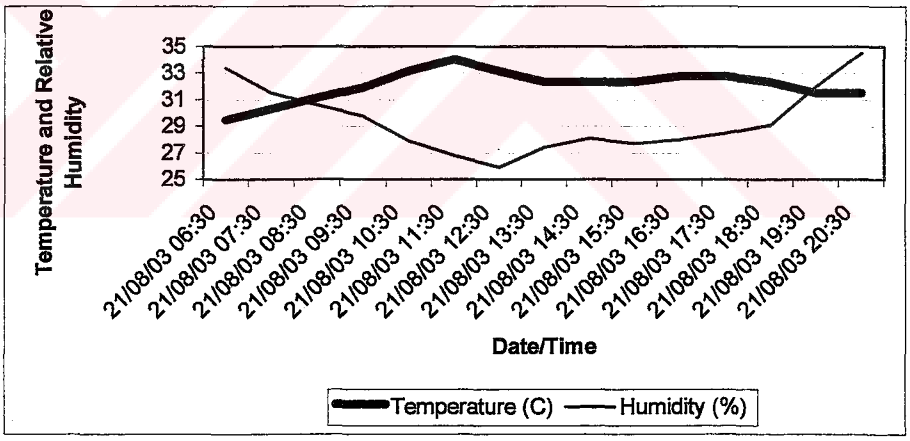

Figure 6.23 Temperature and Relative Humidity, 21.08.2003.

6.2.2 Omega Type Solar Charge Station Without Reflectors

In order to see the effects of reflectors, an experiment carried out without reflectors on 11.09.2003. A plastic black material to prevent reflection covers the reflectors as shown in Figure 6.24. Total solar radiation, direct solar radiation on horizontal and inclined surfaces and efficiencies are shown in Table 6.10 and Figure 6.23.

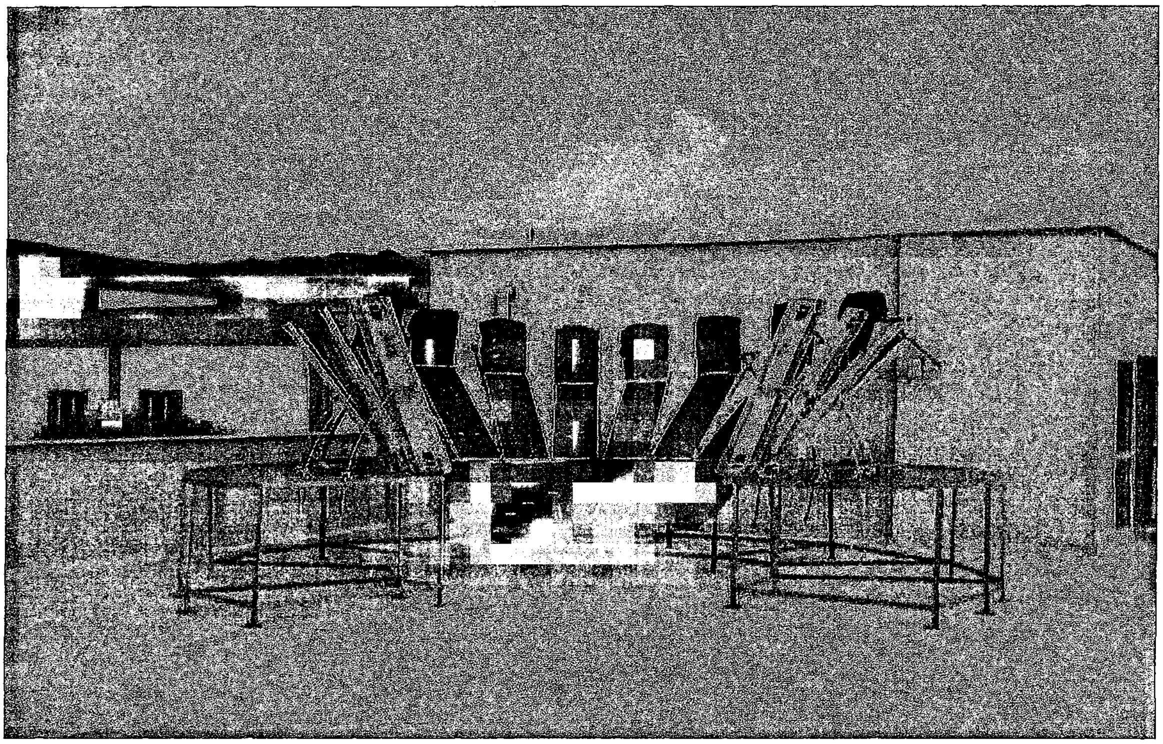

Figure 6.24 Omega Type Solar Charge Station Experiments without Reflectors.

Table 6.10 Total Solar Radiation, Direct solar radiation on horizontal and inclined surfaces and Efficiency for Solar Charge Station Without Reflectors, 11.09.2003.

Date/Time	Total Solar Radiation	Direct Solar Radiation on Horizontal Surface	Direct Solar Radiation on Inclined Surfaces	Energy Obtained from Photovoltaics	% Efficiency, η_I Efficiency
11.09.2003 06:30	0.486381914	0.3891055	0.0880959	0.04199958	47.67481989
11.09.2003 07:30	1.459145742	1.1673166	0.2934368	0.139438606	47.51912744
11.09.2003 08:30	2.334633187	1.8677065	0.5120635	0.758152418	148.0582826
11.09.2003 09:30	3.988331694	3.1906654	0.9321972	0.217077829	23.28668423
11.09.2003 10:30	7.198452326	5.7587619	1.6859119	0.366116339	21.71621954
11.09.2003 11:30	11.47861317	9.1828905	2.6394777	0.581574184	22.03368439
11.09.2003 12:30	11.96499508	9.5719961	2.6906038	0.758152418	28.17778011
11.09.2003 13:30	20.13621124	16.108969	4.469848	1.417485825	31.71217065
11.09.2003 14:30	12.06227147	9.6498172	2.5903007	0.508674913	19.63767846
11.09.2003 15:30	19.16344741	15.330758	3.7955843	1.22794772	32.35200788
11.09.2003 16:30	16.63426146	13.307409	2.9913714	0.960650393	32.11404628
11.09.2003 17:30	9.922191044	7.9377528	1.5861139	0.178198218	11.23489399
11.09.2003 18:30	4.18288446	0	0	0.103678963	0
11.09.2003 19:30	1.459145742	0	0	0.075599244	0
11.08.2003 20:30	0.486381914	0	0	0.04199958	0

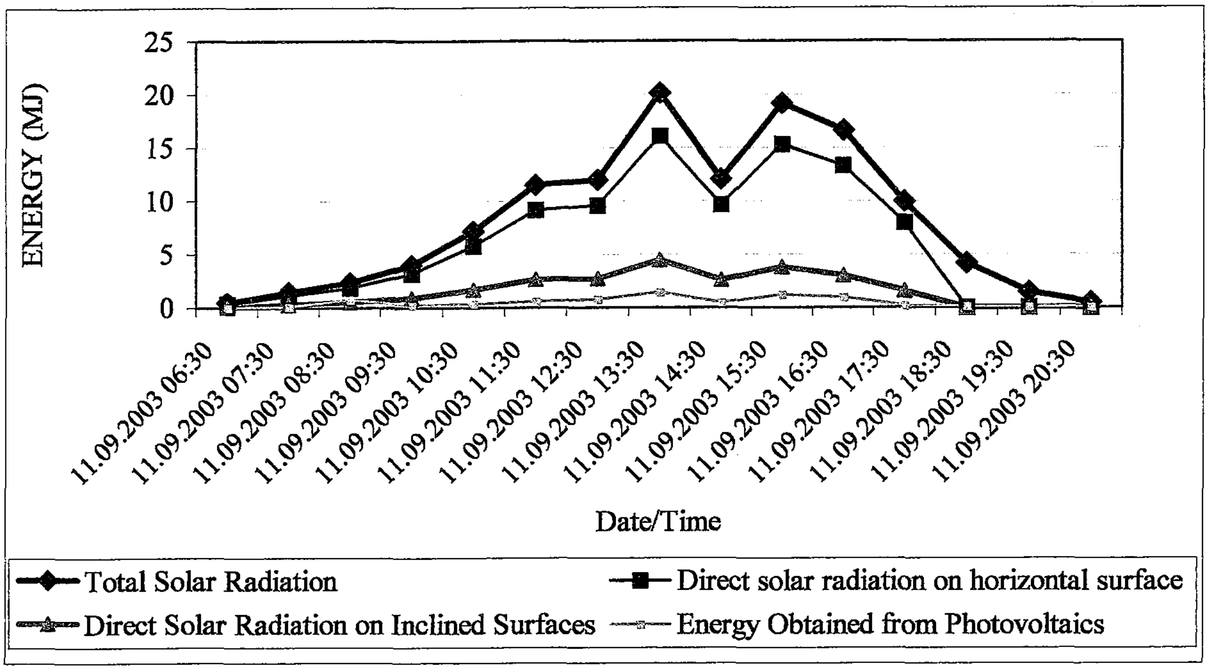

Figure 6.25 Total Solar Radiation, Direct Solar Radiation on horizontal and inclined surfaces for Solar Charge Station Without Reflectors, 11.09.2003.

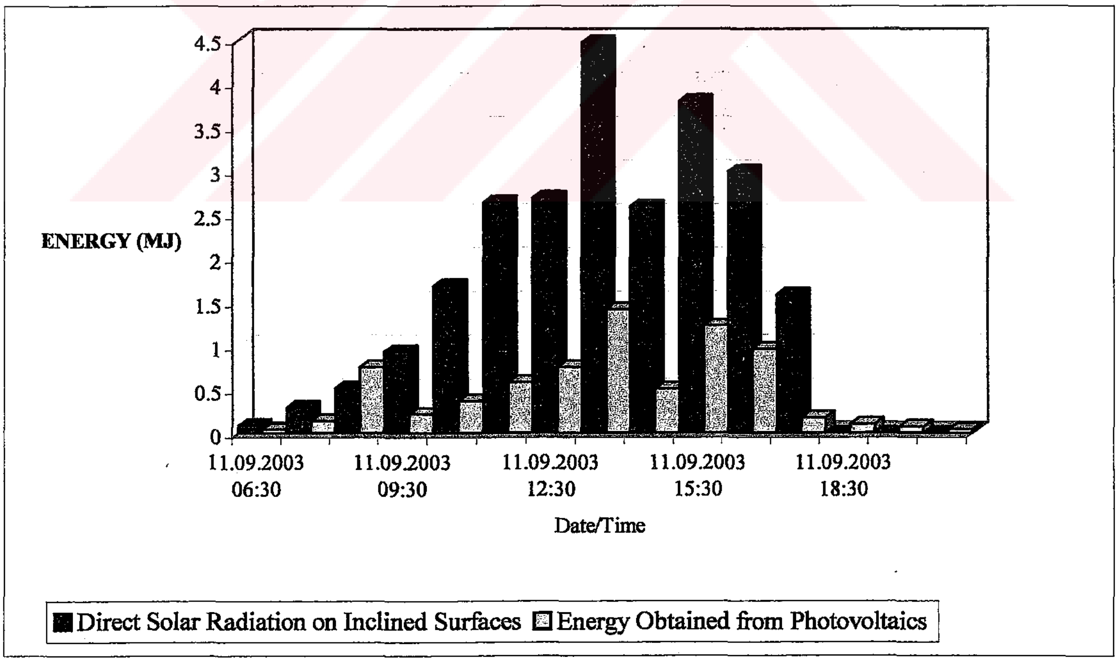

Figure 6.26 Direct Solar Radiation on Inclined Surfaces and Energy obtained from Photovoltaic Generator for Solar Charge Station Without Reflectors, 11.09.2003.

The efficiencies $\eta$and η_I are shown in Figure 6.27.

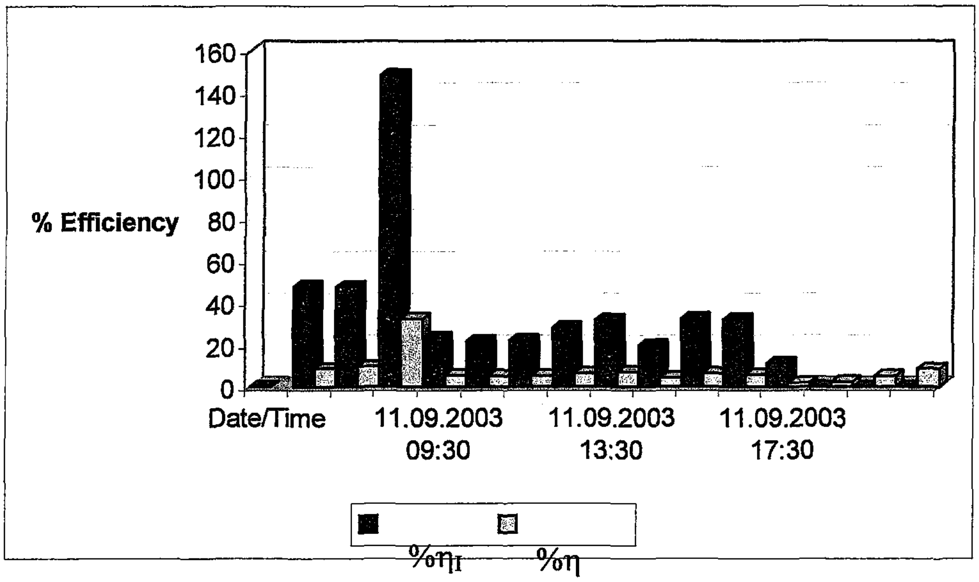

Figure 6.27 Percentage Efficiencies $\eta$and η_I for Solar Charge Station Without Reflectors, 11.09.2003.

Daily percentage efficiency using direct solar radiation data, $\%\eta_I$, is 27.9037935% and using total radiation data, $\%\eta$, is 5.903793%.

As it is understood from Figure 6.23 and Figure 6.26, the day that experiments carried out is a cloudy day but as soon as direct solar radiation is calculated and used to calculate efficiency, the cloudiness is also included to the calculations and we gain a high efficiency value. Although the efficiency is high the effect of reflector is seen (efficiency with reflectors = 31.65315%).

6.2.3 Omega Type Solar Charge Station with Optimum Inclination Angles (Fifth Combination)

Calculated optimum inclination angles given in Section 6.1.6 are the angles, which Omega Type Solar Charge Station collects the most solar radiation, theoretically. In order to observe the solar charge stations behavior with optimum inclination angles, experiments carried out on 12.09.2003 for the angles of the month *September*.

The photovoltaic generator for Omega Type Solar Charge Station with optimum inclination angles is shown in Figure 6.28.

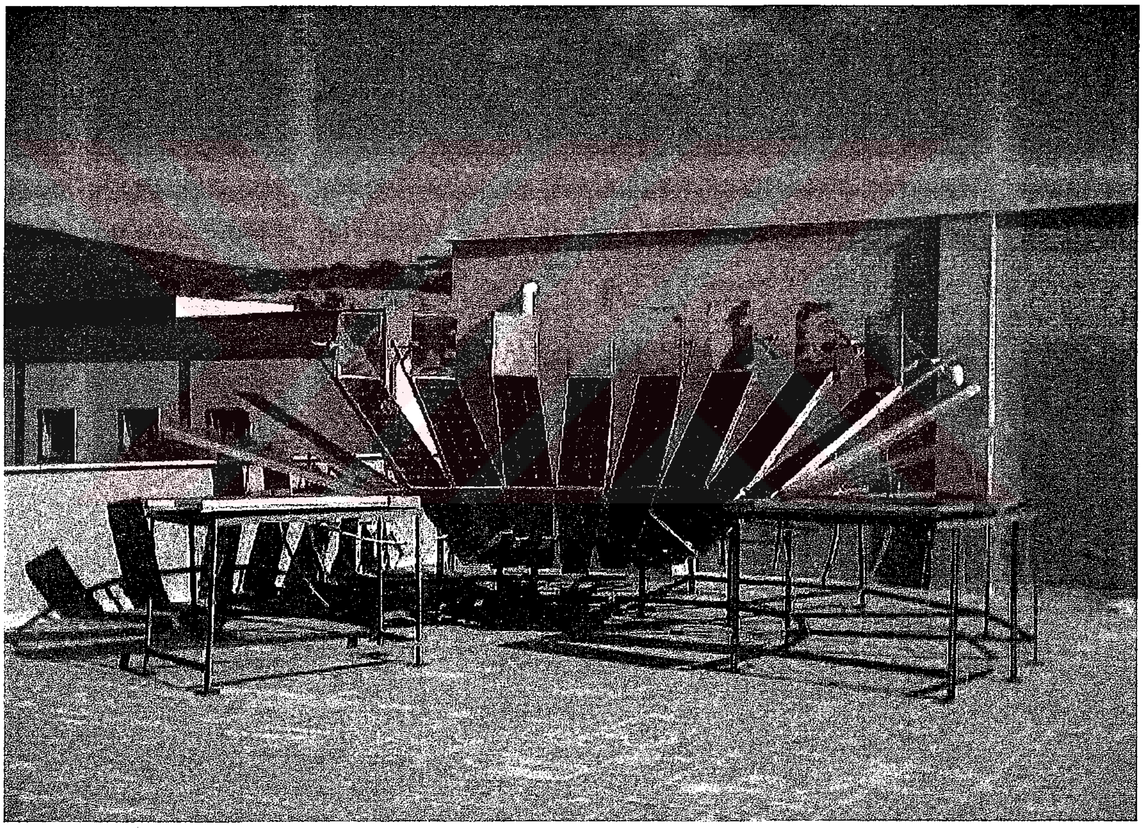

Figure 6.28 Omega Type Solar Charge Station with Optimum Inclination Angles.

Table 6.11 Total Solar Radiation, Direct solar radiation on horizontal and inclined surfaces and Efficiencies for Solar Charge Station with Optimum Inclination Angles, 12.09.2003.

Date/Time	Total Solar Radiation	Direct Solar Radiation on Horizontal Surface	Direct Solar Radiation on Inclined Surfaces	Energy Obtained from Photovoltaics	Efficiency
12.09.2003 06:30	0.486381914	0.3891055	0.1064071	0.04199958	39.4706739
12.09.2003 07:30	1.459145742	1.1673166	0.3498356	0.139438606	39.85832316
12.09.2003 08:30	2.334633187	1.8677065	0.6356221	0.758152418	119.2772242
12.09.2003 09:30	6.128412115	4.9027297	1.8009758	1.182588174	65.66374726
12.09.2003 10:30	6.128412115	4.9027297	1.8841218	0.32399676	17.19616853
12.09.2003 11:30	8.073939771	6.4591518	2.5504599	0.466555334	18.29298861
12.09.2003 12:30	7.101175943	5.6809408	2.2249684	0.40499595	18.20232377
12.09.2003 13:30	6.128412115	4.9027297	1.8439601	0.307796922	16.69216795
12.09.2003 14:30	8.073939771	6.4591518	2.2798943	0.511914881	22.45344821
12.09.2003 15:30	7.101175943	5.6809408	1.7998078	0.468175318	26.012517
12.09.2003 16:30	13.81324636	11.050597	3.0179715	1.368886311	45.35782725
12.09.2003 17:30	10.01946743	8.0155739	1.978873	1.116168838	56.40426921
12.09.2003 18:30	5.25292467	0	0	0.220077799	0
12.09.2003 19:30	1.459145742	0	0	0.075599244	0
12.09.2003 20:30	0.486381914	0	0	0.04199958	0

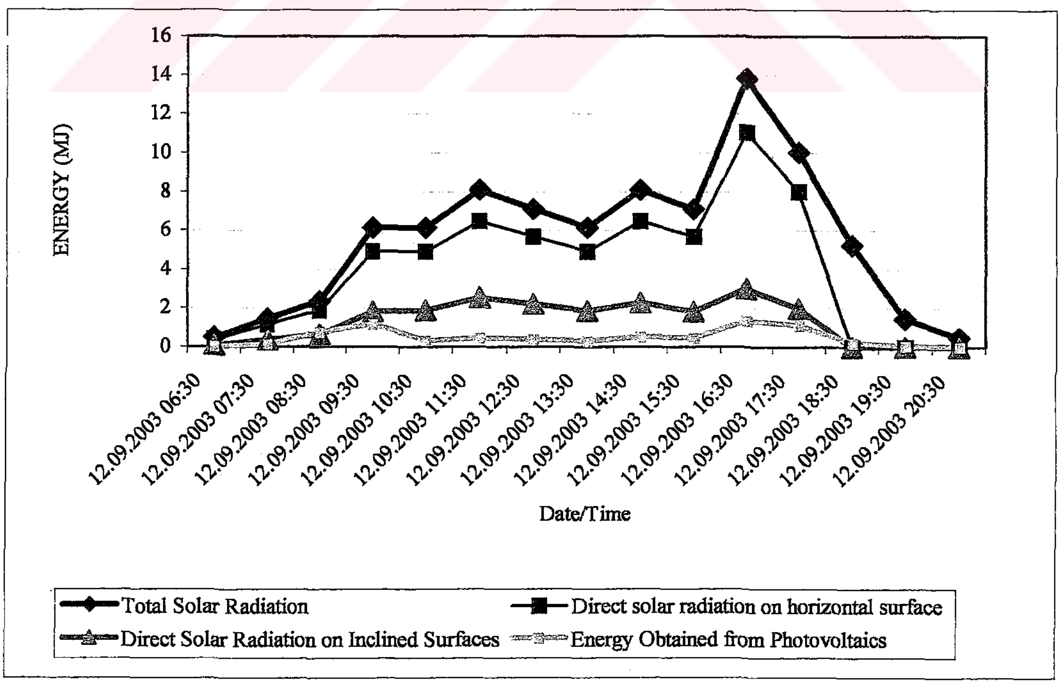

Figure 6.29 Total Solar Radiation, Direct Solar Radiation on horizontal and inclined surfaces for Solar Charge Station with Optimum Inclination Angles, 12.09.2003.

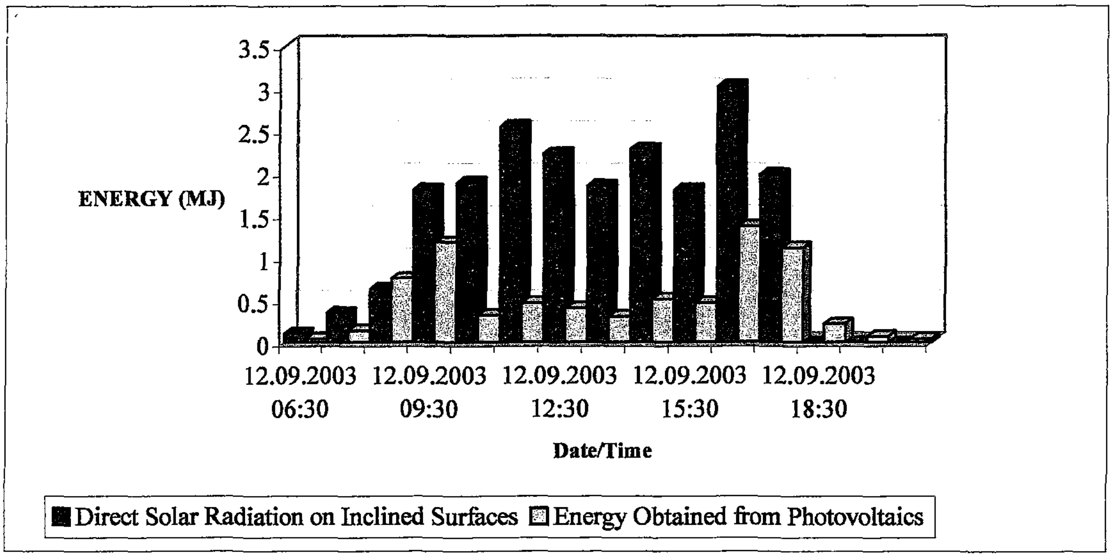

Figure 6.30 Direct Solar Radiation on Inclined Surfaces and Energy obtained from Photovoltaic Generator for Solar Charge Station with Optimum Inclination Angles, 12.09.2003.

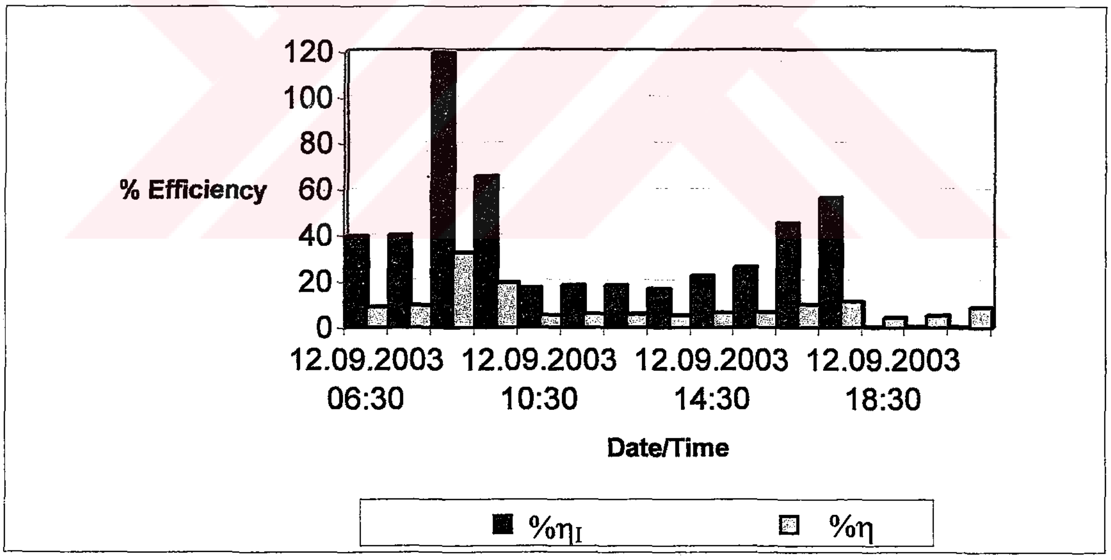

Figure 6.31 Percentage Efficiencies η and η_I for Solar Charge Station with Optimum Inclination Angles, 12.09.2003.

Daily percentage efficiency using direct solar radiation data, $\%\eta_I$, is 35.7093906% and total radiation data, $\%\eta$, is 8.698424%. The efficiency, $\%\eta_I$, is much more higher than the efficiency calculated for Omega Type Solar Charge Station (First Combination).

The experiment is done on 12.09.2003. The recommended day for September is 15th from Table 3.1. By changing the modules inclination angles every month the efficiency can be enhanced. According to Figure 6.16 in theoretical calculations section, we understand that total energy reaching onto the station is very high during summer and must be enhanced during winter. A more effective reflector construction can be solution to the problem.

Chapter 7

CONCLUSION

Increasing energy demand with the increasing population of the world made us realize that we need to change our conventional style of living. Energy, the very important "E" of the *3E-Trilemma* has a power to start wars; thus, who has the energy has the power.

Renewable energy sources, unlike fossil fuels, are environmental friendly and sustainable. As long as we know that acid rains, green house effect, depletion of the ozone layer, smog and air pollution is caused by the fossil fuels, and that fossil fuels are used as the raw material for the production of many useful polymers or other chemicals, we have to stop and think before burning it.

The subject of this study is thus, a solar charge station that charges the batteries of an electric or hybrid vehicle, which does not use fossil fuels like internal combustion engines and prevent CO_2 and other green house gas emissions.

In order to satisfy the expectations of the other important "E" of the trilemma, Economics, a new design is developed. The idea of the design, Ω-shape of the photovoltaic generator, is to create a fix mirror area, which acts as if it were a Sun-tracking array. The generator is constructed to be modular. All the photovoltaic modules inclination angles can be modified when wanted so it gives flexibility to the generator.

Another important design element of the Omega Type Solar Charge Station is the reflectors. Eight photovoltaic modules having the lowest surface azimuth angles have vertical and tilted reflectors in order to increase the solar radiation falling on the modules and the efficiency of the generator. With this reflectors an increase during the winter season and a linearity of energy collection through a year period is expected

Other components of the photovoltaic system are; lead-acid battery, charge controllers, data loggers, pyranometer, loads and wiring. The system is mounted on a rooftop at İzmir Institute of Technology Campus area.

Theoretical results carried with the program MATHCAD have shown that the reflectors add a considerable energy to the photovoltaic generator. Especially in winter the energy gain due to the reflectors is high and the expectation is satisfied.

Comparing the calculated results with other concepts shows that Omega Type Solar Charge Station with reflectors is an efficient design.

When the station is compared with a mostly preferred design, south facing charge station with fixed inclination angles equal to the latitude it is seen that a more linear and stable energy, approximately 240 MJ, is obtained through a year period.

Reflectors are highly effective during winter period. The efficiency has an increase of 12% during winter period and 3% during summer, theoretically.

The daily analysis has shown that the reflectors mostly effect before solar noon and balance the energy collection during the day.

Experimental results have shown that Omega Type Solar Charge Station has a satisfying daily efficiency during summer days, e.g. the efficiencies calculated by using direct solar radiation on inclined surface is 31.65315%, for the experiment on 21.08.2003, 27.90379% for the experiment carried out without reflectors on 11.09.2003 and 35.70939% for the experiment carried out with optimum inclination angles for September, on 12.09.2003. The experimental results confirm the previously calculated theoretical results. Reflectors increase the efficiency nearly 4% during the experiments.

In order to show the effect of reflectors better and obtain a higher enhancement of the efficiency, the experiments must be carried out during winter period, according to theoretical results. Direct solar radiation on horizontal surface values are calculated to be considerably higher than diffuse solar radiation values. The reason is again the summer season. In summer the days are mostly clear not cloudy.

During experiments, it has been realized that although there isn't any conflict between the equipments that are used, some problems may occur frequently. The sudden increase of current intensity on the wiring can cause the fuse of the solar charge regulators burn. Many problems occur due to the materials chosen for the equipments. Most of them are hardly resist to high temperatures. Especially the wirings and the measurement devices may melt when exposed to sunlight.

The summer of 2003 is said to be the hottest one among 20 years. Although the results of the experiments are successful, the reason beyond the high temperatures is believed to be global warming which we try to protect our world.

REFERENCES

[1] G. Atagündüz, "Omega Type Solar Charge Station", *Strojarttsvo* **44**, 2002, 5-16.

[2] R. Sims, H.Rogner, "K. Gregory, Carbon emissions and mitigation cost comparisons between fossil fuel, nuclear and renewable energy resources for electricity generation", *Energy Policy*, Article in Press.

[3] A. Çantay, "Photovoltaic charge station on garage roofs with passive reflectors", *Master of Science Thesis*, Izmir, 2000.

[4] G. E. Ahmad, H. M. S. Hussein, "Comparative Study of PV modules with and without a tilted plane reflector", *Energy Conversion and Management* **42**, 2001, 1327-1333.

[5] Y. Hamakawa, "Solar energy conversion and 21st century's civilization", Solar *Energy Materials & Solar Cells 74*, 2002, 13-23.

[6] T. Muneer, M. Asif, J. Kubie, " Generation and transmission prospects for solar electricity: UK and global markets", *Energy Conversion and Management* **44**, 2003, 35-52.

[7] G. Purvis, "Is PV on a slow, downward slope, or can industry make the multi-MW breakthrough?", *Photovoltaics Bulletin*, March 2002, 7-10.

[8] J. B. Lesourd, "Solar photovoltaic systems: the economics of a renewable energy resource", *Environmental Modeling & Software* **16**, 2001, 147-156.

[9] K. Kaygusuz, A. Sarı, "Renewable energy potential and utilization in Turkey", *Energy Conversion and Management* **44**, 2003, 459-478.

[10] J. M. Pearce, " Photovoltaics – a path to sustainable futures ", *Futures* **34**, 2002, 663-674.

[11] M. A. Green, "Third generation photovoltaics: solar cells for 2020 and beyond", *Physica* **E 14**, 2002, 65-70.

[12] K. Bücher, "Site dependence of the energy collection of PV modules", *Solar Energy Materials and Solar Cells* **47**, 1997, 85-94.

[13] M. Rönnelid, B. Karlsson, P. Krohn, J. Wennerberg, "Booster reflectors for PV modules in Sweden", *Progress in Photovoltaics Research and Applications* **8**, 2000, 279-291.

[14] H. M. S. Hussein, G. E. Ahmad, M. A. Mohamad, "Optimization of operational and design parameters of plane reflector-tilted flat plate solar collector systems", *Energy* **25**, 2000, 529-542.

[15] M. D. J. Pucar, A. R. Despic, "The enhancement of energy gain of solar collectors and photovoltaic panels by the reflection of solar beams", *Energy* **27**, 2002, 205-223.

[16] G. E. Ahmad, H. M. S. Hussein, "Comparative study of PV modules with and without a tilted plane reflector", *Energy Conversion and Management* **42**, 2001, 1327-1333.

[17] M. Oliver, T. Jackson, "The market for solar photovoltaics", *Energy Policy* **27**, 1999, 371-385.

[18] T. Markvart, *Solar Electricity,* Second Edition, John Wiley & Sons, England, 2000.

[19] J. A. Duffie, W.A. Beckman, *Solar Engineering of Thermal Processe*s, Second Edition, John Wiley & Sons, Canada, 1991.

[20] G. Atagündüz, Güneş Enerjisi Temelleri ve Uygulamaları, Ege University Press, Izmir, 1989.

[21] R. Messenger, J. Ventre, Photovoltaic System Engineering, CRC Press,Florida, 2000.

[22] Mathcad Software

[23] M. A. Green, "Photovoltaic Principles", *Physica* **E 0**, 2002, Article in Press.

[24] M. A. Green, "Photovoltaics: Technology overview", *Energy Policy* **28**, 2000, 989-998.

[25] M. A. Green, "Recent developments in photovoltaics", *Solar Energy* **0**, 2003, Article in Press.

[26] A. Goetzberger, C. Hebling, "Photovoltaic materials, past, present, future", *Solar Energy Materials & Solar Cells* **62**, 2000, 1-19.

[27] M. A. Green, "Crystalline and thin-film silicon solar cells: state of the art and future potential", *Solar Energy* **74**, 2003, 181-192.

[28] D. E. Carlson, K. Rajan, R. R. Arya, F. Willing, L. Yang, "Advances in amorphous silicon photovoltaic technology", *Journal of Materials Research* **13**, 1998, 2754-2762.

[29] B. Rech, H. Wagner, "Potential of amorphous silicon for solar cells", *Applied Physics* **A69**, 1999, 155-167.

[30] T. M. Bruton, "General trends about photovoltaics based on crystalline silicon ", *Solar Energy Materials & Solar Cells* **72**, 2002, 3-10.

[31] www.eren.doe.gov

[32] www.pvpower.com

[33] www.etvi.org

[34] www.oft.doe.gov

[35] www.hobohelp.com

[36] www.campbell.sci.com

[37] www.apogee-inst.com

[38] Boxcar Software

APPENDIX A

Table A 1 First Combination, hourly average daily extraterrestrial solar radiation falling on Omega Type Solar Charge Station for selected days of the year, theoretically.

n	First Combination Without Reflectors (MJ)	First Combination Reflected Energy (MJ)	First Combination With Reflectors (MJ)
17	201,4281383	27,56445102	228,9925893
47	217,2479774	25,11037786	242,3583553
75	231,1702224	20,92124582	252,0914683
105	236,7329463	14,59237772	251,325324
135	233,7584955	9,697490664	243,4559861
162	230,0692836	7,59895091	237,6682345
198	230,7623985	8,481244599	239,2436431
228	233,9652036	12,28942048	246,2546241
258	231,9260556	18,29264325	250,2186988
288	220,2797596	23,32228663	243,6020463
318	204,4509012	26,91403658	231,3649377
344	195,9565998	27,70318009	223,6597799

Table A 2 Second Combination, hourly average daily extraterrestrial solar radiation falling on South-facing Solar Charge Station with different inclination angles for selected days of the year, theoretically.

n	Second Combination Without Reflectors (MJ)	Second Combination Reflected (MJ)	Second Combination With Reflectors (MJ)
17	245,3417158		245,3417158
47	252,344254		252,344254
75	245,4990698	22,85148495	268,3505548
105	221,8543553	16,59368234	238,4480376
135	197,313218	10,81619593	208,1294139
162	184,4804889	8,174853619	192,6553425
198	189,3530829	9,301492789	198,6545757
228	209,8053512	13,98000293	223,7853541
258	234,6698365	20,43157807	255,1014145
288	249,4334102		249,4334102
318	246,5426953		246,5426953
344	240,8440151		240,8440151

Table A 3 Third Combination, hourly average daily extraterrestrial solar radiation falling on South-facing Solar Charge Station with fixed inclination angles for selected days of the year, theoretically.

n	Third Combination Without Reflectors (MJ)	Third Combination Reflected (MJ)	Third Combination With Reflectors (MJ)
17	232,5322309	51,02348832	283,5557192
47	248,1912746	40,37761065	288,5688852
75	255,2019296	29,13414271	284,3360723
105	247,9205291	19,81272225	267,7332513
135	234,3537894	12,1857524	246,5395418
162	225,7688259	9,017593854	234,7864197
198	228,6342917	10,3520047	238,9862964
228	240,5541984	16,27242975	256,8266282
258	250,8393148	28,51637401	279,3556888
288	249,4388491	36,14745136	285,5863005
318	235,8022539	47,76839275	283,5706466
344	226,103252	54,26542765	280,3686797

Table A 4 Fourth Combination, hourly average daily extraterrestrial solar radiation falling on Inverse of Omega Type Solar Charge Station for selected days of the year, theoretically.

n	Fourth Combination Without Reflectors (MJ)	Fourth Combination Reflected (MJ)	Fourth Combination With Reflectors (MJ)
17	170,3969998	31,65914944	202,0561493
47	187,9296045	28,80376181	216,7333663
75	203,2705645	24,42612273	227,6966873
105	210,8373788	15,7179488	226,5553276
135	210,2229035	9,839483286	220,0623868
162	207,9627155	7,472894381	215,4356099
198	208,0922192	8,468677	216,5608962
228	209,2391288	12,88524025	222,124369
258	205,0299764	20,97687923	226,0068556
288	191,74808	27,06876878	218,8168488
318	174,1727929	30,85050164	205,0232946
344	164,3136106	31,98942563	196,3030362

Table A 5 Fifth Combination, hourly average daily extraterrestrial solar radiation falling on optimum inclination angles of Omega Type Solar Charge Station for selected days of the year, theoretically.

n	Fifth Combination Without Reflectors (MJ)	Fifth Combination Reflected (MJ)	Fifth Combination With Reflectors (MJ)
17	176,6870779	31,82268625	208,5097641
47	198,3247661	28,38840787	226,713174
75	225,1750006	20,73281155	245,9078121
105	255,8402312	12,61091539	268,4511466
135	283,8008973	7,386315199	291,1872125
162	299,1887513	4,150477542	303,3392288
198	292,1355989	6,252140414	298,3877393
228	267,2217333	9,470939191	276,6926725
258	236,9224515	15,3863152	252,3087667
288	207,0096154	22,17500057	229,184616
318	182,3204855	30,65845149	212,9789369
344	170,5167425	32,47884194	202,9955844

APPENDIX B

Table B 1 Current Intensity Raw Data.

Date Time	Voltage (V) (*1)	Voltage (V) (*2)	Voltage (V) (*3)	Voltage (V) (*4)	Voltage (V) (*5)	Voltage Total	Current (A)
20/08/03 17:30	0.005	0.005	0.337	0.21	0.034	0.591	19.699803
20/08/03 18:30	0.005	0.005	0.122	0.015	0.024	0.171	5.699943
20/08/03 19:30	0.005	0.005	0.015	0.005	0.015	0.045	1.499985
20/08/03 20:30	0.005	0.005	0.005	0.005	0.005	0.025	0.833325
21/08/03 06:30	0.005	0.005	0.005	0.005	0.005	0.025	0.833325
21/08/03 07:30	0.005	0.034	0.005	0.005	0.034	0.083	2.766639
21/08/03 08:30	0.005	0.249	0.005	0.005	0.171	0.435	14.499855
21/08/03 09:30	0.132	0.347	0.005	0.005	0.259	0.748	24.933084
21/08/03 10:30	0.259	0.396	0.005	0.054	0.239	0.953	31.766349
21/08/03 11:30	0.308	0.376	0.005	0.132	0.19	1.011	33.699663
21/08/03 12:30	0.337	0.347	0.005	0.249	0.151	1.089	36.299637
21/08/03 13:30	0.308	0.22	0.034	0.298	0.103	0.963	32.099679
21/08/03 14:30	0.288	0.034	0.161	0.337	0.063	0.883	29.433039
21/08/03 15:30	0.229	0.005	0.239	0.337	0.044	0.854	28.466382
21/08/03 16:30	0.093	0.005	0.269	0.308	0.034	0.709	23.633097
21/08/03 17:30	0.005	0.005	0.278	0.171	0.034	0.493	16.433169
21/08/03 18:30	0.005	0.005	0.073	0.024	0.024	0.131	4.366623
21/08/03 19:30	0.005	0.005	0.015	0.005	0.015	0.045	1.499985
21/08/03 20:30	0.005	0.005	0.005	0.005	0.005	0.025	0.833325
22/08/03 06:30	0.005	0.005	0.005	0.005	0.005	0.025	0.833325
22/08/03 07:30	0.005	0.024	0.005	0.005	0.034	0.073	2.433309
22/08/03 08:30	0.005	0.239	0.005	0.005	0.161	0.415	13.833195
22/08/03 09:30	0.112	0.337	0.005	0.005	0.259	0.718	23.933094
22/08/03 10:30	0.249	0.376	0.005	0.054	0.229	0.913	30.433029
22/08/03 11:30	0.376	0.454	0.005	0.19	0.19	1.215	40.499595
22/08/03 12:30	0.376	0.396	0.005	0.278	0.151	1.206	40.199598
22/08/03 13:30	0.327	0.249	0.044	0.308	0.103	1.031	34.366323
22/08/03 14:30	0.269	0.005	0.132	0.308	0.063	0.777	25.899741
22/08/03 15:30	0.19	0.005	0.19	0.288	0.044	0.717	23.899761
22/08/03 16:30	0.034	0.005	0.229	0.259	0.034	0.561	18.699813
22/08/03 17:30	0.005	0.005	0.249	0.132	0.034	0.425	14.166525
22/08/03 18:30	0.015	0.005	0.034	0.024	0.024	0.102	3.399966
22/08/03 19:30	0.005	0.005	0.015	0.005	0.015	0.045	1.499985
22/08/03 20:30	0.005	0.005	0.005	0.005	0.005	0.025	0.833325
23/08/03 06:30	0.015	0.024	0.005	0.005	0.005	0.054	1.799982
23/08/03 07:30	0.015	0.034	0.015	0.015	0.034	0.113	3.766629
23/08/03 08:30	0.005	0.298	0.015	0.024	0.171	0.513	17.099829
23/08/03 09:30	0.171	0.396	0.024	0.024	0.249	0.864	28.799712
23/08/03 10:30	0.317	0.454	0.005	0.103	0.229	1.108	36.932964
23/08/03 11:30	0.376	0.454	0.005	0.19	0.19	1.215	40.499595
23/08/03 12:30	0.386	0.396	0.005	0.278	0.151	1.216	40.532928
23/08/03 13:30	0.327	0.249	0.044	0.308	0.103	1.031	34.366323
23/08/03 14:30	0.269	0.005	0.132	0.308	0.063	0.777	25.899741

23/08/03 15:30	0.19	0.005	0.19	0.288	0.044	0.717	23.899761
23/08/03 16:30	0.034	0.005	0.22	0.249	0.034	0.542	18.066486
23/08/03 17:30	0.005	0.005	0.239	0.142	0.034	0.425	14.166525
23/08/03 18:30	0.015	0.015	0.024	0.034	0.024	0.112	3.733296
23/08/03 19:30	0.005	0.005	0.015	0.005	0.015	0.045	1.499985
23/08/03 20:30	0.005	0.005	0.005	0.005	0.005	0.025	0.833325
24/08/03 06:30	0.015	0.024	0.005	0.005	0.005	0.054	1.799982
24/08/03 07:30	0.015	0.044	0.015	0.015	0.024	0.113	3.766629
24/08/03 08:30	0.015	0.278	0.015	0.024	0.161	0.493	16.433169
24/08/03 09:30	0.151	0.386	0.015	0.034	0.249	0.835	27.833055
24/08/03 10:30	0.327	0.464	0.005	0.103	0.229	1.128	37.599624
24/08/03 11:30	0.376	0.454	0.005	0.19	0.19	1.215	40.499595
24/08/03 12:30	0.376	0.405	0.005	0.269	0.142	1.197	39.899601
24/08/03 13:30	0.317	0.269	0.044	0.298	0.093	1.021	34.032993
24/08/03 14:30	0.259	0.034	0.142	0.288	0.063	0.786	26.199738
24/08/03 15:30	0.19	0.005	0.2	0.278	0.044	0.717	23.899761
24/08/03 16:30	0.034	0.005	0.229	0.249	0.034	0.551	18.366483
24/08/03 17:30	0.005	0.005	0.259	0.151	0.034	0.454	15.133182
24/08/03 18:30	0.024	0.054	0.015	0.015	0.024	0.132	4.399956
24/08/03 19:30	0.015	0.044	0.005	0.005	0.015	0.084	2.799972
24/08/03 20:30	0.005	0.005	0.005	0.005	0.005	0.025	0.833325
25/08/03 06:30	0.005	0.024	0.005	0.005	0.005	0.044	1.466652
25/08/03 07:30	0.015	0.034	0.015	0.015	0.024	0.103	3.433299
25/08/03 08:30	0.005	0.278	0.015	0.015	0.161	0.474	15.799842
25/08/03 09:30	0.142	0.396	0.015	0.034	0.249	0.836	27.866388
25/08/03 10:30	0.308	0.435	0.005	0.093	0.22	1.061	35.366313
25/08/03 11:30	0.356	0.415	0.005	0.181	0.181	1.138	37.932954
25/08/03 12:30	0.337	0.347	0.005	0.269	0.142	1.1	36.6663
25/08/03 13:30	0.269	0.21	0.044	0.288	0.093	0.904	30.133032
25/08/03 14:30	0.21	0.005	0.122	0.278	0.063	0.678	22.599774
25/08/03 15:30	0.151	0.005	0.171	0.269	0.044	0.64	21.33312
25/08/03 16:30	0.015	0.005	0.2	0.239	0.034	0.493	16.433169
25/08/03 17:30	0.005	0.005	0.22	0.142	0.034	0.406	13.533198
25/08/03 18:30	0.005	0.005	0.024	0.024	0.024	0.082	2.733306
25/08/03 19:30	0.005	0.005	0.015	0.005	0.015	0.045	1.499985
25/08/03 20:30	0.005	0.034	0.005	0.005	0.005	0.054	1.799982
26/08/03 06:30	0.024	0.054	0.005	0.005	0.005	0.093	3.099969
26/08/03 07:30	0.024	0.054	0.005	0.015	0.034	0.132	4.399956
26/08/03 08:30	0.024	0.229	0.015	0.024	0.142	0.434	14.466522
26/08/03 09:30	0.132	0.347	0.015	0.034	0.229	0.757	25.233081
26/08/03 10:30	0.298	0.415	0.005	0.103	0.22	1.041	34.699653
26/08/03 11:30	0.337	0.396	0.005	0.181	0.181	1.1	36.6663
26/08/03 12:30	0.327	0.337	0.005	0.259	0.142	1.07	35.66631
26/08/03 13:30	0.278	0.21	0.044	0.288	0.093	0.913	30.433029
26/08/03 14:30	0.22	0.005	0.122	0.288	0.063	0.698	23.266434
26/08/03 15:30	0.151	0.005	0.171	0.269	0.044	0.64	21.33312
26/08/03 16:30	0.015	0.005	0.19	0.239	0.044	0.493	16.433169
26/08/03 17:30	0.005	0.005	0.22	0.132	0.034	0.396	13.199868
26/08/03 18:30	0.005	0.005	0.034	0.024	0.024	0.092	3.066636
26/08/03 19:30	0.005	0.005	0.015	0.005	0.015	0.045	1.499985

26/08/03 20:30	0.005	0.054	0.005	0.005	0.005	0.074	2.466642
27/08/03 06:30	0.024	0.054	0.005	0.005	0.005	0.093	3.099969
27/08/03 07:30	0.015	0.044	0.005	0.015	0.024	0.103	3.433299
27/08/03 08:30	0.015	0.249	0.015	0.024	0.142	0.445	14.833185
27/08/03 09:30	0.132	0.386	0.024	0.034	0.229	0.805	26.833065
27/08/03 10:30	0.269	0.396	0.005	0.103	0.21	0.983	32.766339
27/08/03 11:30	0.288	0.347	0.005	0.181	0.171	0.992	33.066336
27/08/03 12:30	0.278	0.298	0.005	0.259	0.142	0.982	32.733006
27/08/03 13:30	0.269	0.21	0.044	0.288	0.103	0.914	30.466362
27/08/03 14:30	0.21	0.005	0.122	0.278	0.073	0.688	22.933104
27/08/03 15:30	0.151	0.005	0.171	0.269	0.054	0.65	21.66645
27/08/03 16:30	0.015	0.005	0.2	0.239	0.044	0.503	16.766499
27/08/03 17:30	0.005	0.005	0.22	0.142	0.034	0.406	13.533198
27/08/03 18:30	0.005	0.005	0.024	0.024	0.024	0.082	2.733306
27/08/03 19:30	0.005	0.005	0.015	0.005	0.005	0.035	1.166655
27/08/03 20:30	0.005	0.034	0.005	0.005	0.005	0.054	1.799982
28/08/03 06:30	0.269	0.366	0.005	0.005	0.005	0.65	21.66645
28/08/03 07:30	0.005	0.044	0.005	0.015	0.034	0.103	3.433299
28/08/03 08:30	0.015	0.229	0.015	0.024	0.132	0.415	13.833195
28/08/03 09:30	0.132	0.366	0.024	0.034	0.229	0.785	26.166405
28/08/03 10:30	0.308	0.435	0.005	0.093	0.21	1.051	35.032983
28/08/03 11:30	0.356	0.415	0.005	0.181	0.171	1.128	37.599624
28/08/03 12:30	0.337	0.347	0.005	0.269	0.142	1.1	36.6663
28/08/03 13:30	0.269	0.21	0.044	0.288	0.093	0.904	30.133032
28/08/03 14:30	0.21	0.005	0.122	0.278	0.063	0.678	22.599774
28/08/03 15:30	0.151	0.005	0.171	0.269	0.044	0.64	21.33312
28/08/03 16:30	0.015	0.005	0.2	0.239	0.034	0.493	16.433169
28/08/03 17:30	0.005	0.005	0.22	0.142	0.034	0.406	13.533198
28/08/03 18:30	0.005	0.005	0.024	0.024	0.024	0.082	2.733306
28/08/03 19:30	0.005	0.005	0.015	0.005	0.015	0.045	1.499985
28/08/03 20:30	0.005	0.034	0.005	0.005	0.005	0.054	1.799982
29/08/03 06:30	0.005	0.005	0.005	0.005	0.005	0.025	0.833325
29/08/03 07:30	0.005	0.044	0.005	0.015	0.024	0.093	3.099969
29/08/03 08:30	0.005	0.229	0.015	0.024	0.122	0.395	13.166535

Table B 2 Temperature, Humidity and Total Solar Radiation Raw Data.

Date Time	Temperature (*C) (1)	RH (%) (1,2)	Abs Humidity (g/m^3) (1,2)	Voltage (V) (*4)
20/08/03 10:30	31.52	31.6	10.4	0.22
20/08/03 11:30	31.93	30.4	10.2	0.259
20/08/03 12:30	31.93	29.3	9.9	0.278
20/08/03 13:30	31.52	29.1	9.6	0.288
20/08/03 14:30	31.93	27.3	9.2	0.269

20/08/03 15:30	32.76	26	9.1	0.239
20/08/03 16:30	33.17	25.4	9.1	0.2
20/08/03 17:30	33.17	24.6	8.8	0.132
20/08/03 18:30	32.76	24.5	8.6	0.063
20/08/03 19:30	31.93	25.1	8.5	0.015
21/08/03 06:30	29.5	33.4	9.9	0.005
21/08/03 07:30	30.31	31.5	9.7	0.015
21/08/03 08:30	31.12	30.6	9.9	0.024
21/08/03 09:30	31.93	29.8	10	0.151
21/08/03 10:30	33.17	27.9	10	0.21
21/08/03 11:30	34.01	26.8	10.1	0.249
21/08/03 12:30	33.17	25.9	9.3	0.269
21/08/03 13:30	32.34	27.4	9.4	0.269
21/08/03 14:30	32.34	28.1	9.6	0.259
21/08/03 15:30	32.34	27.7	9.5	0.229
21/08/03 16:30	32.76	28	9.8	0.181
21/08/03 17:30	32.76	28.5	10	0.122
21/08/03 18:30	32.34	29.1	10	0.054
21/08/03 19:30	31.52	32	10.5	0.015
21/08/03 20:30	31.52	34.5	11.4	0.005
22/08/03 06:30	29.5	37.3	11	0.005
22/08/03 07:30	30.31	36.2	11.2	0.015
22/08/03 08:30	31.12	34.9	11.2	0.024
22/08/03 09:30	31.93	32.6	11	0.151
22/08/03 10:30	32.76	31.2	11	0.21
22/08/03 11:30	33.59	30.4	11.2	0.249
22/08/03 12:30	33.59	30	11	0.269
22/08/03 13:30	32.76	30.7	10.8	0.278
22/08/03 14:30	32.76	29.6	10.4	0.259
22/08/03 15:30	32.76	28.3	9.9	0.229
22/08/03 16:30	33.17	28.4	10.2	0.19
22/08/03 17:30	33.17	28.2	10.1	0.122
22/08/03 18:30	33.17	29.3	10.5	0.063
22/08/03 19:30	32.34	32.6	11.2	0.015
22/08/03 20:30	31.93	33.2	11.2	0.005
23/08/03 06:30	29.5	44.9	13.2	0.005
23/08/03 07:30	29.9	43.5	13.1	0.015
23/08/03 08:30	30.71	41.3	13	0.024
23/08/03 09:30	31.52	39.1	12.8	0.151
23/08/03 10:30	32.76	36.7	12.9	0.2
23/08/03 11:30	34.01	34	12.7	0.249
23/08/03 12:30	34.01	32.6	12.2	0.269
23/08/03 13:30	33.17	33.9	12.2	0.278
23/08/03 14:30	32.76	33.2	11.7	0.259
23/08/03 15:30	32.76	32.4	11.4	0.229
23/08/03 16:30	33.17	31.1	11.2	0.181
23/08/03 17:30	33.17	30	10.8	0.122

23/08/03 18:30	33.17	29.3	10.5	0.063
23/08/03 19:30	32.34	30.2	10.4	0.015
23/08/03 20:30	31.93	30.4	10.2	0.005
24/08/03 06:30	29.9	34.9	10.5	0.005
24/08/03 07:30	30.31	34.2	10.5	0.015
24/08/03 08:30	31.12	33.3	10.7	0.024
24/08/03 09:30	32.34	31.4	10.8	0.151
24/08/03 10:30	33.17	30.1	10.8	0.21
24/08/03 11:30	33.17	28.2	10.1	0.249
24/08/03 12:30	33.17	28.2	10.1	0.269
24/08/03 13:30	31.93	29.2	9.8	0.278
24/08/03 14:30	31.93	26.7	9	0.269
24/08/03 15:30	31.93	26.3	8.9	0.239
24/08/03 16:30	32.76	25.6	9	0.19
24/08/03 17:30	32.76	25.2	8.9	0.132
24/08/03 18:30	32.76	25.4	8.9	0.063
24/08/03 19:30	32.34	27.7	9.5	0.015
24/08/03 20:30	31.93	28.3	9.5	0.005
25/08/03 06:30	25.95	39	9.5	0.005
25/08/03 07:30	26.73	39.2	9.9	0.015
25/08/03 08:30	29.1	39.2	11.3	0.024
25/08/03 09:30	31.12	32.7	10.5	0.151
25/08/03 10:30	31.52	29.9	9.8	0.21
25/08/03 11:30	32.76	27.4	9.6	0.249
25/08/03 12:30	34.43	25.7	9.9	0.269
25/08/03 13:30	33.17	26.7	9.6	0.269
25/08/03 14:30	32.76	26.4	9.3	0.259
25/08/03 15:30	32.34	29.2	10	0.229
25/08/03 16:30	32.34	28.6	9.8	0.181
25/08/03 17:30	32.34	28.4	9.8	0.112
25/08/03 18:30	33.17	28.2	10.1	0.054
25/08/03 19:30	31.93	26.7	9	0.015
25/08/03 20:30	31.52	27.7	9.1	0.005
26/08/03 06:30	28.7	34.4	9.7	0.005
26/08/03 07:30	29.5	34.2	10.1	0.015
26/08/03 08:30	30.71	32.5	10.2	0.024
26/08/03 09:30	32.76	32.4	11.4	0.132
26/08/03 10:30	32.34	29.4	10.1	0.2
26/08/03 11:30	35.27	25.2	10.1	0.239
26/08/03 12:30	34.85	24.4	9.6	0.259
26/08/03 13:30	33.17	25.7	9.2	0.269
26/08/03 14:30	32.76	24.8	8.7	0.249
26/08/03 15:30	33.59	23.7	8.7	0.229
26/08/03 16:30	34.01	23.7	8.9	0.171
26/08/03 17:30	33.59	23.9	8.8	0.112
26/08/03 18:30	33.59	28.6	10.5	0.054
26/08/03 19:30	32.34	26.3	9	0.015

26/08/03 20:30	31.93	25.7	8.7	0.005
27/08/03 06:30	25.56	36.7	8.7	0.005
27/08/03 07:30	27.91	33.9	9.2	0.015
27/08/03 08:30	30.31	31.3	9.6	0.044
27/08/03 09:30	31.52	32.7	10.8	0.142
27/08/03 10:30	34.01	32.3	12.1	0.2
27/08/03 11:30	37	26.5	11.6	0.239
27/08/03 12:30	36.13	26.8	11.2	0.259
27/08/03 13:30	34.85	27.4	10.7	0.259
27/08/03 14:30	34.43	27.8	10.6	0.249
27/08/03 15:30	34.43	26.9	10.3	0.22
27/08/03 16:30	34.01	27.7	10.4	0.171
27/08/03 17:30	34.01	27.2	10.2	0.112
27/08/03 18:30	33.17	31.4	11.3	0.044
27/08/03 19:30	31.12	44.2	14.2	0.005
27/08/03 20:30	31.93	34.4	11.6	0.005
28/08/03 06:30	29.5	44	13	0.005
28/08/03 07:30	29.5	44.6	13.1	0.015
28/08/03 08:30	31.12	42.3	13.6	0.073
28/08/03 09:30	32.76	38.6	13.5	0.132
28/08/03 10:30	33.17	36.6	13.1	0.19
28/08/03 11:30	36.13	30.9	13	0.239
28/08/03 12:30	35.27	30.6	12.3	0.259
28/08/03 13:30	33.17	29.5	10.6	0.259
28/08/03 14:30	31.93	38.7	13	0.249
28/08/03 15:30	31.52	37.6	12.4	0.21
28/08/03 16:30	31.93	31.9	10.7	0.171
28/08/03 17:30	31.93	36.5	12.3	0.103
28/08/03 18:30	32.76	35.8	12.6	0.044
28/08/03 19:30	31.93	39.9	13.4	0.015
28/08/03 20:30	31.93	42.1	14.2	0.005
29/08/03 06:30	28.7	39.4	11.1	0.005
29/08/03 07:30	29.1	38.6	11.1	0.015
29/08/03 08:30	30.31	39	12	0.073
29/08/03 09:30	31.52	35.6	11.7	0.142
29/08/03 10:30	33.59	31.5	11.5	0.2
29/08/03 11:30	35.27	28.1	11.3	0.239
29/08/03 12:30	34.43	30.1	11.5	0.259
29/08/03 13:30	32.76	31.1	10.9	0.269
29/08/03 14:30	32.34	29.7	10.2	0.259
29/08/03 15:30	32.76	29.4	10.3	0.22
29/08/03 16:30	33.17	29.5	10.6	0.171
29/08/03 17:30	33.59	28.9	10.6	0.103
29/08/03 18:30	33.17	27.5	9.9	0.044
29/08/03 19:30	32.76	31.5	11.1	0.015
29/08/03 20:30	32.34	32.4	11.1	0.005
30/08/03 06:30	28.31	52.2	14.4	0.005

30/08/03 07:30	29.1	47.2	13.6	0.015
30/08/03 08:30	29.1	55.2	15.9	0.073
30/08/03 09:30	31.52	40.8	13.4	0.142
30/08/03 10:30	32.76	36.7	12.9	0.2
30/08/03 11:30	34.43	32.9	12.6	0.239
30/08/03 12:30	34.85	30.7	12	0.269
30/08/03 13:30	33.17	35.4	12.7	0.269
30/08/03 14:30	32.76	30.5	10.7	0.259
30/08/03 15:30	32.76	31.1	10.9	0.229
30/08/03 16:30	34.01	25.2	9.5	0.181
30/08/03 17:30	34.43	24.3	9.3	0.122
30/08/03 18:30	33.59	28.1	10.3	0.054
30/08/03 19:30	33.17	31.1	11.2	0.005
30/08/03 20:30	32.76	32.4	11.4	0.005
31/08/03 06:30	27.12	38.1	9.9	0.005
31/08/03 07:30	27.52	37.6	10	0.015
31/08/03 08:30	29.5	34.2	10.1	0.073
31/08/03 09:30	32.34	32.4	11.1	0.132
31/08/03 10:30	34.43	29.5	11.3	0.19
31/08/03 11:30	36.57	25.7	11	0.229
31/08/03 12:30	37	25.2	11	0.259
31/08/03 13:30	34.85	26	10.2	0.259
31/08/03 14:30	34.85	24.6	9.6	0.239
31/08/03 15:30	34.85	25.8	10.1	0.21
31/08/03 16:30	34.85	26.2	10.3	0.161
31/08/03 17:30	34.01	32.6	12.2	0.103
31/08/03 18:30	33.17	35	12.6	0.044
31/08/03 19:30	32.76	37.1	13	0.005
09.01.2003 06:30	27.91	34.5	9.3	0.005
09.01.2003 07:30	27.91	35.9	9.7	0.015
09.01.2003 08:30	30.71	32.1	10.1	0.063
09.01.2003 09:30	32.76	29.6	10.4	0.122
09.01.2003 10:30	33.59	33.8	12.4	0.171

Table B 3 Efficiencies, experimentally.

Date/Time	Total Solar Radiation (MJ)	Direct solar radiation on horizontal surface (MJ)	Direct Solar Radiation on Inclined Surfaces (MJ)	Energy Obtained from Photovoltaics (MJ)	Efficiency
21/08/03 06:30	0.486381914	0.3891055	0.0867154	0.04199958	48.43380249
21/08/03 07:30	1.459145742	1.1673166	0.2865215	0.139438606	48.66601629
21/08/03 08:30	2.334633187	1.8677065	0.5026385	0.730792692	145.3912978
21/08/03 09:30	14.6887338	11.750987	3.3997417	1.256627434	36.96243862
21/08/03 10:30	20.42804038	16.342432	4.8681441	1.60102399	32.88776909
21/08/03 11:30	24.22181931	19.377455	5.8156507	1.698463015	29.20503824

Date/Time	Total Solar Radiation (MJ)	Direct solar radiation on horizontal surface (MJ)	Direct Solar Radiation on Inclined Surfaces (MJ)	Energy Obtained from Photovoltaics (MJ)	Efficiency
21/08/03 13:30	26.16734697	20.933878	6.2358608	1.617823822	25.94387336
21/08/03 14:30	25.19458314	20.155667	5.831345	1.483425166	25.43881665
21/08/03 15:30	22.27629166	17.821033	4.7960094	1.434705653	29.9145715
21/08/03 16:30	17.60702528	14.08562	3.4573596	1.191108089	34.4513801
21/08/03 17:30	11.8677187	9.494175	2.1158565	0.828231718	39.14404037
21/08/03 18:30	5.25292467	4.2023397	0.7821024	0.220077799	28.13925495
21/08/03 19:30	1.459145742	0	0	0.075599244	0
21/08/03 20:30	0.486381914	0	0	0.04199958	0
22/08/03 06:30	0.486381914	0.3891055	0.0868775	0.04199958	48.34344426
22/08/03 07:30	1.459145742	1.1673166	0.2867722	0.122638774	42.7652287
22/08/03 08:30	2.334633187	1.8677065	0.5031561	0.697193028	138.5639729
22/08/03 09:30	14.6887338	11.750987	3.4024277	1.206227938	35.45197878
22/08/03 10:30	20.42804038	16.342432	4.8735638	1.533824662	31.47234186
22/08/03 11:30	24.22181931	19.377455	5.8224625	2.041179588	35.05698148
22/08/03 12:30	26.16734697	20.933878	6.2901301	2.026059739	32.21014027
22/08/03 13:30	27.04283441	21.634268	6.4516702	1.732062679	26.84673318
22/08/03 14:30	25.19458314	20.155667	5.8359521	1.305346946	22.3673348
22/08/03 15:30	22.27629166	17.821033	4.8009474	1.204547954	25.08979686
22/08/03 16:30	18.48251273	14.78601	3.6324475	0.942470575	25.94588317
22/08/03 17:30	11.8677187	9.494175	2.1198112	0.71399286	33.68190789
22/08/03 18:30	6.128412115	4.9027297	0.9124528	0.171358286	18.77996078
22/08/03 19:30	1.459145742	0	0	0.075599244	0
22/08/03 20:30	0.486381914	0	0	0.04199958	0
23/08/03 06:30	0.486381914	0.3891055	0.0870466	0.090719093	104.2190462
23/08/03 07:30	1.459145742	1.1673166	0.2870294	0.189838102	66.13890771
23/08/03 08:30	2.334633187	1.8677065	0.5036842	0.861831382	171.1054972
23/08/03 09:30	14.6887338	11.750987	3.4051618	1.451505485	42.62662276
23/08/03 10:30	19.45527656	15.564221	4.6467368	1.861421386	40.05867948
23/08/03 11:30	24.22181931	19.377455	5.8294273	2.041179588	35.01509661
23/08/03 12:30	26.16734697	20.933878	6.2976544	2.042859571	32.43842004
23/08/03 13:30	27.04283441	21.634268	6.4589641	1.732062679	26.81641596
23/08/03 14:30	25.19458314	20.155667	5.8406418	1.305346946	22.34937513
23/08/03 15:30	22.27629166	17.821033	4.8059869	1.204547954	25.06348814
23/08/03 16:30	17.60702528	14.08562	3.4634879	0.910550894	26.28999754
23/08/03 17:30	11.8677187	9.494175	2.123936	0.71399286	33.61649562
23/08/03 18:30	6.128412115	4.9027297	0.9124528	0.188158118	20.6211334
23/08/03 19:30	1.459145742	0	0	0.075599244	0
23/08/03 20:30	0.486381914	0	0	0.04199958	0
24/08/03 06:30	0.486381914	0.3891055	0.0871174	0.090719093	104.1343159
24/08/03 07:30	1.459145742	1.1673166	0.2872933	0.189838102	66.07814307
24/08/03 08:30	2.334633187	1.8677065	0.5042231	0.828231718	164.2589664
24/08/03 09:30	14.6887338	11.750987	3.4079444	1.402785972	41.1622312
24/08/03 10:30	20.42804038	16.342432	4.8846738	1.89502105	38.79524293
24/08/03 11:30	24.22181931	19.377455	5.8365023	2.041179588	34.972651
24/08/03 12:30	26.16734697	20.933878	6.3052977	2.01093989	31.89286199
24/08/03 13:30	27.04283441	21.634268	6.4663776	1.715262847	26.52586878
24/08/03 14:30	26.16734697	20.933878	6.0711063	1.320466795	21.75001924
24/08/03 15:30	23.24905549	18.599244	5.0212221	1.204547954	23.9891391

24/08/03 16:30	18.48251273	14.78601	3.6390489	0.925670743	25.43716127
24/08/03 17:30	12.84048253	10.272386	2.299899	0.762712373	33.16286434
24/08/03 19:30	1.459145742	0	0	0.141118589	0
24/08/03 20:30	0.486381914	0	0	0.04199958	0
25/08/03 06:30	0.486381914	0.3891055	0.0871522	0.073919261	84.8162841
25/08/03 07:30	1.459145742	1.1673166	0.2875642	0.17303827	60.17378955
25/08/03 08:30	2.334633187	1.8677065	0.504773	0.796312037	157.7564713
25/08/03 09:30	14.6887338	11.750987	3.4107759	1.404465955	41.17731587
25/08/03 10:30	20.42804038	16.342432	4.8903646	1.782462175	36.4484519
25/08/03 11:30	24.22181931	19.377455	5.8436878	1.911820882	32.71599955
25/08/03 12:30	26.16734697	20.933878	6.3130603	1.84798152	29.27235637
25/08/03 13:30	26.16734697	20.933878	6.2643241	1.518704813	24.24371379
25/08/03 14:30	25.19458314	20.155667	5.8502712	1.13902861	19.46967192
25/08/03 15:30	22.27629166	17.821033	4.8163755	1.075189248	22.32361762
25/08/03 16:30	17.60702528	14.08562	3.4699412	0.828231718	23.86875362
25/08/03 17:30	10.89495487	8.7159639	1.9522094	0.682073179	34.93852612
25/08/03 18:30	5.25292467	4.2023397	0.7821024	0.137758622	17.61388478
25/08/03 19:30	1.459145742	0	0	0.075599244	0
25/08/03 20:30	0.486381914	0	0	0.090719093	0
26/08/03 06:30	0.486381914	0.3891055	0.0871886	0.156238438	179.1959807
26/08/03 07:30	1.459145742	1.1673166	0.2878421	0.221757782	77.04146192
26/08/03 08:30	2.334633187	1.8677065	0.5053339	0.729112709	144.2833624
26/08/03 09:30	12.84048253	10.272386	2.9841235	1.271747282	42.61711272
26/08/03 10:30	19.45527656	15.564221	4.6629965	1.748862511	37.5051217
26/08/03 11:30	23.24905549	18.599244	5.6156434	1.84798152	32.90774365
26/08/03 12:30	25.19458314	20.155667	6.0855717	1.797582024	29.538425
26/08/03 13:30	26.16734697	20.933878	6.2717303	1.533824662	24.45616426
26/08/03 14:30	24.22181931	19.377455	5.6291421	1.172628274	20.83138524
26/08/03 15:30	22.27629166	17.821033	4.8217274	1.075189248	22.29883935
26/08/03 16:30	16.63426146	13.307409	3.2814002	0.828231718	25.24019187
26/08/03 17:30	10.89495487	8.7159639	1.9530243	0.665273347	34.06375208
26/08/03 18:30	5.25292467	4.2023397	0.7821024	0.154558454	19.76191951
26/08/03 19:30	1.459145742	0	0	0.075599244	0
26/08/03 20:30	0.486381914	0	0	0.124318757	0
27/08/03 06:30	0.486381914	0.3891055	0.0872266	0.156238438	179.1178408
27/08/03 07:30	1.459145742	1.1673166	0.2881273	0.17303827	60.05617843
27/08/03 08:30	4.280160842	3.4241287	0.9274943	0.747592524	80.6034614
27/08/03 09:30	13.81324636	11.050597	3.2129489	1.352386476	42.0917517
27/08/03 10:30	19.45527656	15.564221	4.6685899	1.651423486	35.37306844
27/08/03 11:30	23.24905549	18.599244	5.6206798	1.666543334	29.65020934
27/08/03 12:30	25.19458314	20.155667	6.0910296	1.649743502	27.08480521
27/08/03 13:30	25.19458314	20.155667	6.0458239	1.535504645	25.39777338
27/08/03 14:30	24.22181931	19.377455	5.6339738	1.155828442	20.51533226
27/08/03 15:30	21.40080421	17.120643	4.6374716	1.09198908	23.54707861
27/08/03 16:30	16.63426146	13.307409	3.2846517	0.84503155	25.72667156
27/08/03 17:30	10.89495487	8.7159639	1.9538763	0.682073179	34.90871896
27/08/03 18:30	4.280160842	3.4241287	0.6372687	0.137758622	21.61704041
27/08/03 19:30	0.486381914	0	0	0.058799412	0
27/08/03 20:30	0.486381914	0	0	0.090719093	0
28/08/03 06:30	0.486381914	0.3891055	0.087266415	1.09198908	1251.327999
28/08/03 07:30	1.459145742	1.1673166	0.288420028	0.17303827	59.99523372
28/08/03 08:30	7.101175943	5.6809408	1.540572166	0.697193028	45.25546049
28/08/03 10:30	18.48251273	14.78601	4.440556929	1.765662343	39.76218235
28/08/03 11:30	23.24905549	18.599244	5.625791794	1.89502105	33.68452156